Del principio de Vernier al procesamiento de imágenes con una resolución subpixel: Teoría y aplicaciones

Patrick Sandoz

Département de Mécanique Appliquée,

Institut FEMTO-ST,

UMR CNRS 6174 – Université de Franche-Comté

Besançon, France

patrick.sandoz@univ-fcomte.fr

slides in english

From Vernier's principle to image processing with a subpixel resolution: Theory and applications

1 Vernier principle and its transposition to image domain

Other contributors: Sounkalo Dembelé, Jean-Christophe Ravassard, André Janex, Tijani Gharbi, Vincent Bonnans, Jean-Michel Friedt, Emile Carry, **July A. Galeano Z.**, Emilie Gaiffe, Sophie Launay, Laurent Robert, Maxime Jacquot, Fabienne Hirchaud, Jean-Luc Prétet, Christiane Mougin, Bertrand Trolard, **Johnson Garzon R., Néstor A. Arias H., Jaime E. Meneses, Miguel A. Suarez,** Rabah Zeggari, Luc Froehly

Vernier Instrument

Measurements with two complementary scales

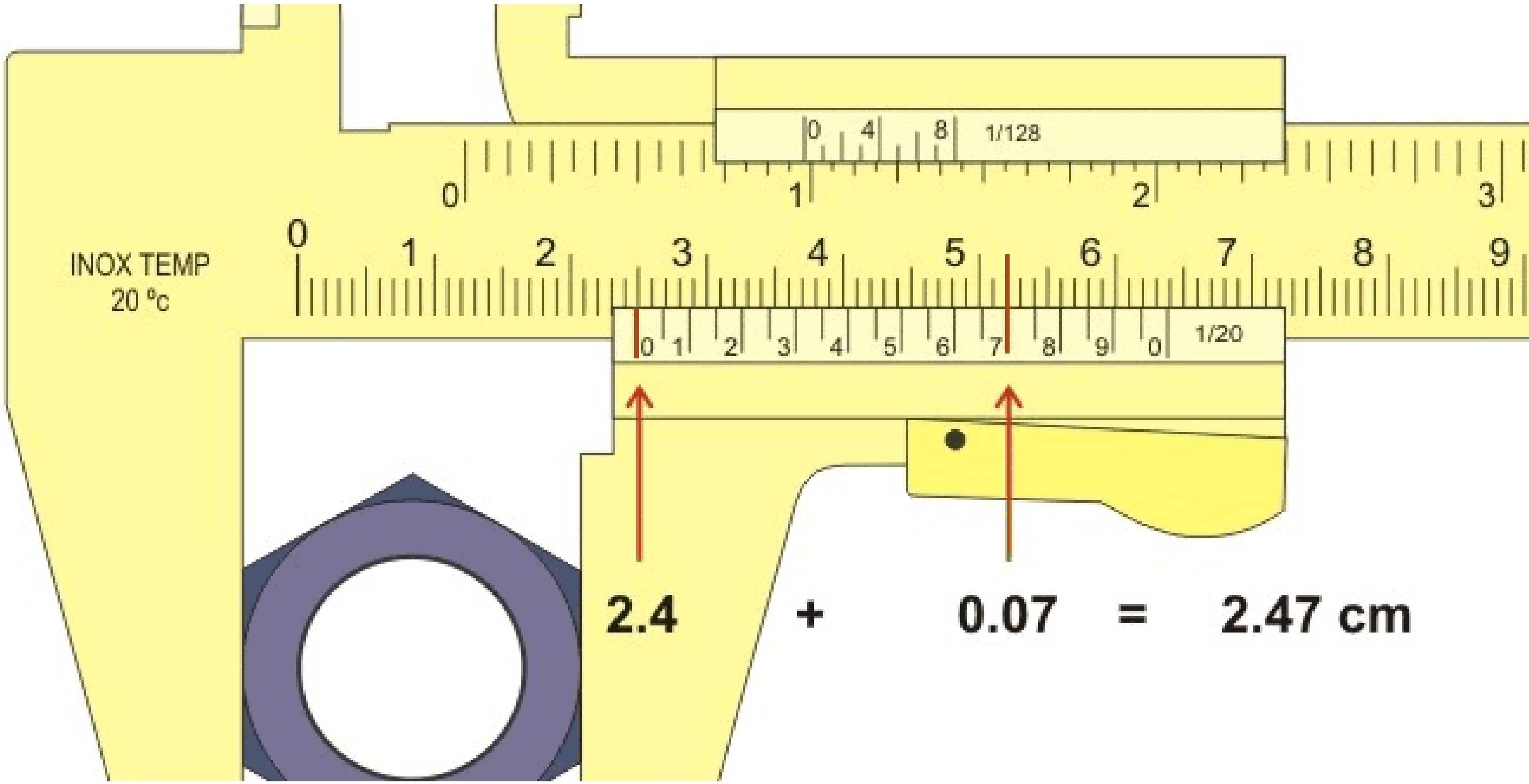

Pierre Vernier: 1580-1637, mathematician

Lived in Ornans; 25 kms from Besançon

Trigonometric phase representation of the Vernier principle

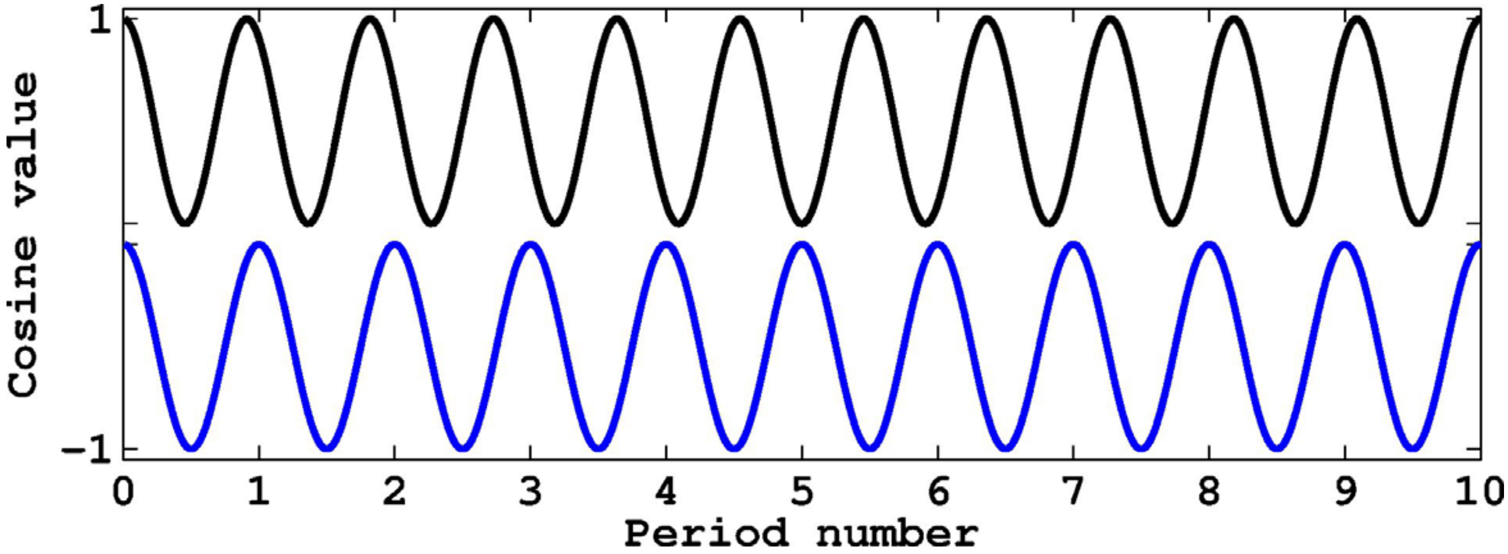

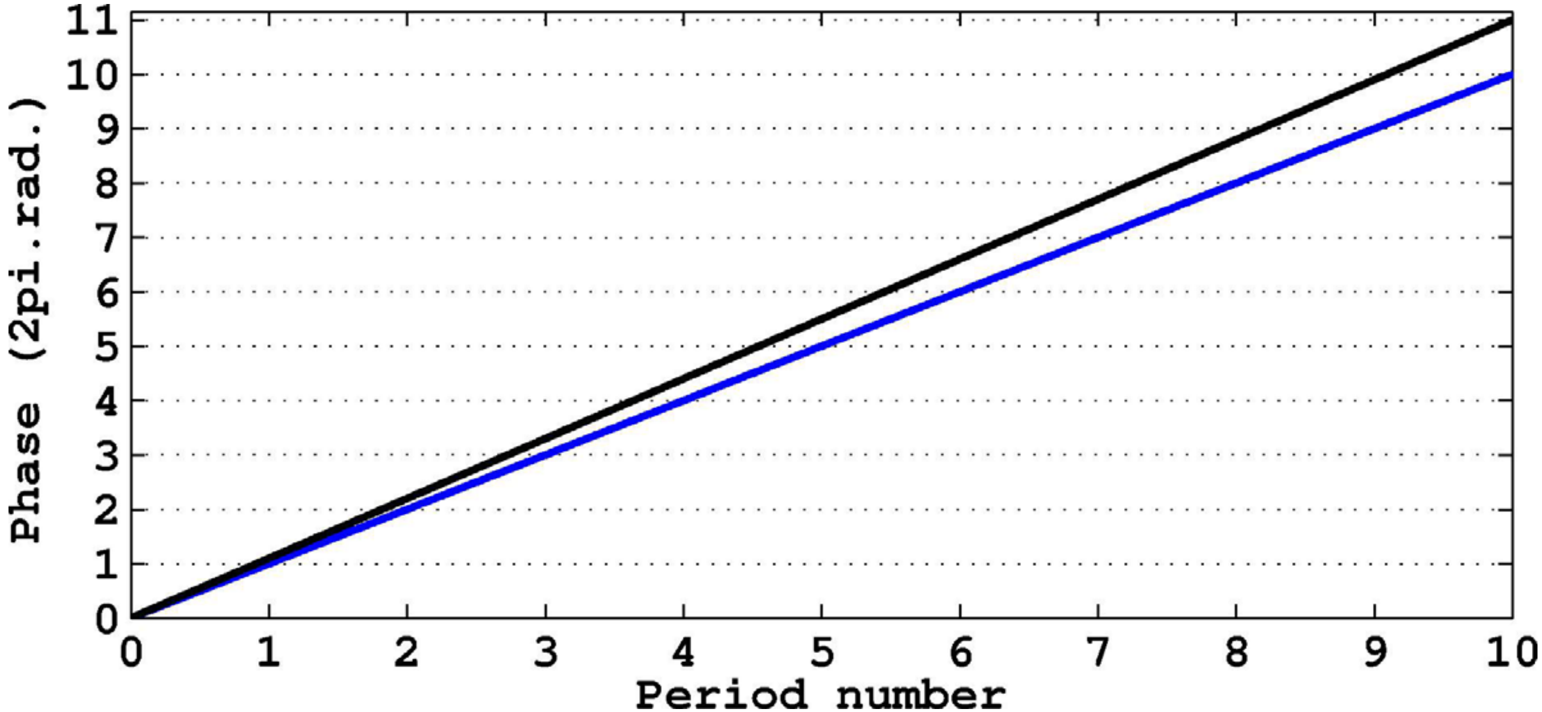

Trigonometric phase representation of the Vernier principle

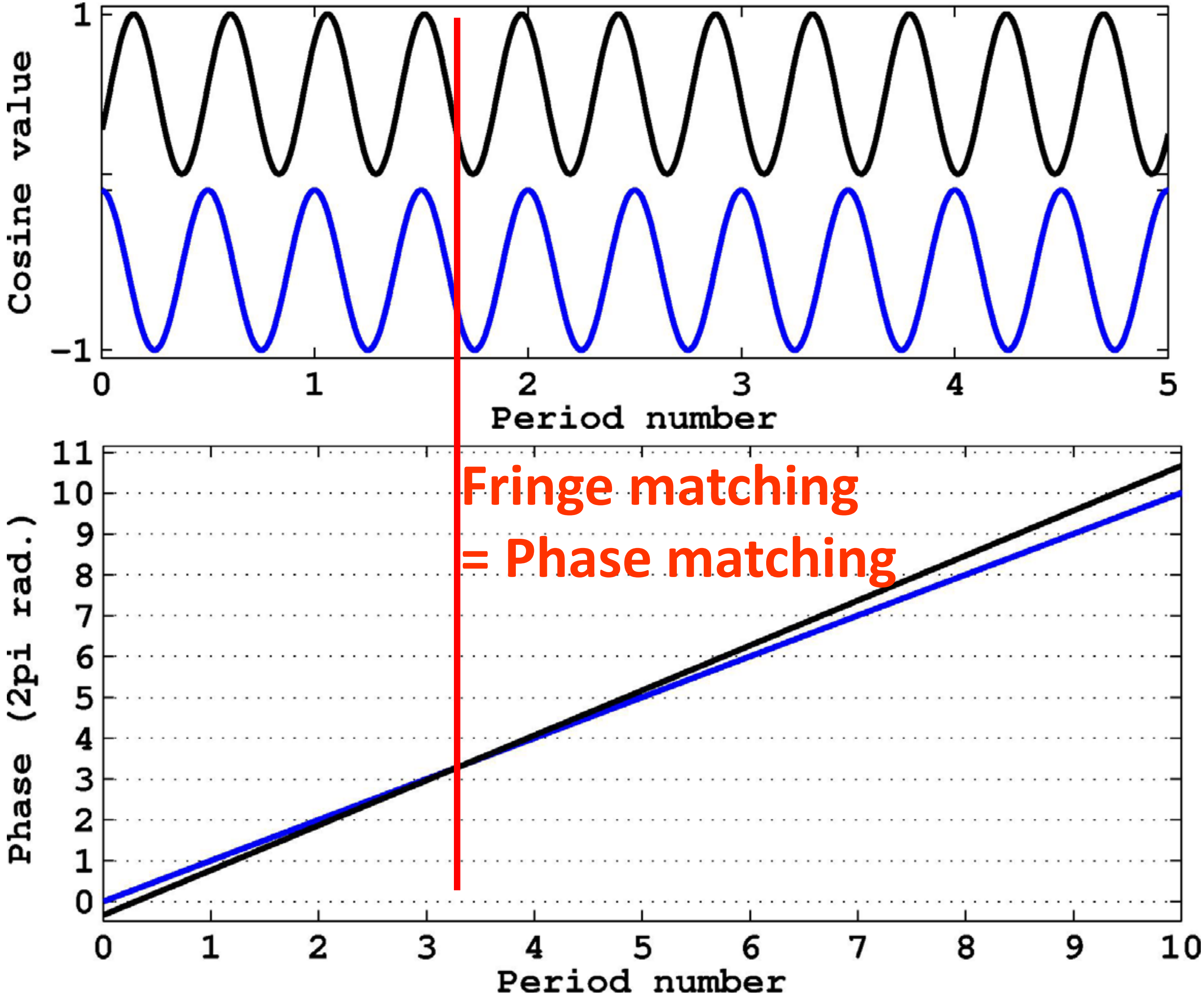

Mathematical phase representation of the Vernier principle

In the space domain:

$$O_{Dis}(x,y) = O_{ini}(x,y) * \delta(\Delta x, \Delta y)$$

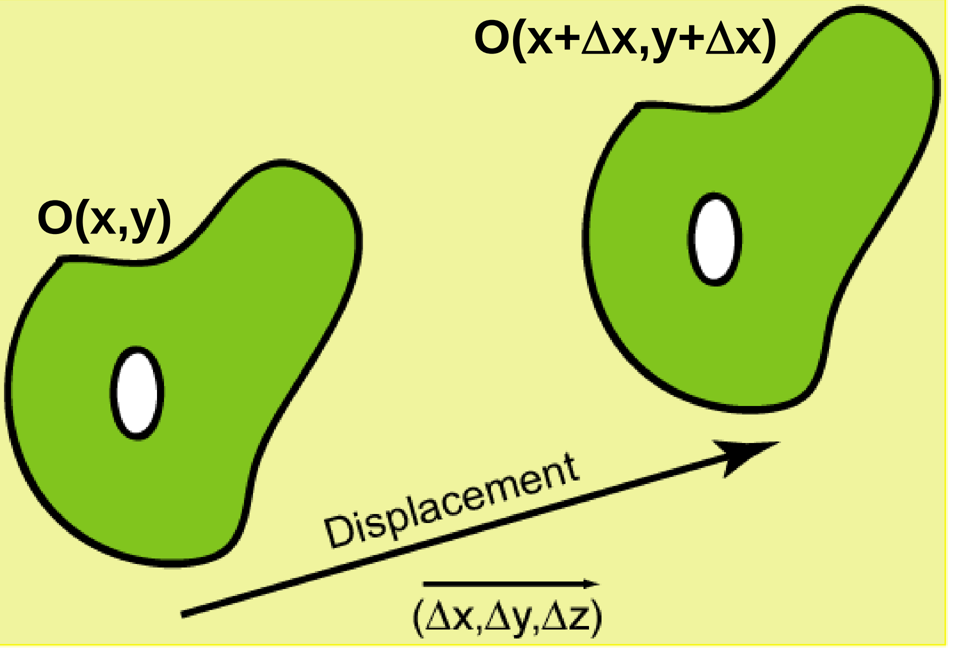

In the Fourier domain:

$$\tilde{O}_{Dis}(\nu_x, \nu_y) = \tilde{O}_{ini}(\nu_x, \nu_y) \, . \, \exp(\mathbf{2}\pi\nu_{\mathbf{x}}\Delta_{\mathbf{x}}) \, . \, \exp(\mathbf{2}\pi\nu_{\mathbf{y}}\Delta_{\mathbf{y}})$$

Pseudo-periodic pattern and pixel frame as Vernier scales

Vernier Instrument
1D (X)

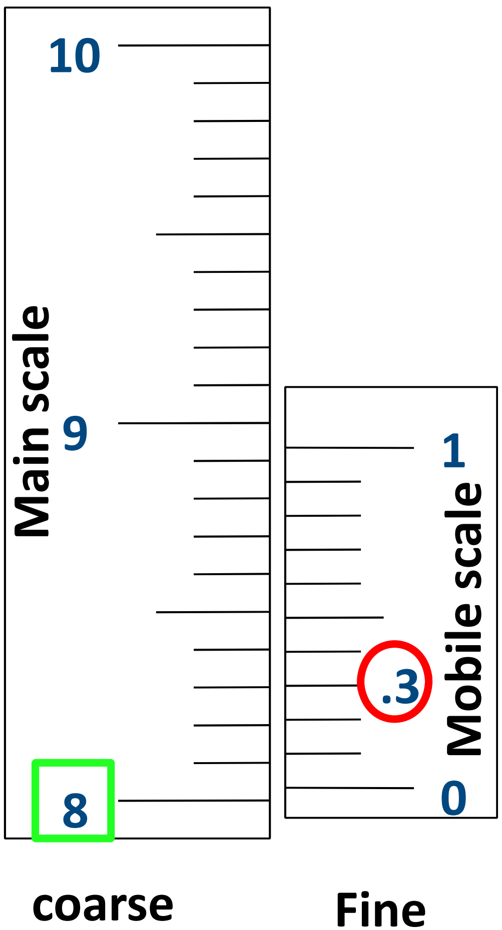

Digital image
2D (X,Y,θ)

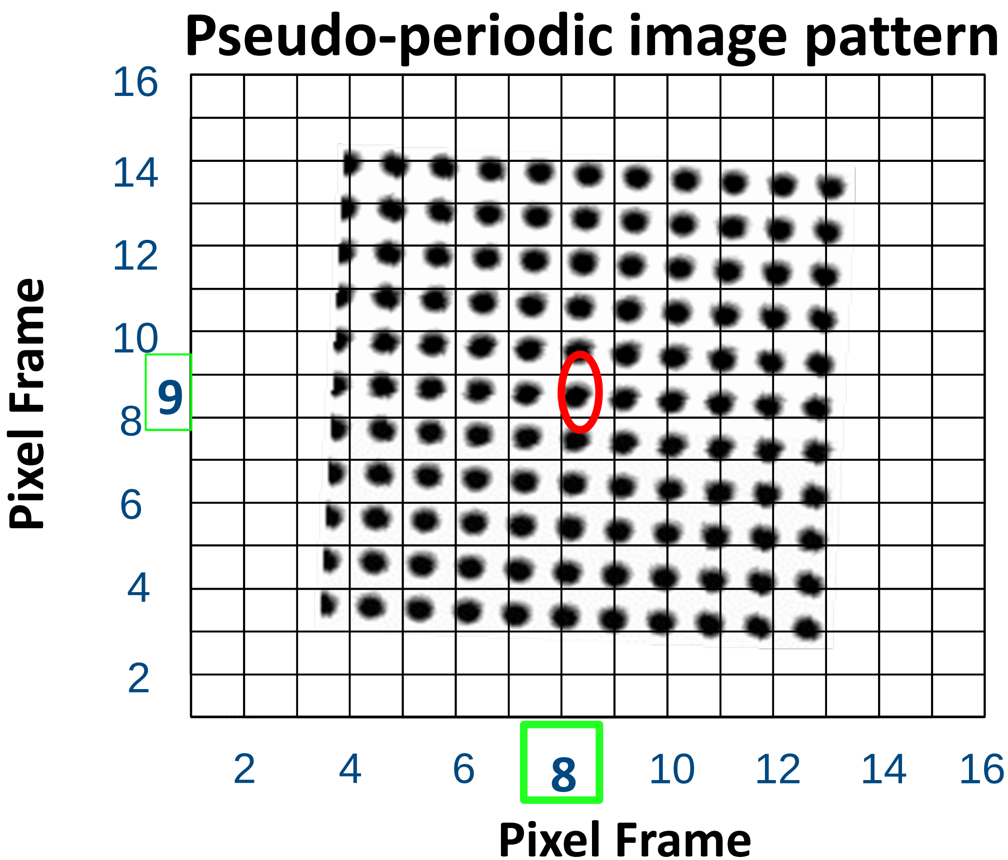

First scale: pixel frame
Second scale: pattern

Coarse: edges
Fine: phase
Orientation: phase

Pseudo-periodic pattern and pixel frame as Vernier scales

Vernier Instrument

1D (X)

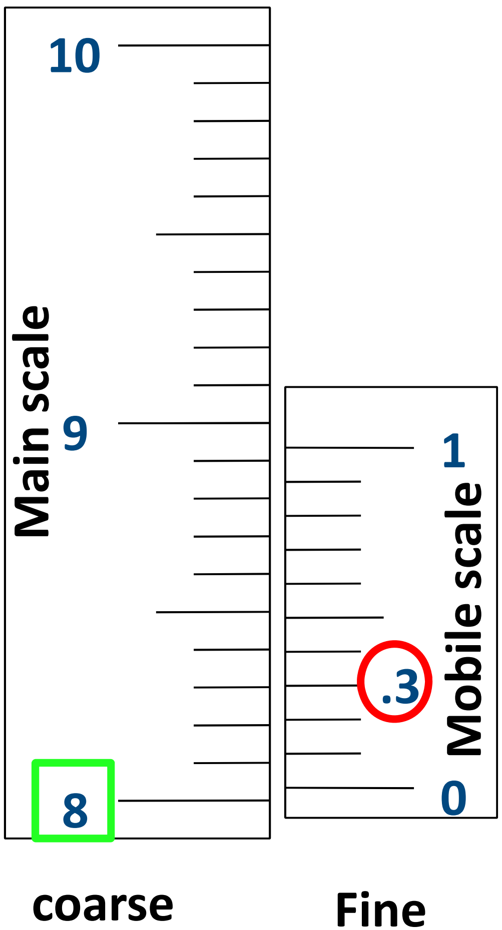

Digital image Variants

2D (X,Y,θ)

Pseudo-periodic image pattern

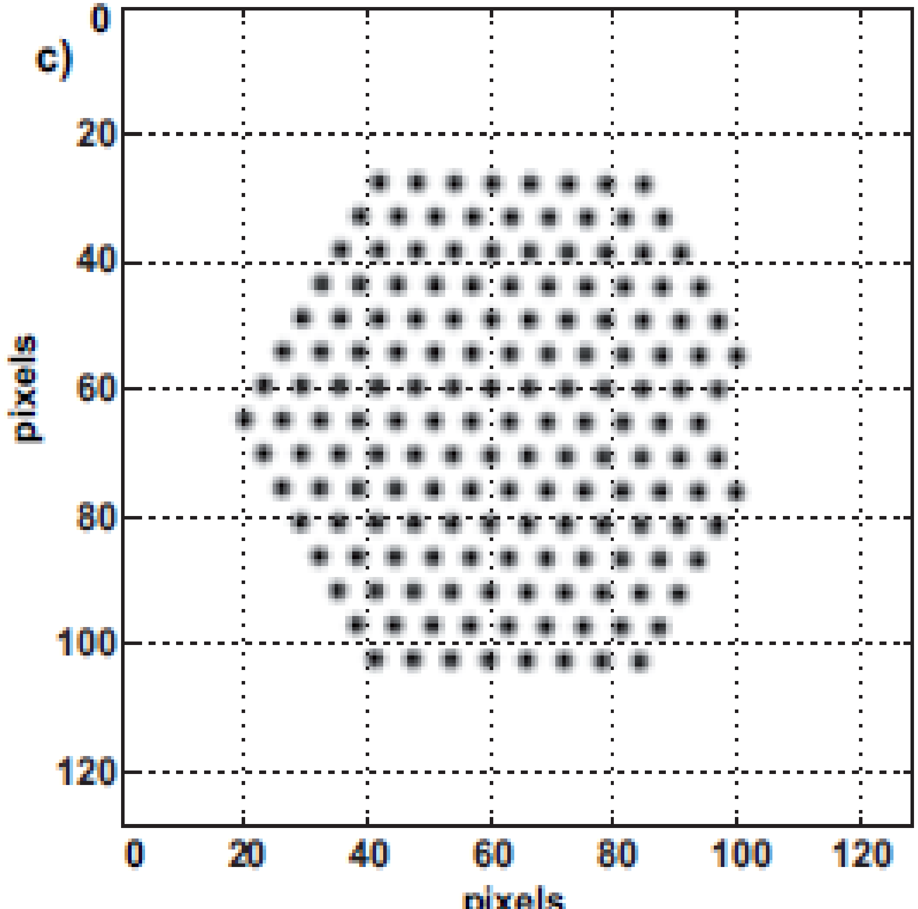

Pseudo-periodic pattern and pixel frame as Vernier scales

Vernier Instrument

1D (X)

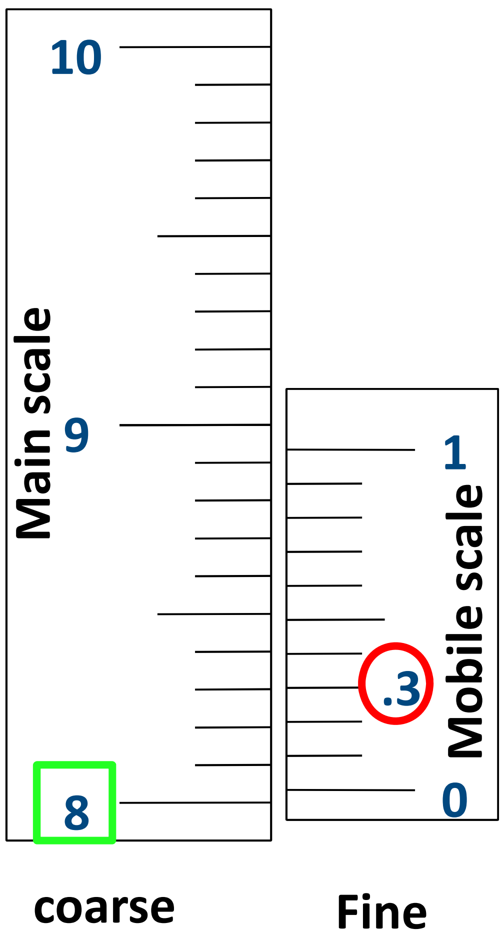

Digital image

2D (X,Y,θ)

Pseudo-periodic image pattern

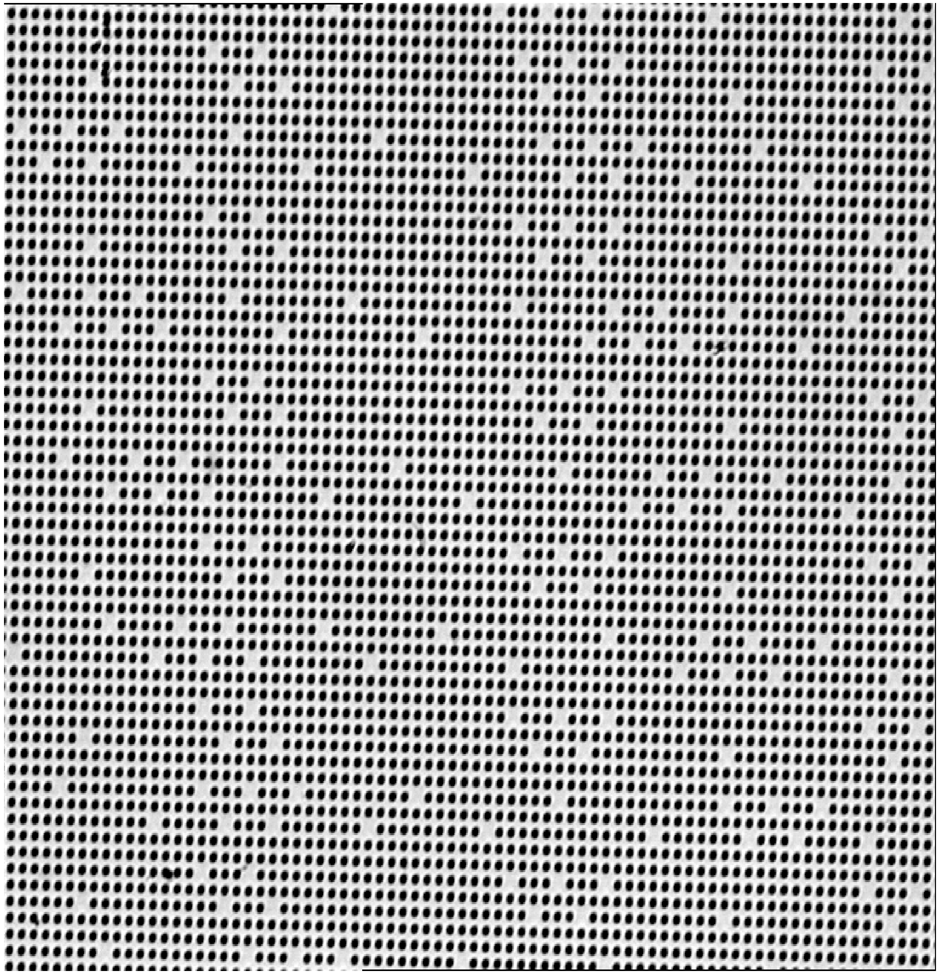

No edges:

encryption of raw and columns orders

Pseudo-periodic position encryption principle

Natural binary sequence

	0	1	2	3	4	5	6	7
sequence of (2^N) positions	000	001	010	011	100	101	110	111

NESTED SEQUENCE

Pseudo Random Sequences

Encoded sequence

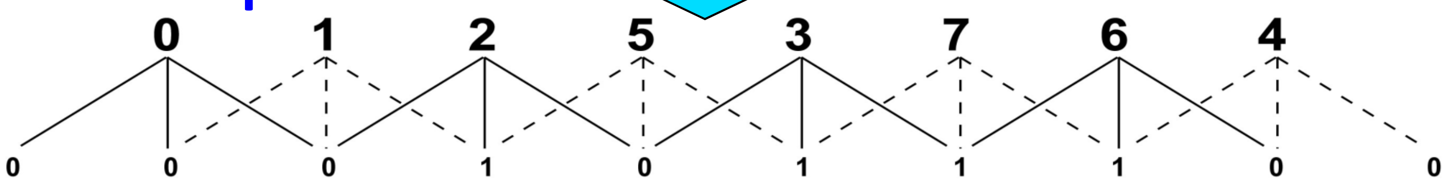

1D Distribution

LFSR (Linear Feedback Shift Register) technique for obtaining pseudorandom sequences

S.W. Golomb, *Shift Register Sequences*, Holden-Day Inc., San Francisco, U.S.A, (1967).

2 Image processing for reconstruction of target position and orientation: two steps

Phase computations: relative but high accuracy measurements

Binary processing:
- **raw and column order identification**
- **coarse but absolute measurement**
- **from edges or from missing dot distribution**

Patrick Sandoz, Sounkalo Dembelé, Jean-Christophe Ravassard, André Janex,
Phase-sensitive vision method for high accuracy position measurement of moving targets,
IEEE Transactions on Instrumentation and Measurement 49 (2000), no. 4, 867–872

Patrick Sandoz, Vincent Bonnans, Tijani Gharbi,
High-accuracy position and orientation measurement of extended 2D surfaces by a phase-sensitive vision method,
Applied Optics, 41, (2002), no. 26, 5503-5511

Fourier Processing: fine measurement (Sub-Pixel)

Image

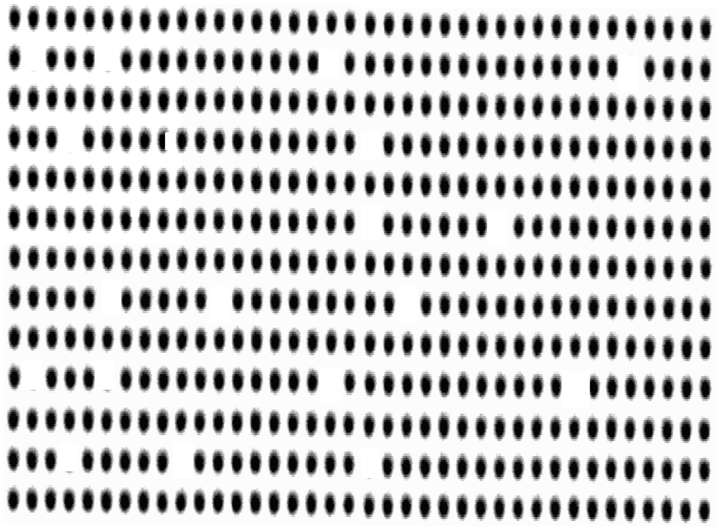

Fourier spectrum

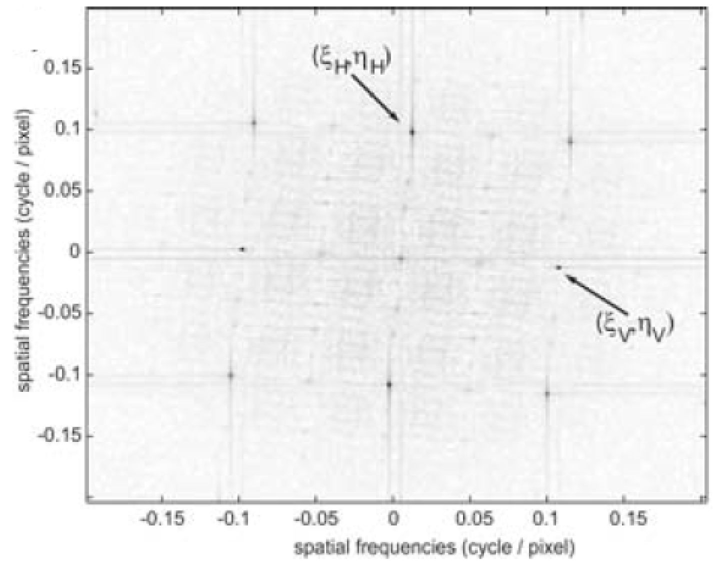

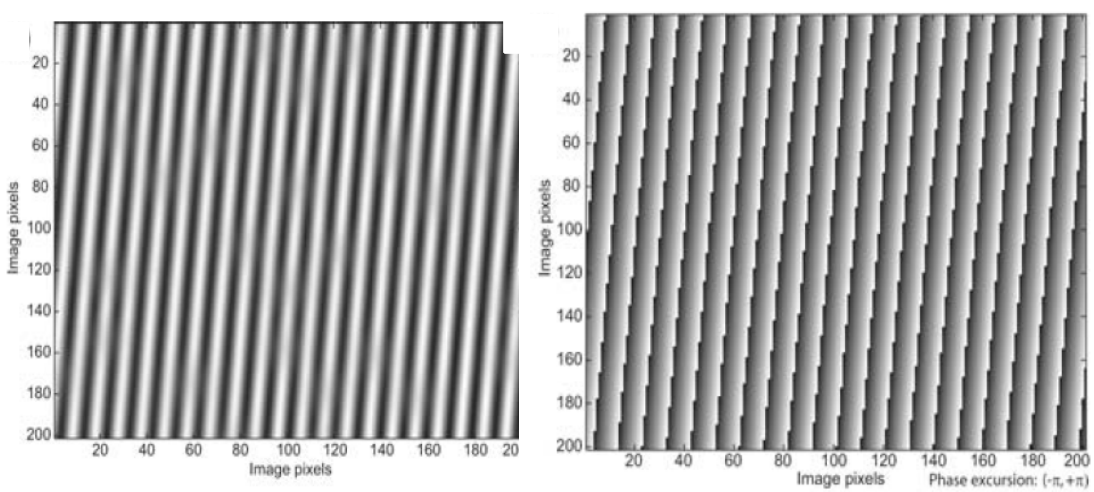

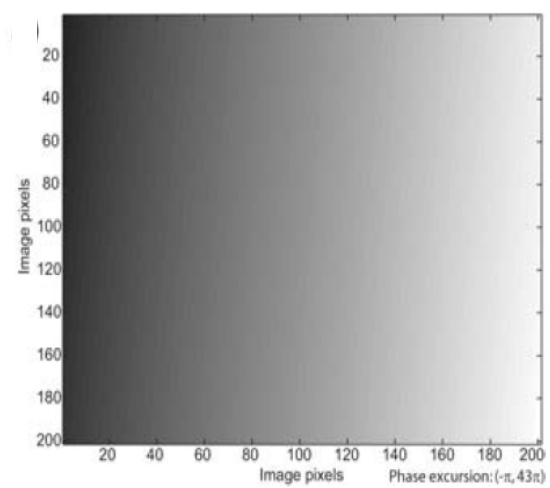

Inverse Fourier transform: real part and angle

Unwrapped phase

Fourier Processing: fine measurement (Sub-Pixel)

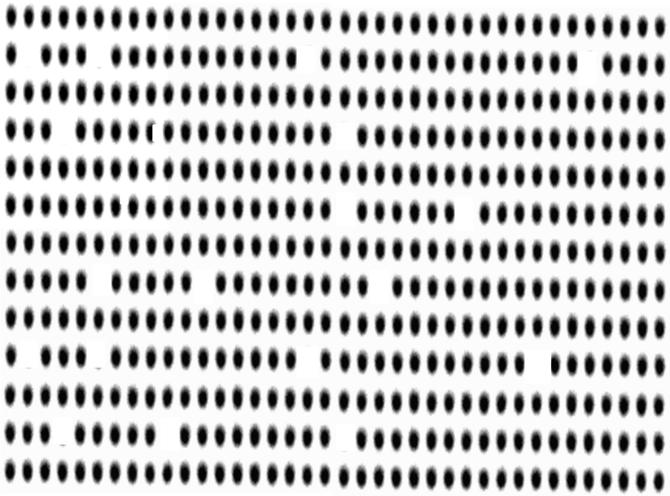

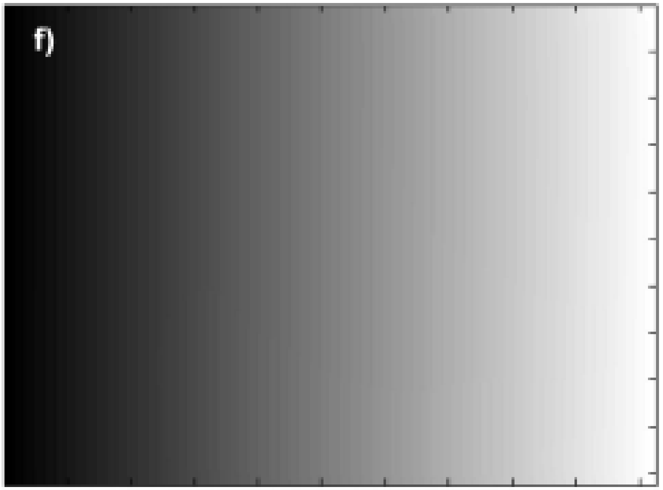

From the unwrapped Phase

$$\Phi_V(i,j) = A_V \cdot i + B_V \cdot j + C_V$$

$$\Phi_H(i,j) = A_H \cdot i + B_H \cdot j + C_H$$

Orientation $\alpha = tan^{-1}(B_V/A_V) \quad or \quad tan^{-1}(B_H/A_H)$

C_V C_H Phase constants with an ambiguity of 2π → Compensation by The Binary Code (coarse measurement)

Binary Processing: coarse measurement (absolute)

Identification of the missing dot distribution

Position decryption from code reading

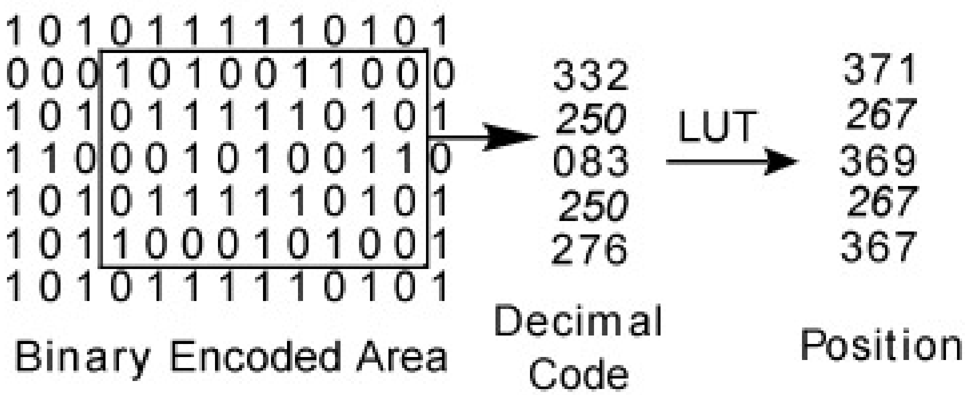

Binary Processing: coarse measurement (absolute)

Local contrast computation from phase data for robust dot presence identification

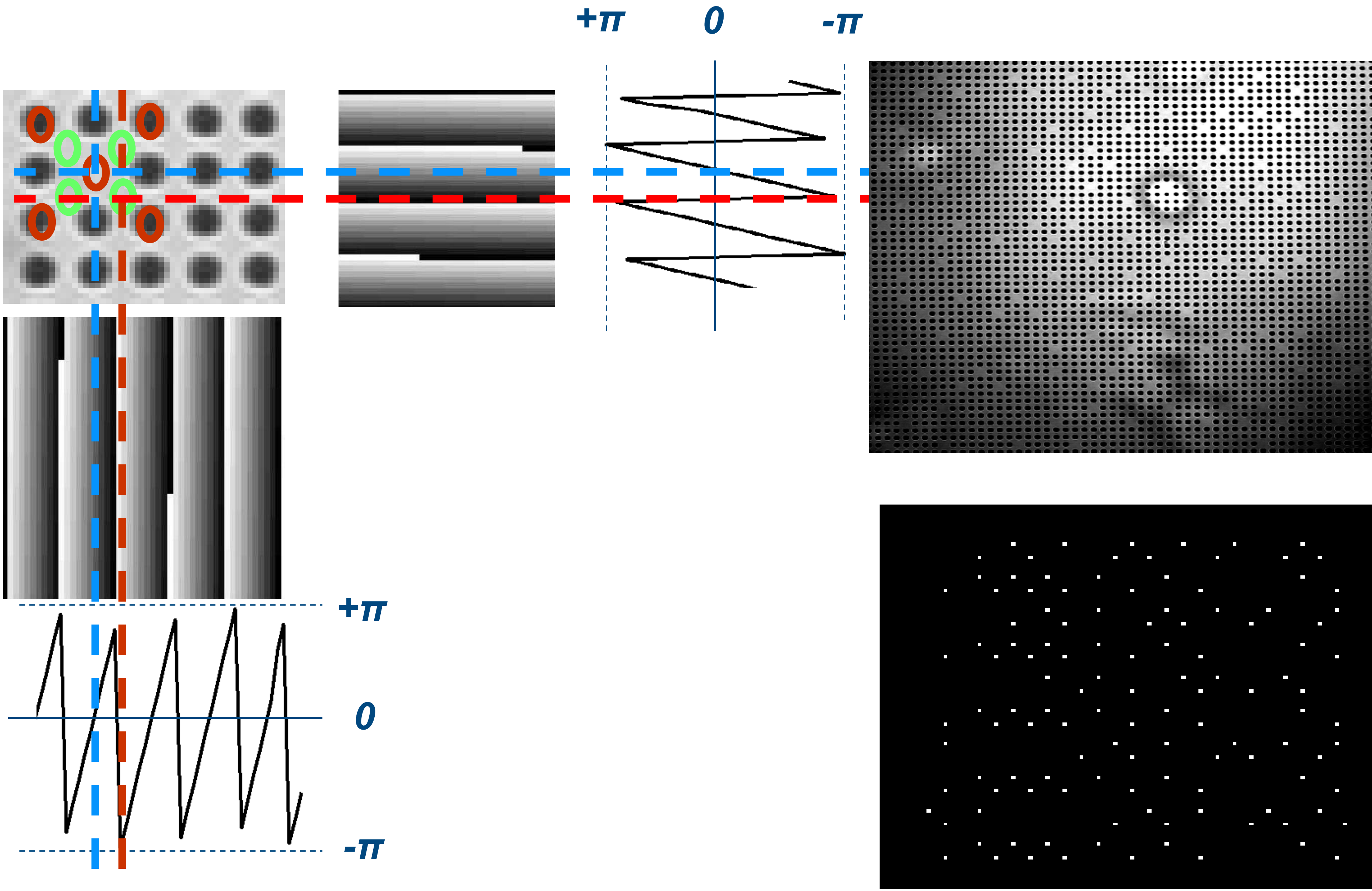

Spectral phase and modulus processing (Sub-Pixel and absolute)

Image **Fourier spectrum**

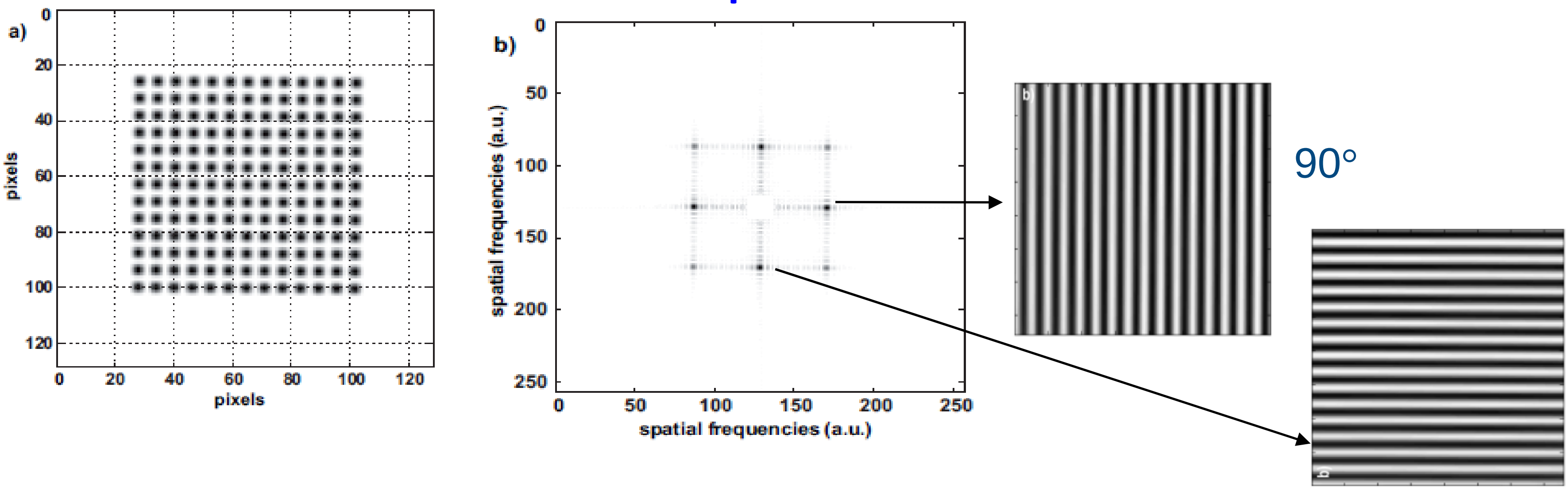

Inverse Fourier transforms from complementary spectral lobes

Spectral phase and modulus processing (Sub-Pixel and absolute)

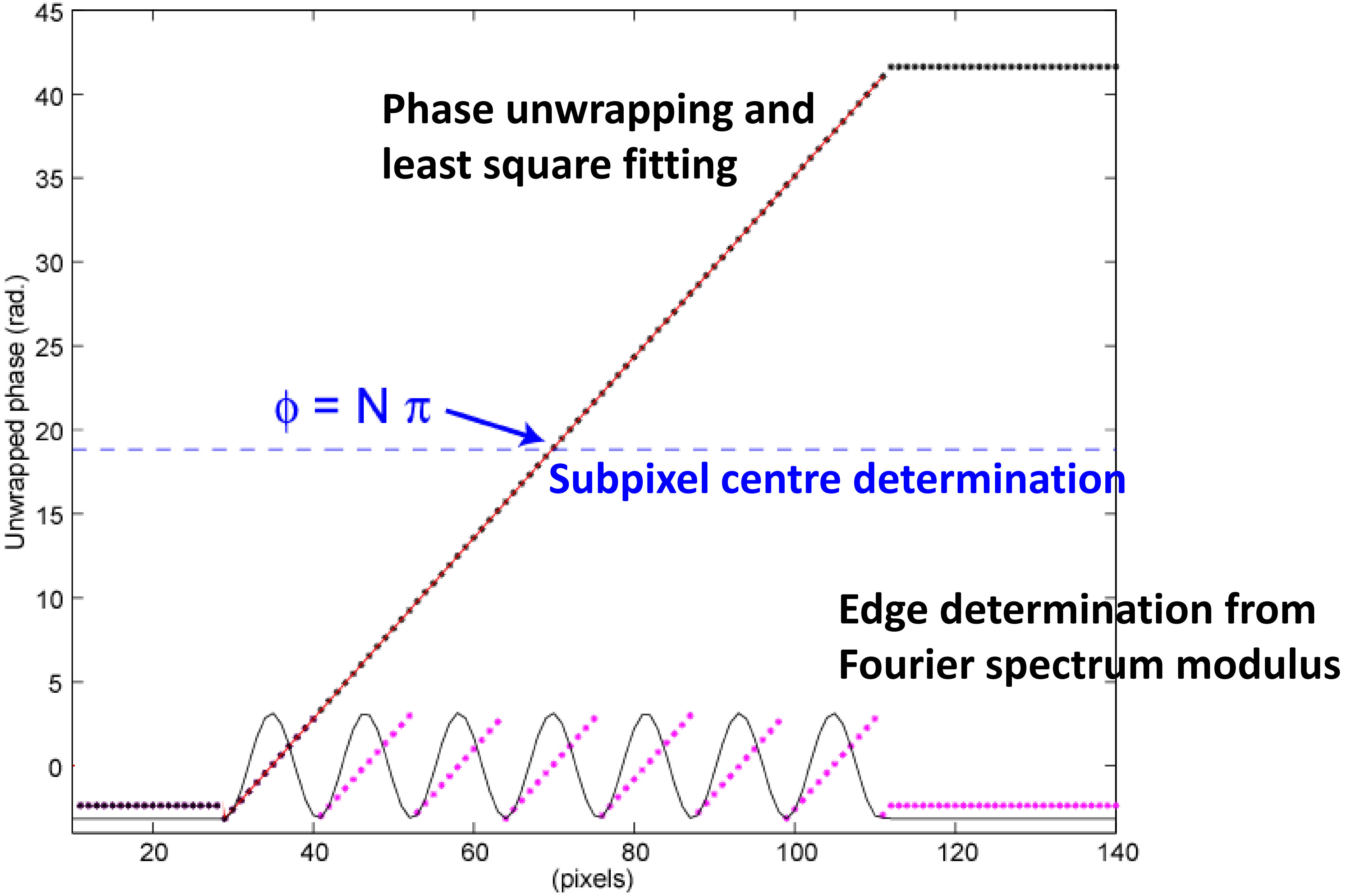

Spectral phase and modulus processing (Sub-Pixel and absolute)

Inverse Fourier transforms from complementary spectral lobes

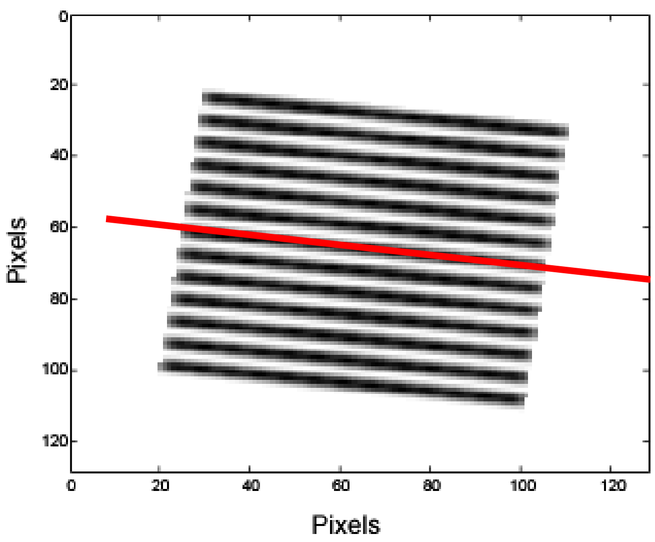

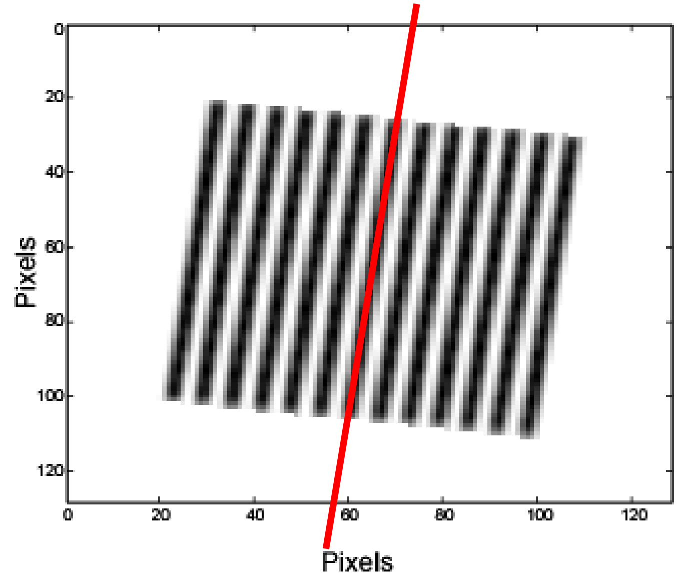

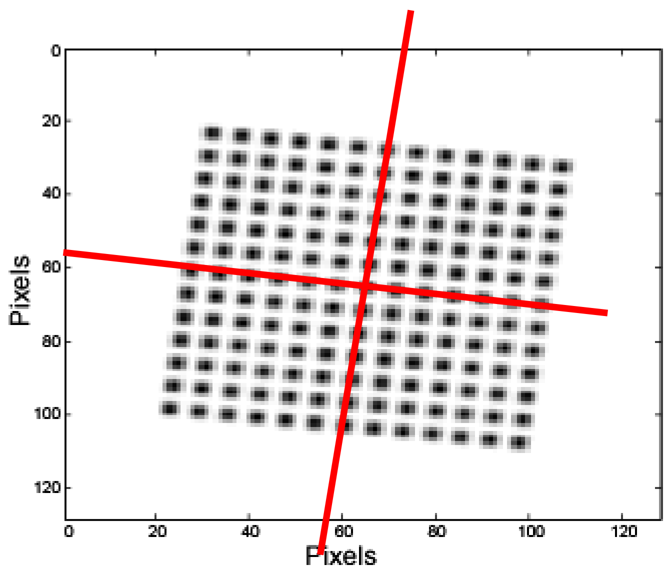

Subpixel center position determination

Orientation determination (slope)

Spectral phase and modulus processing (Sub-Pixel and absolute)

Synthetization of a digital pattern with angle and period retrieved from phase computation for image correlation

Pattern center identified from image correlation peak

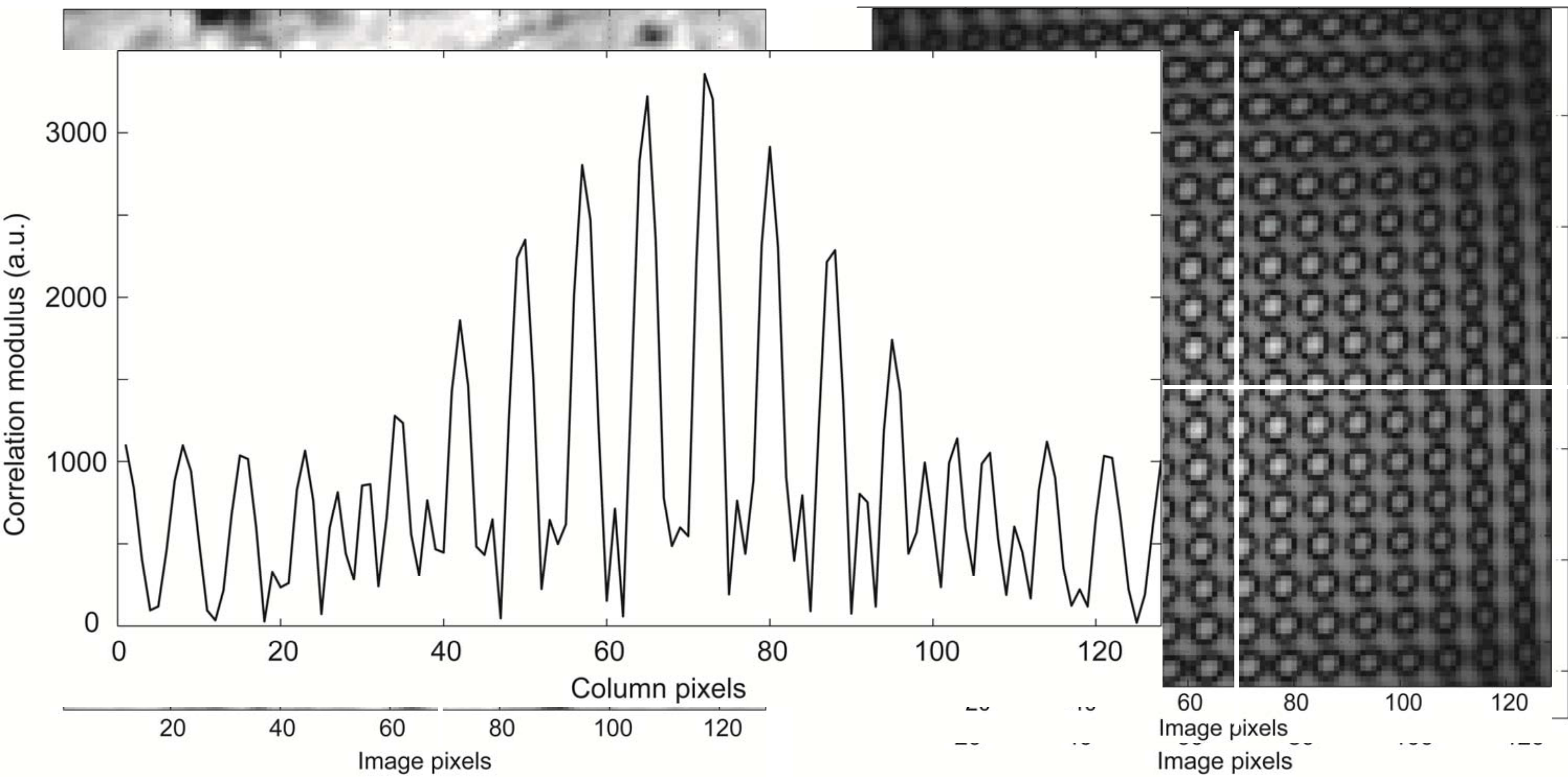

3 Performances

- Position
- Orientation
- Depth of focus

Repeatability test

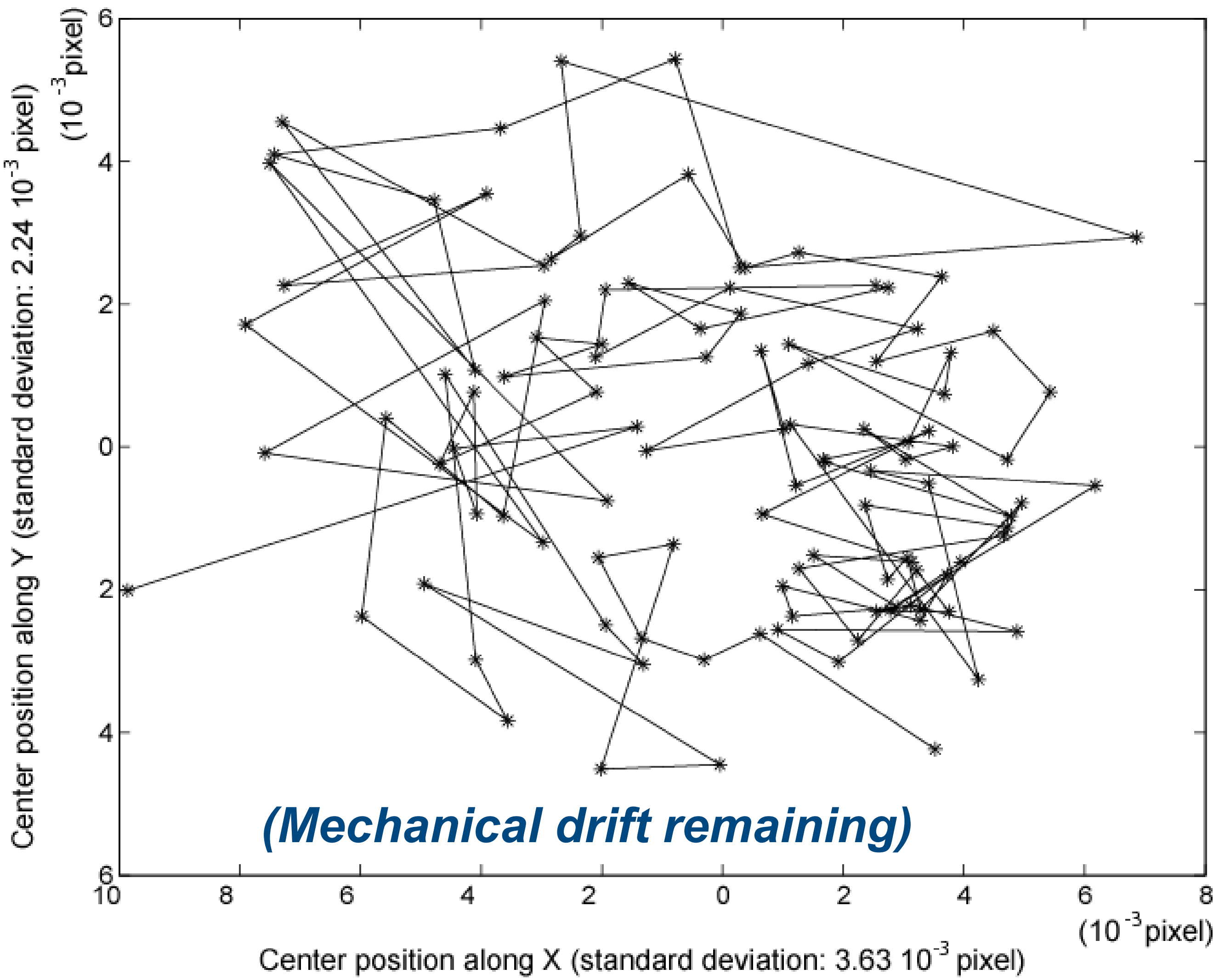

Statistics (100pts)

PV in X :

1.67.10^{-2} pixel

PV in Y :

0.99.10^{-2} pixel

σ in X :

3.63 10^{-3} pixel

σ in Y :

2.24 10^{-3} pixel

Scale:

Pattern period ⬄ 10µm & 1 pixel ⬄ 1µm **lens: 10x**

Resolution in linear displacement reconstruction

Phase computation versus image correlation

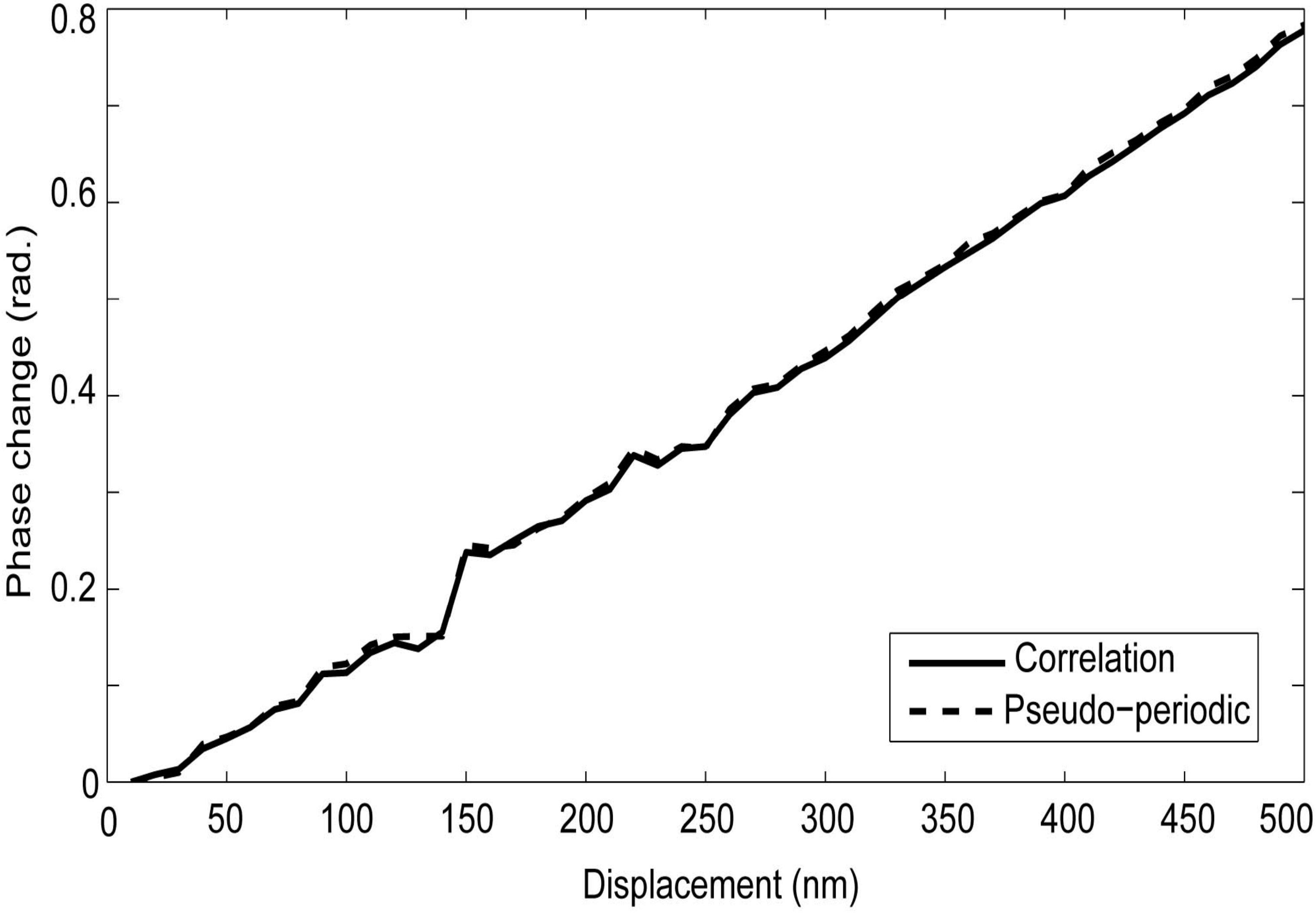

Piezo motor

StD:

σ=25 *nm*

period: 4μm

10x lens

Demonstration of displacement reconstruction

Phase computation versus PZT capacitive sensor (bandwidth mismatch)

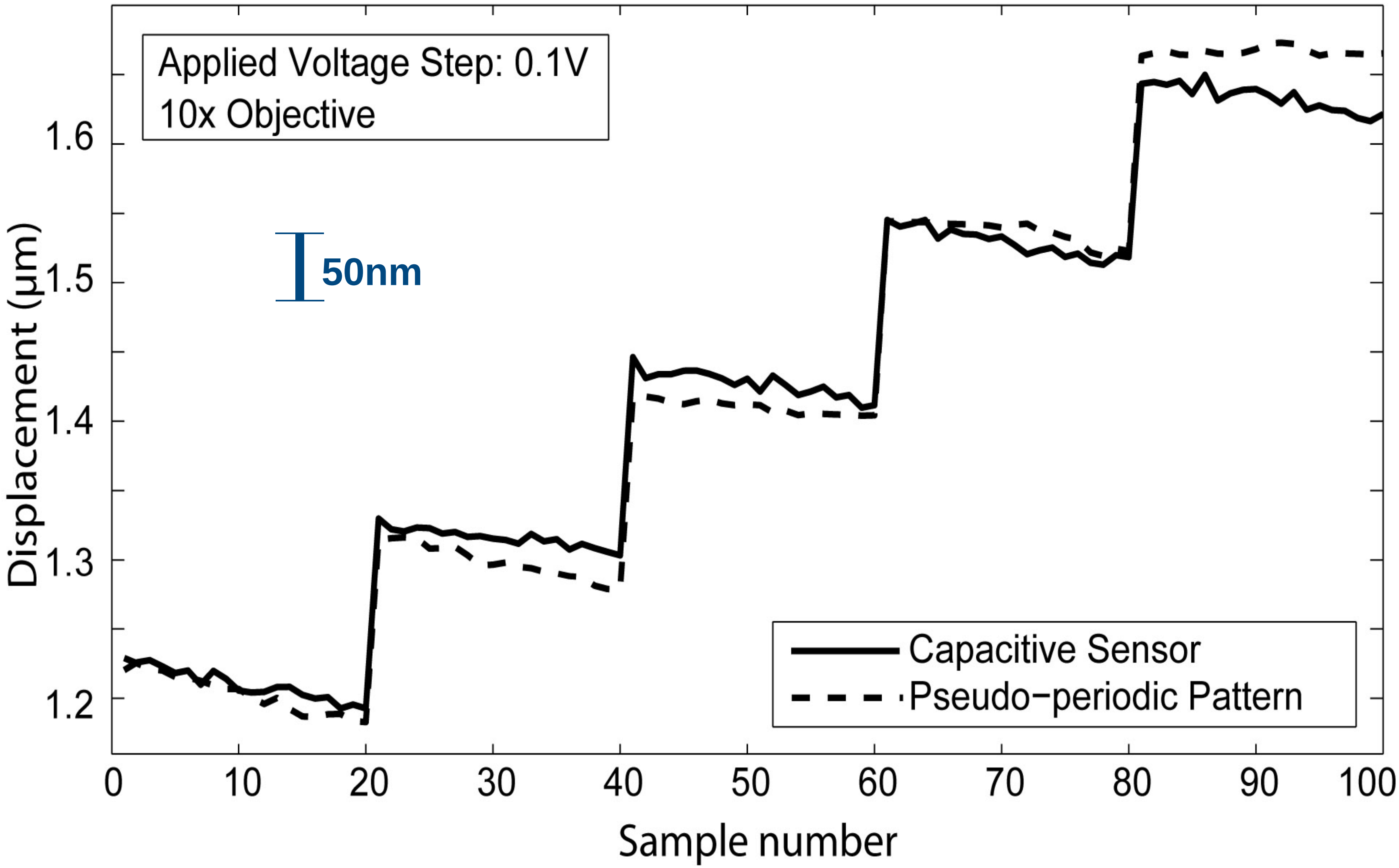

Demonstration of displacement reconstruction

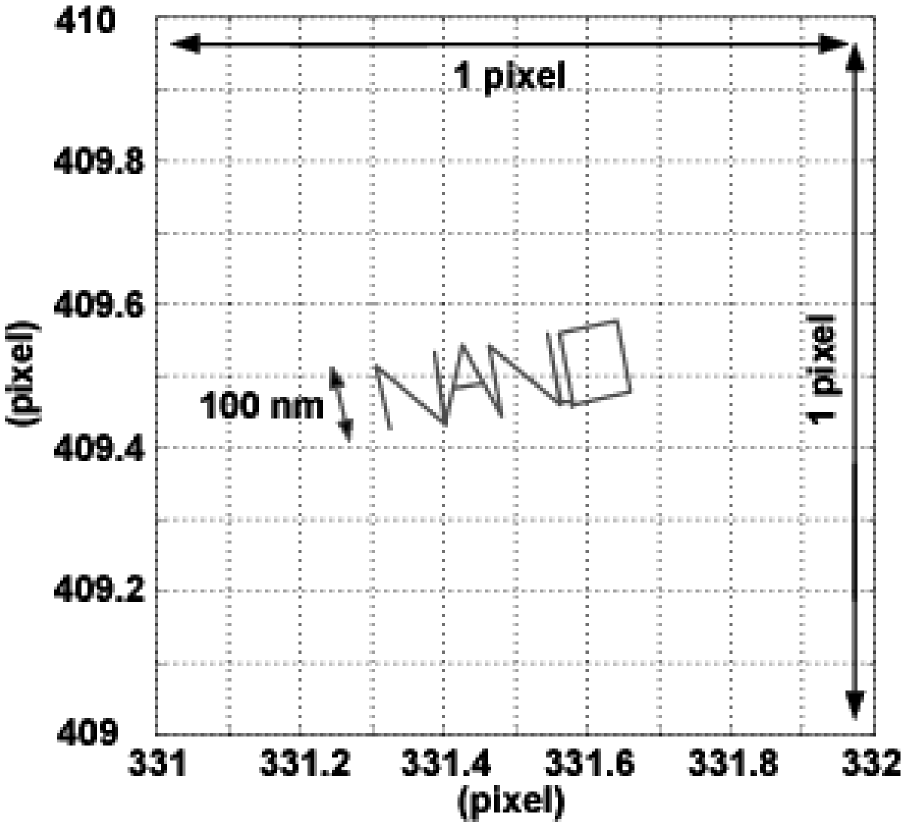

- PZT driven displacement
- Measurement synchronized with displacement
- Measurement rate : ~10 s^{-1}
- Full scale: 1 pixel

Characterization of a motorized stage capabilities

Stage data (c) versus pseudo-periodic pattern data (d)

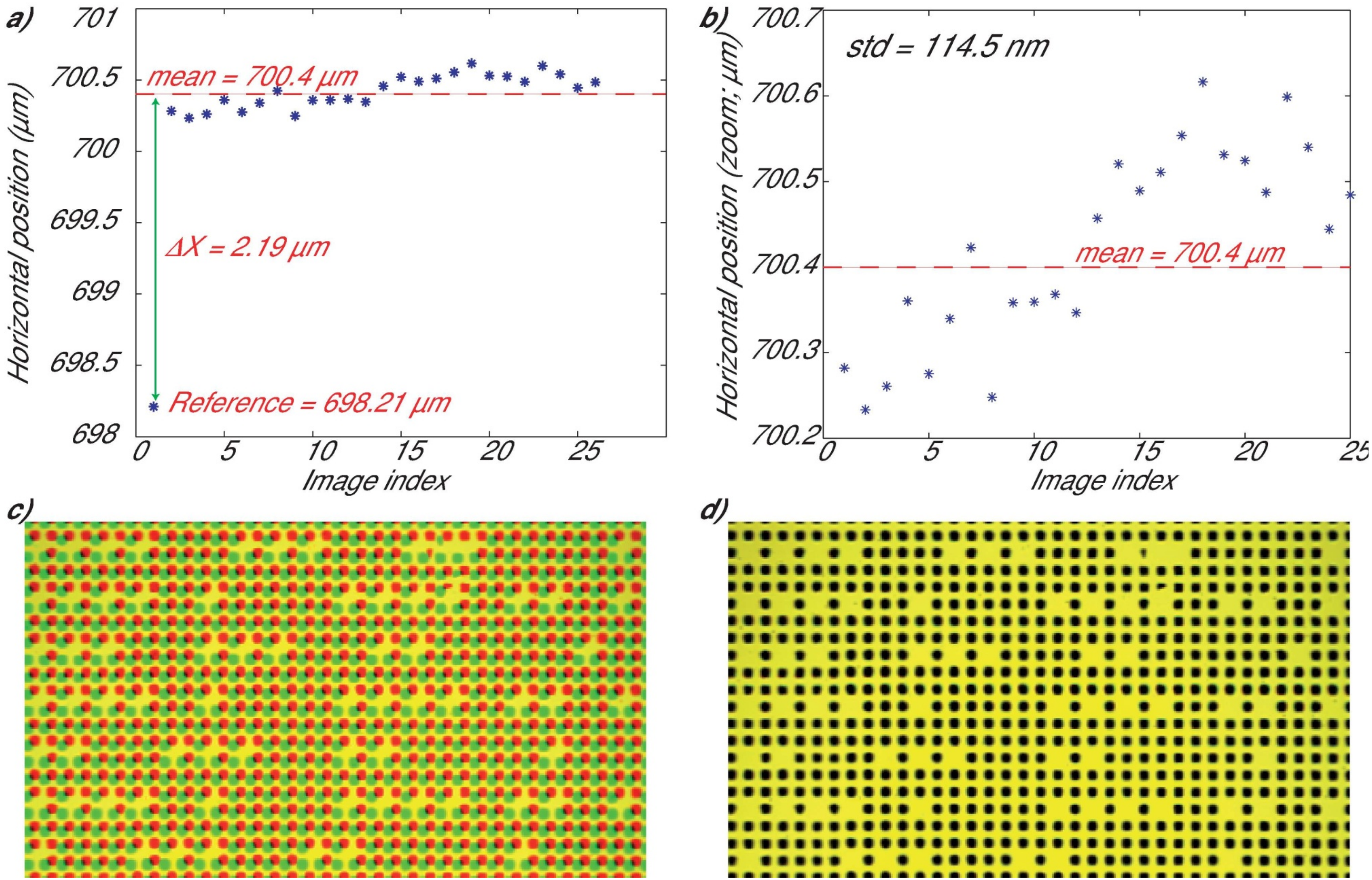

Position error while the stage was driven repeatedly on a given position cycle

Resolution in in-plane orientation measurement

Following of a progressive target rotation

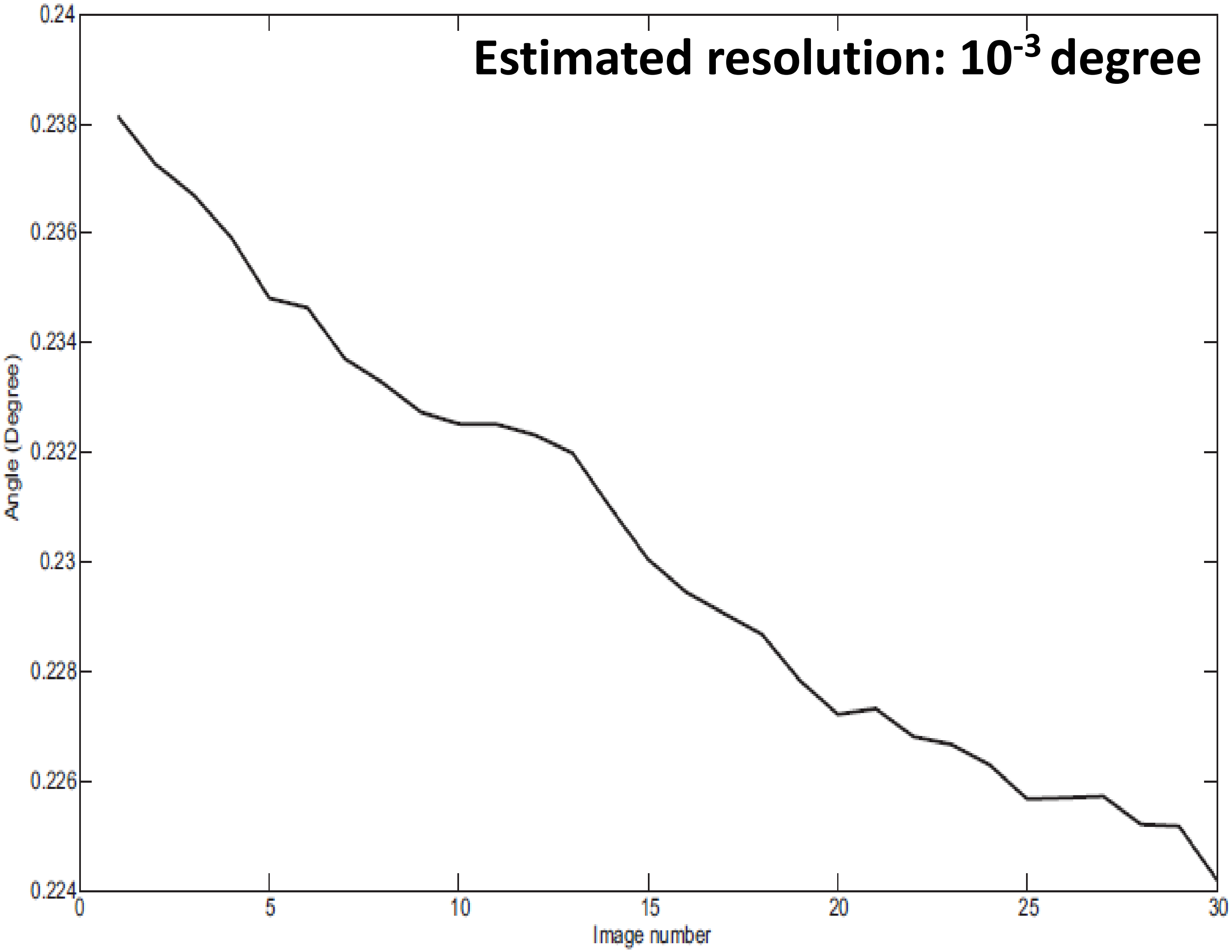

Out of focus robustness => extended depth of operation

Low contrast images can be processed successfully

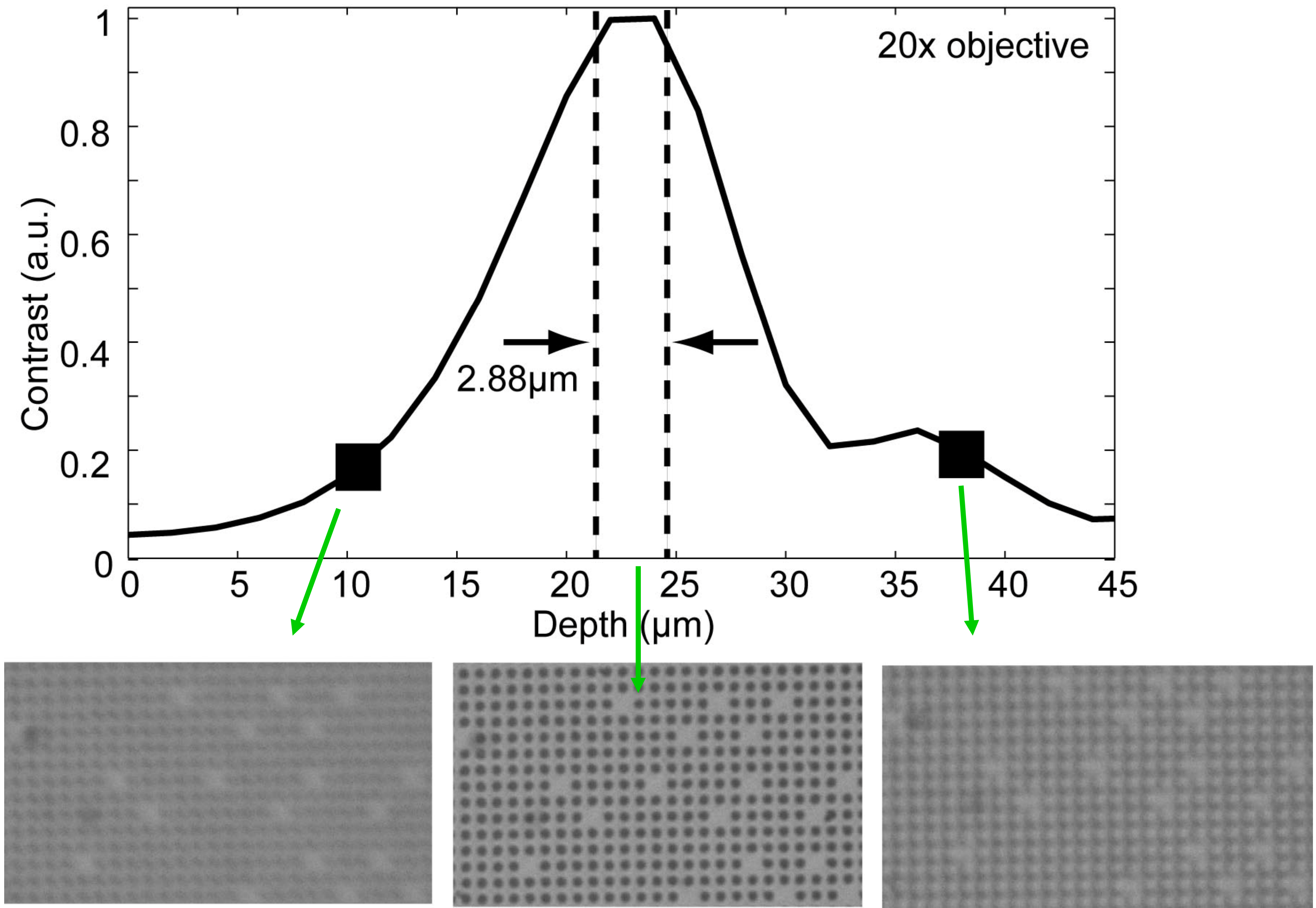

4 Applications

Three examples : - Vibration amplitude control
- Positionning of live-cell-cultures
- Didactic experiment

Vibration amplitude control:

Patrick Sandoz, Jean-Michel Friedt, Émile Carry,
In-plane rigid-body vibration mode characterization with nanometer resolution by stroboscopic imaging of a microstructured pattern,
Review of Scientific Instruments, 78, 023706, 2007

Patrick Sandoz, Jean-Michel Friedt, Émile Carry,
Vibration amplitude of a tip-loaded quartz tuning fork during shear force microscopy scanning,
Review of Scientific Instruments 79, 086102 2008

Application to Vibration Amplitude Measurement

Problematic

Control of probe displacement in Scanning Probe Microscopy

Potential effect of probe vibration on lateral resolution ?

Trade-off between vibration amplitude and ease of servo-control

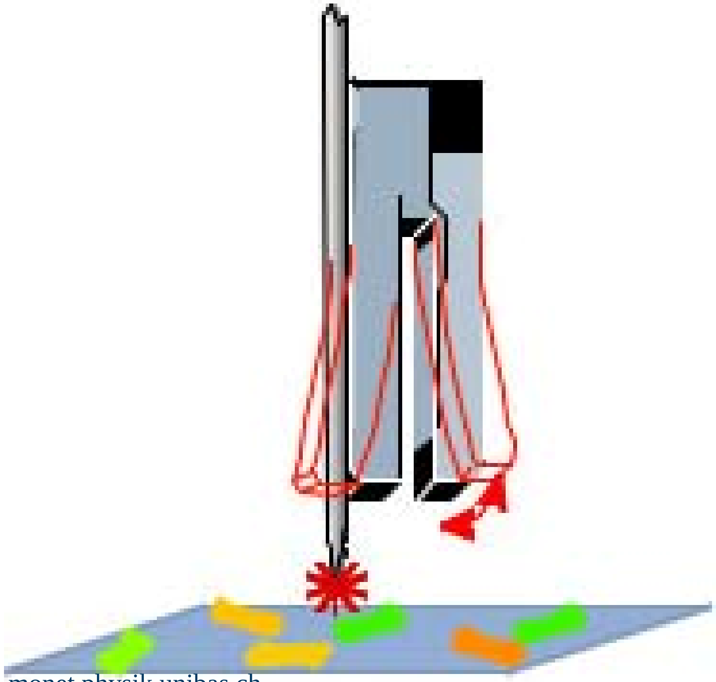
monet.physik.unibas.ch

Demonstration

Visual control of the prong displacement

Representative of the tip displacement

SEM image of the tip-loaded tuning-fork used

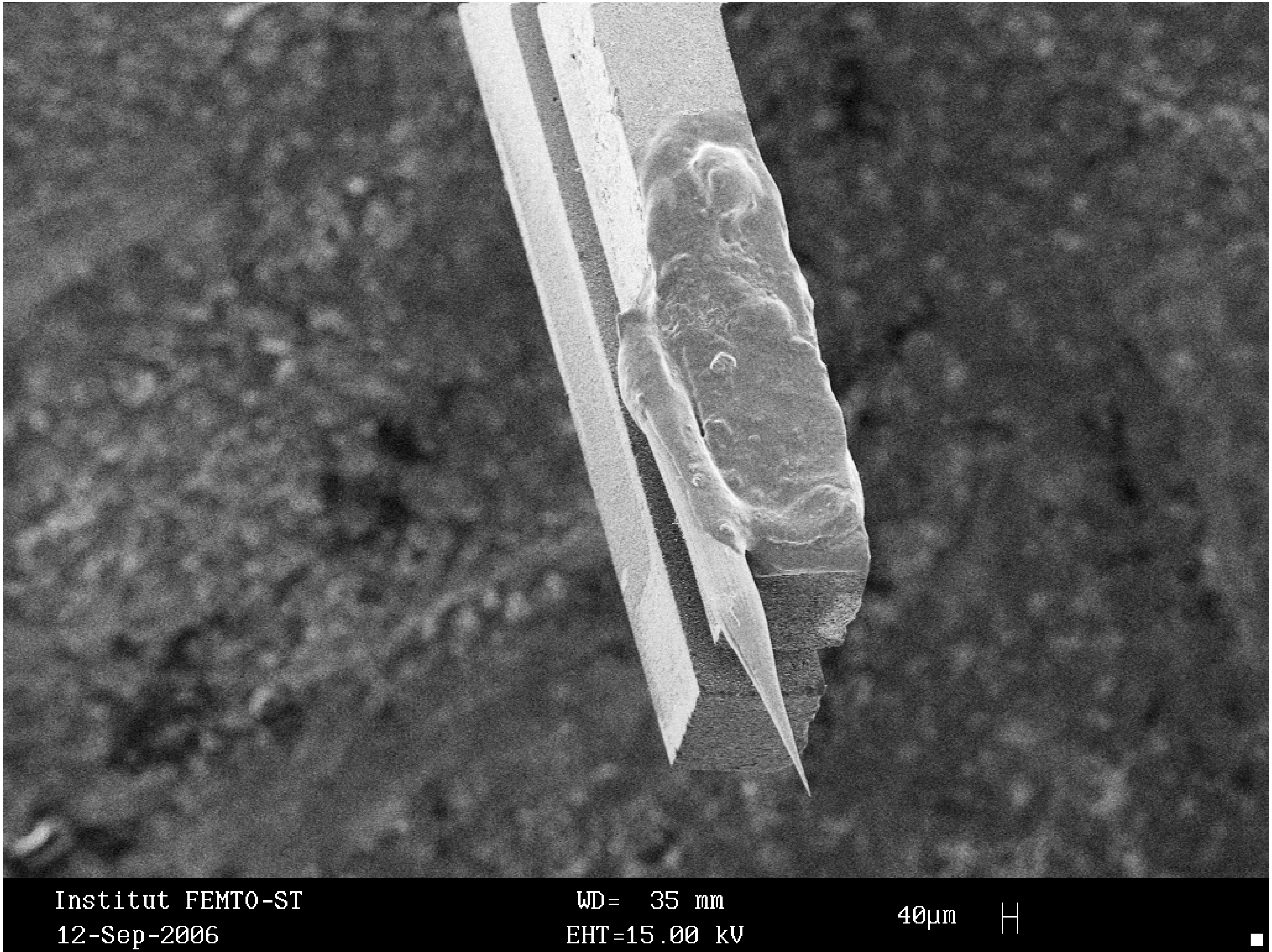

Measurement principle and experimental device

Pseudo-periodic pattern on the prong end face observed by vision

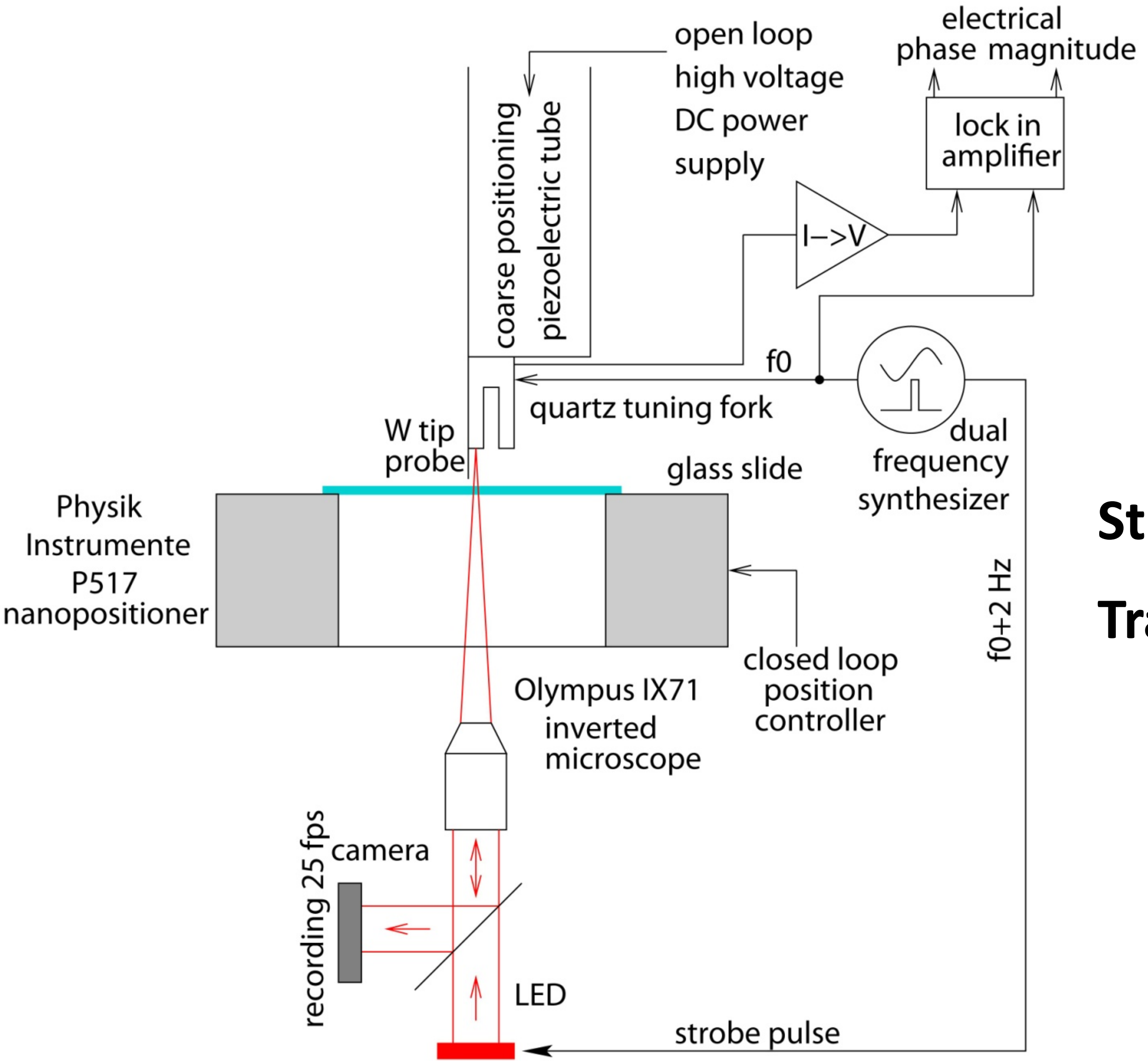

Stroboscopic illumination

Transparent sample

Experimentally recorded image

Pseudo-periodic pattern drilled by FIB on the prong end face
or
Sticking of a patterned glass plate obtained by photolithography

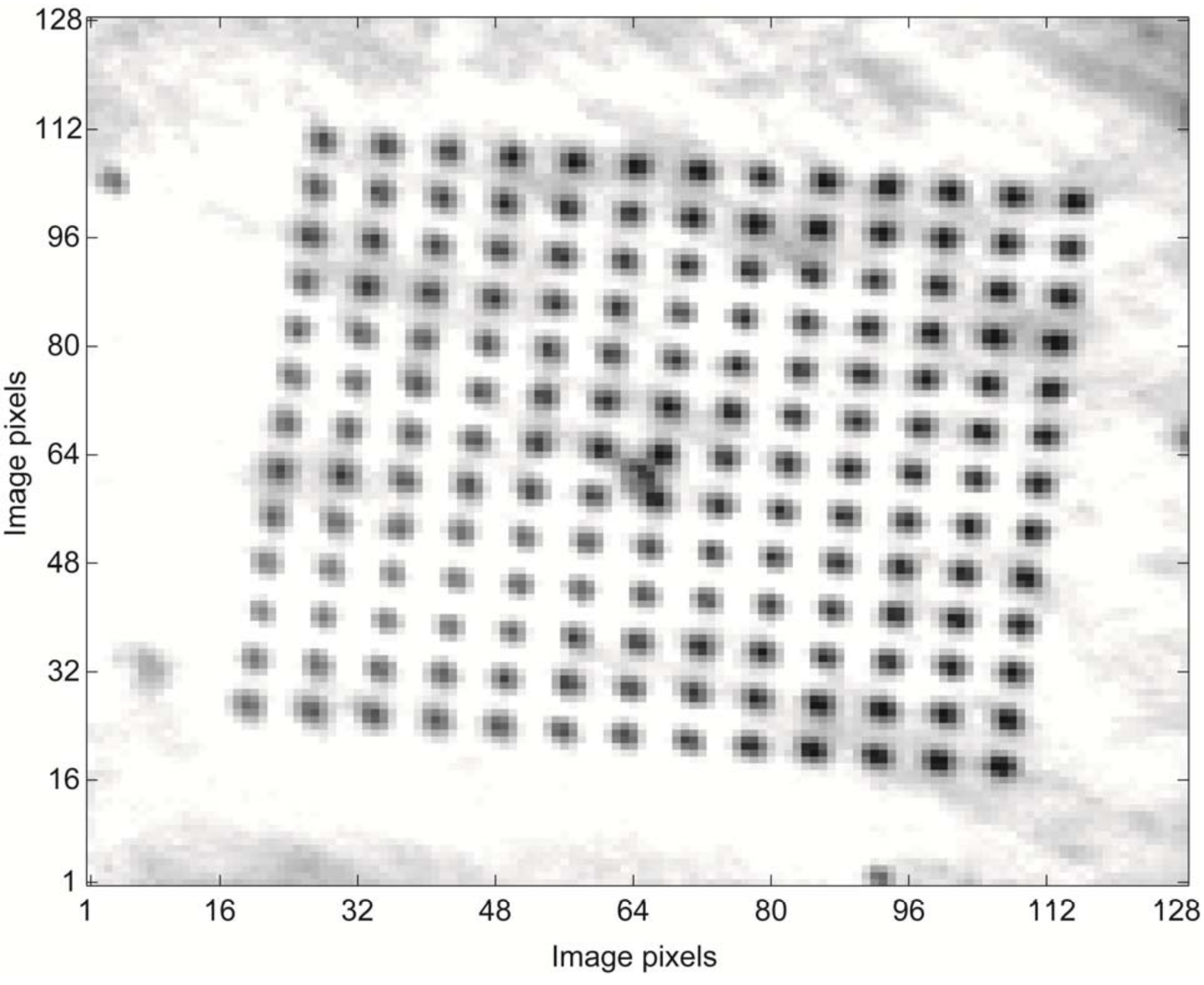

Typical period: 3µm

Detection noise level (electrical and mechanical)

Prong position without tuning-fork excitation

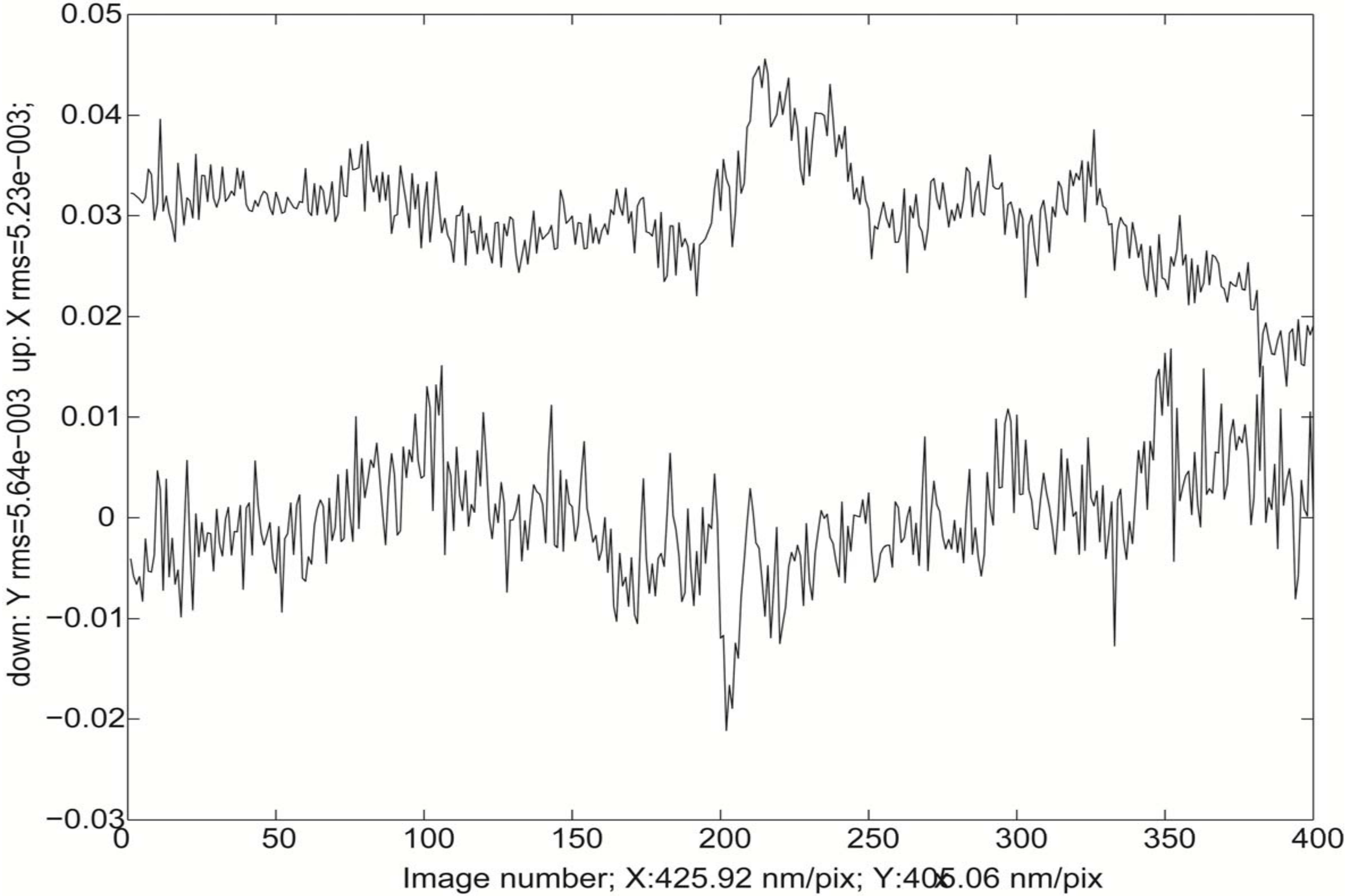

Vibration observation and measurement

2Hz frequency-shift between tuning-fork excitation and LED driving current => The 2Hz resulting frequency fits with standard video rate

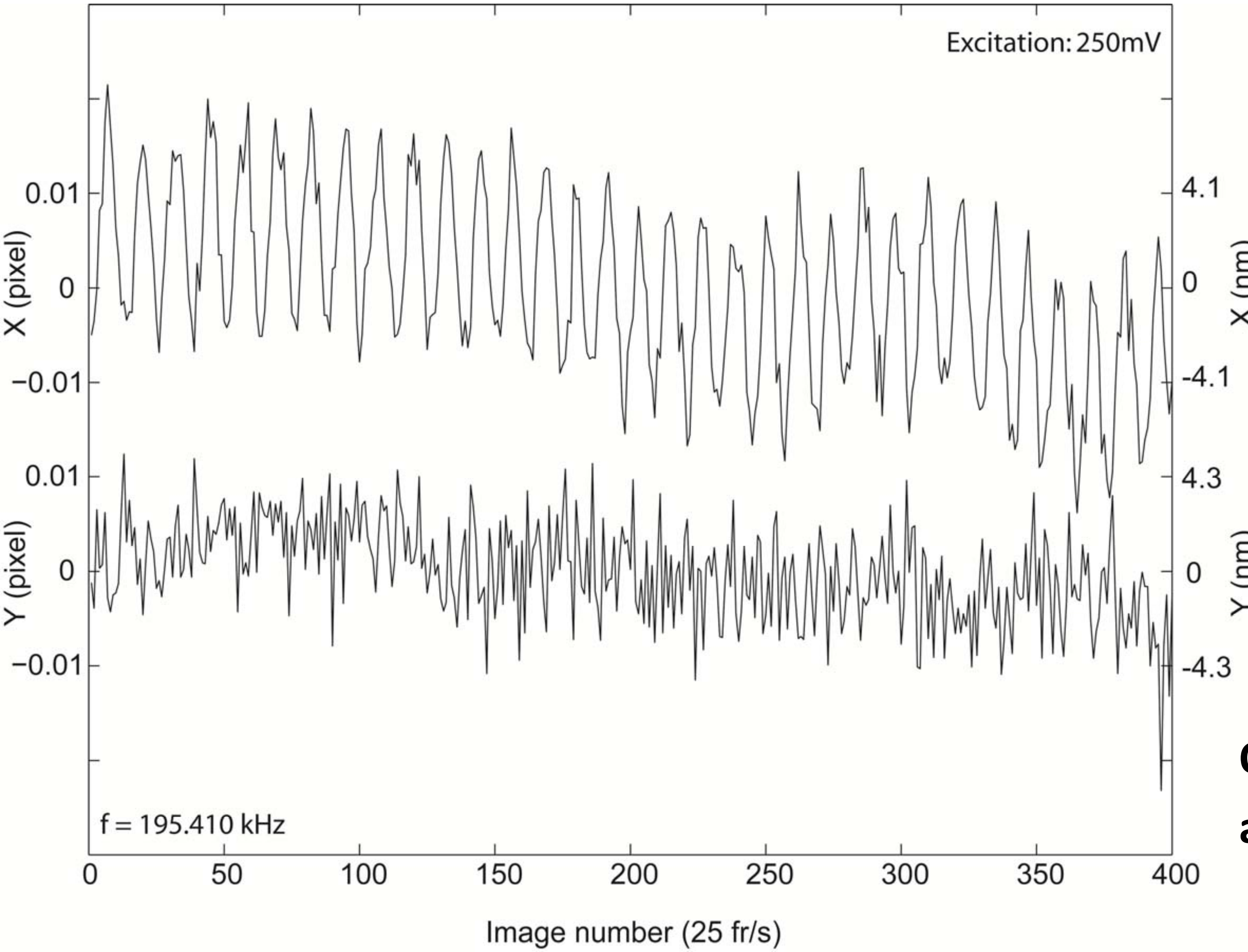

Overtone mode at 195.41 kHz

Measurement of the prong rotation amplitude

Observation of a torsion mode at 181.552 kHz

Variation of the pseudo-periodic pattern orientation

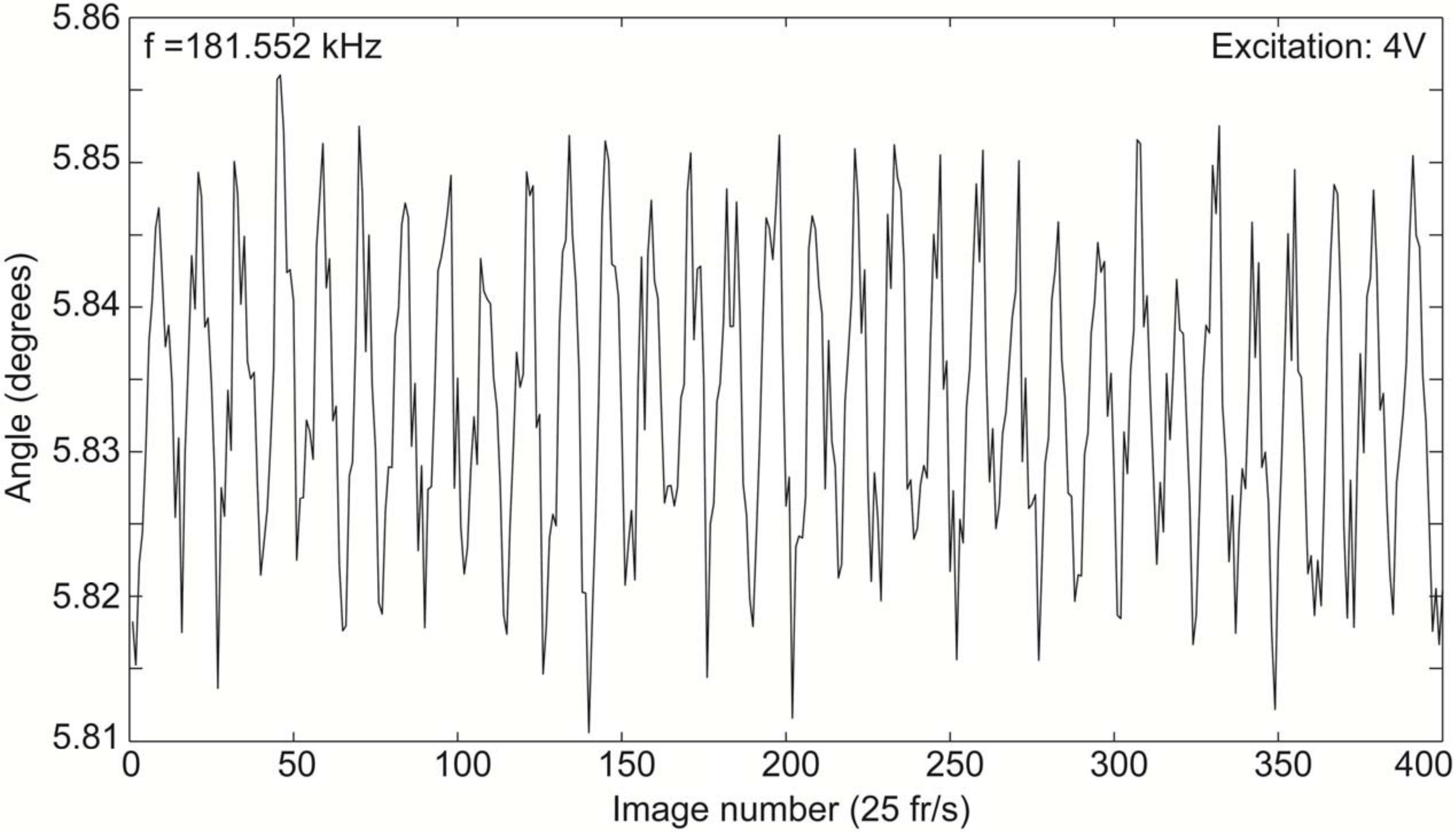

Calibration of the prong rotation amplitude

Observation of a torsion mode at 181.552 kHz

Rotation amplitude versus excitation voltage

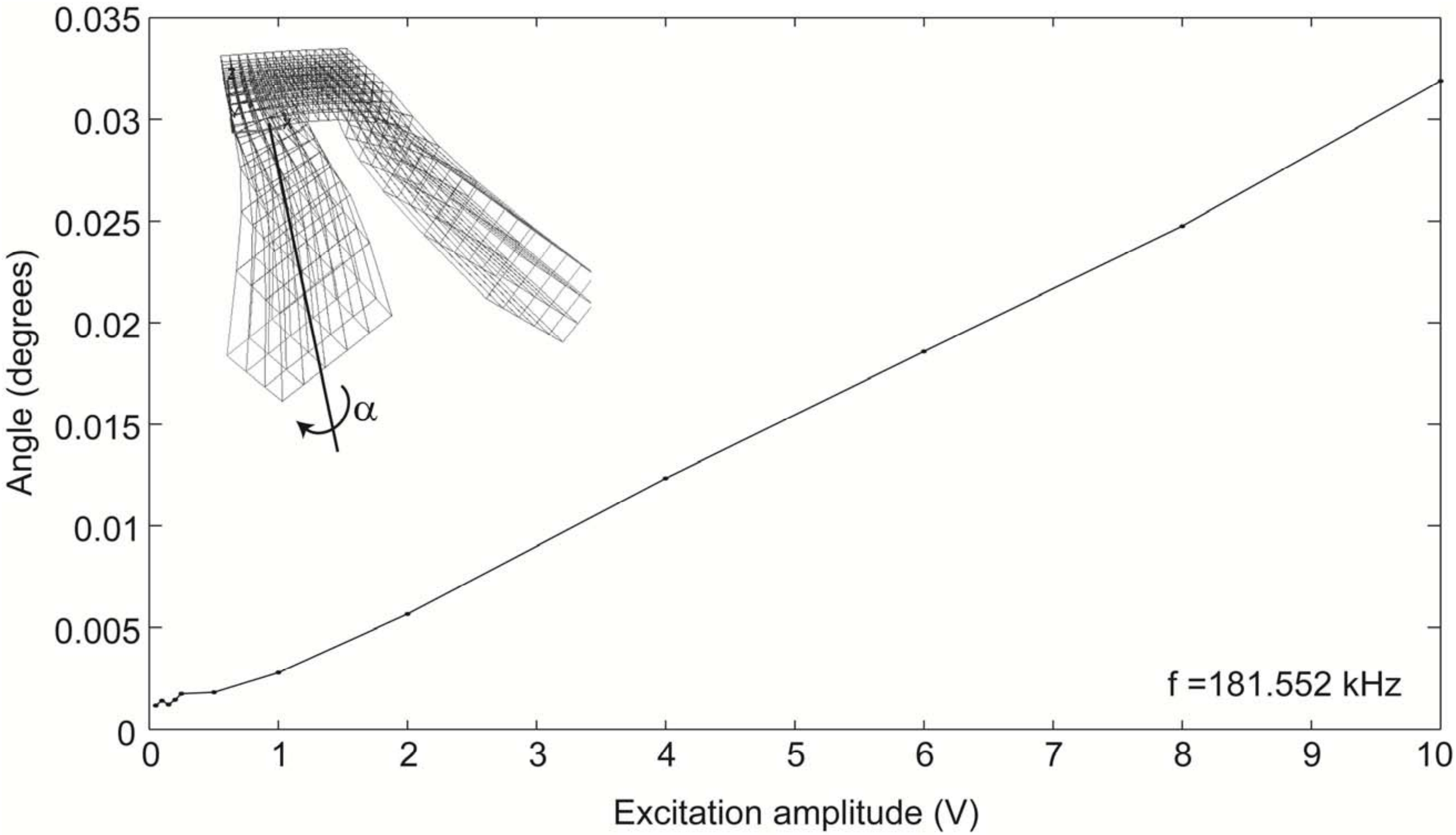

Tuning-Fork resonance characterization

Natural mode at 33 kHz

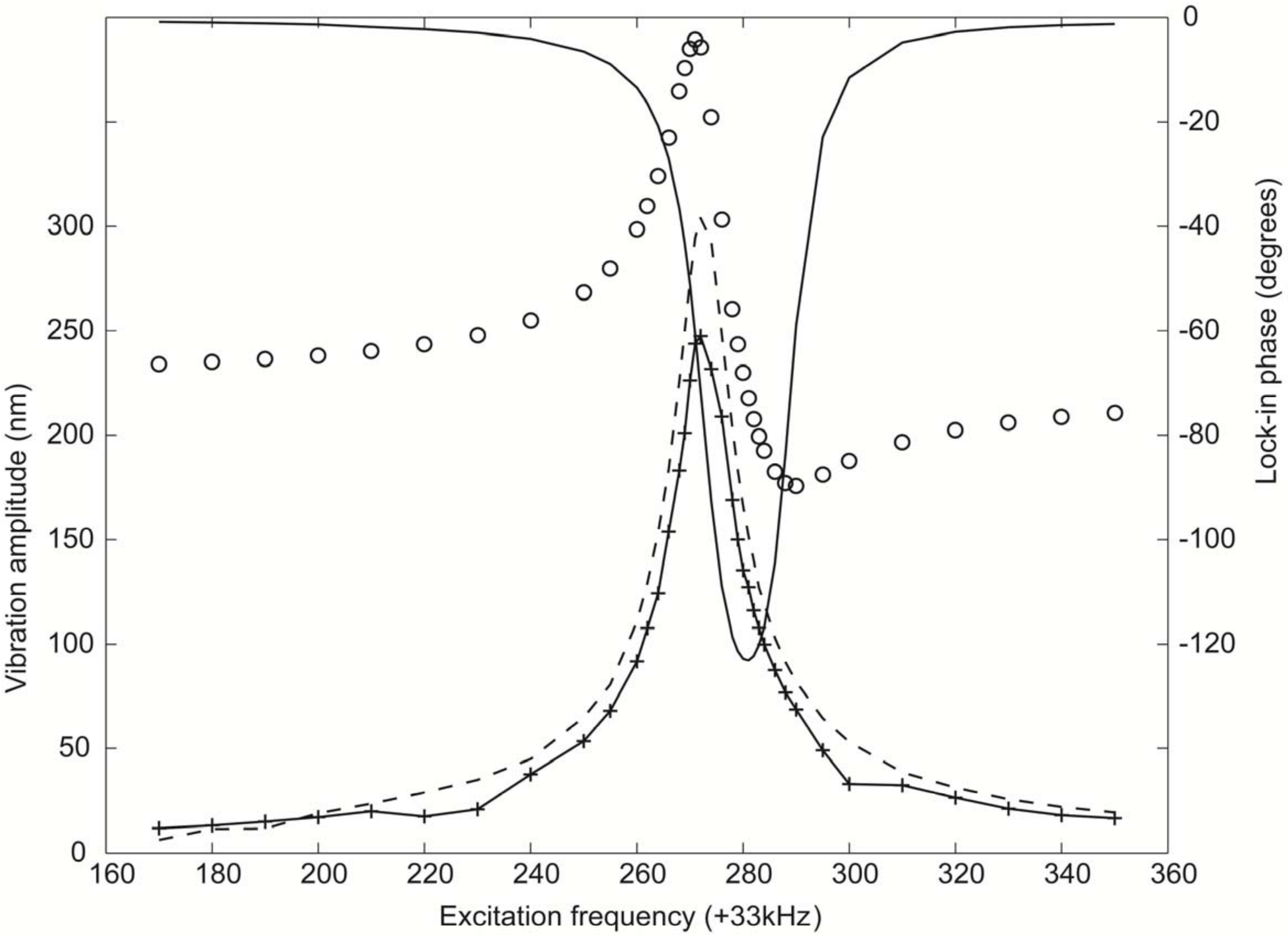

dotted line: Free prong vibration amplitude (nm)

solid plus crosses: Tip-loaded prong vibration amplitude (nm)

solid: Lock-in phase (degrees); circle: Lock-in amplitude (a.u.)

Excitation voltag amplitude: 500mV

Calibration of the vibration amplitude

Natural mode at 33 kHz

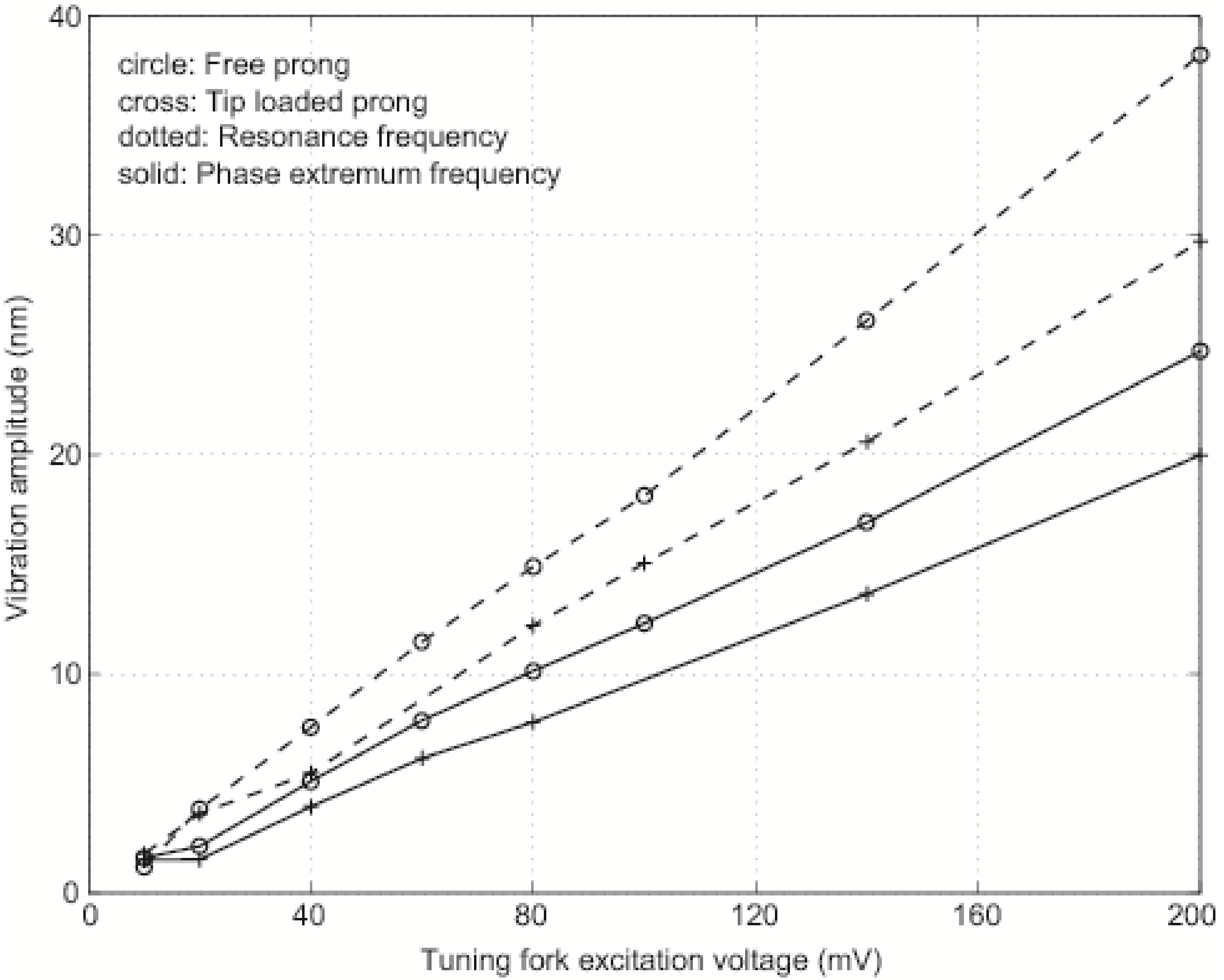

Vibration amplitude during tip-surface approach

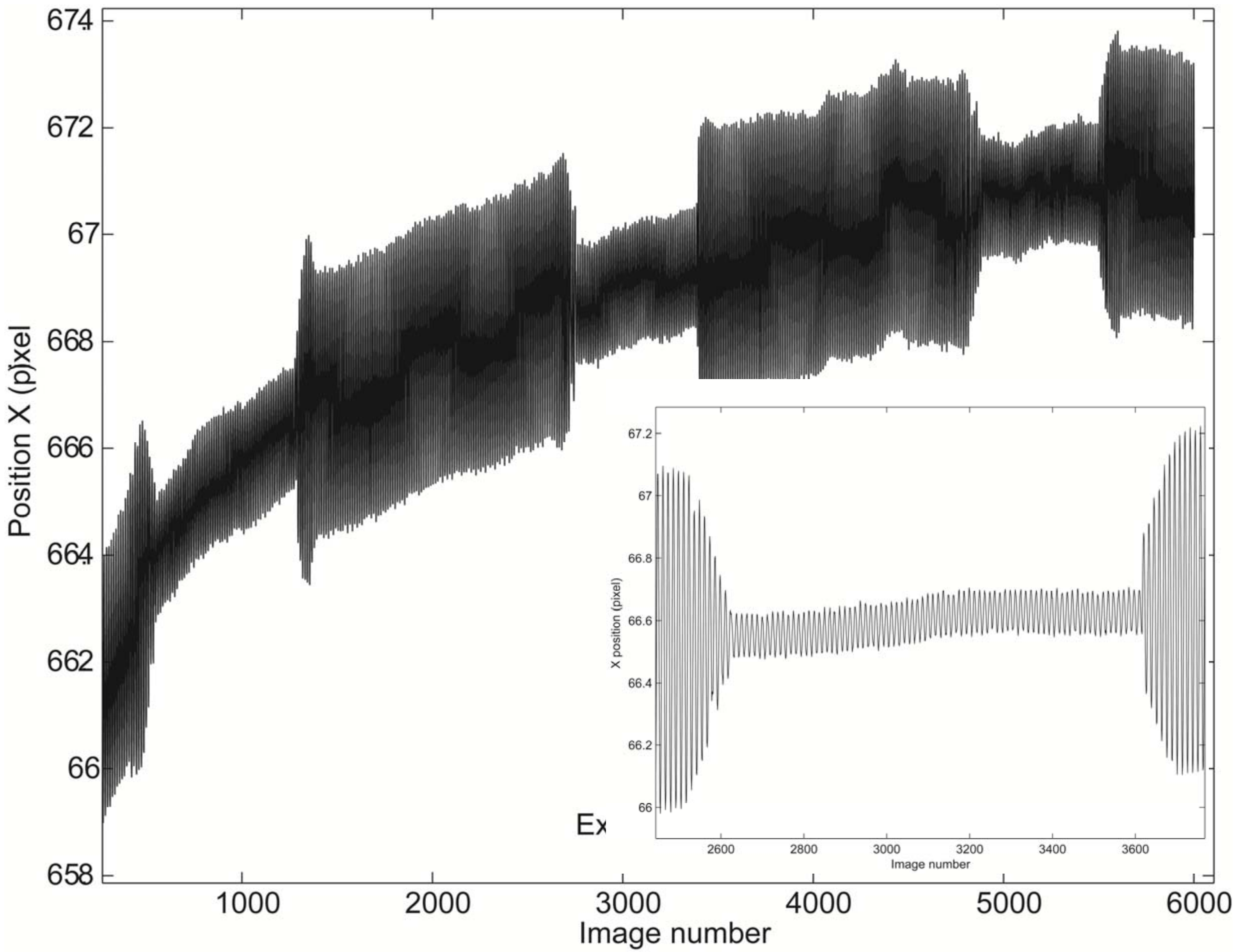

Tuning-fork vibration amplitude during surface scanning

detection of servo-control failures (amplitude damping means surface contact)

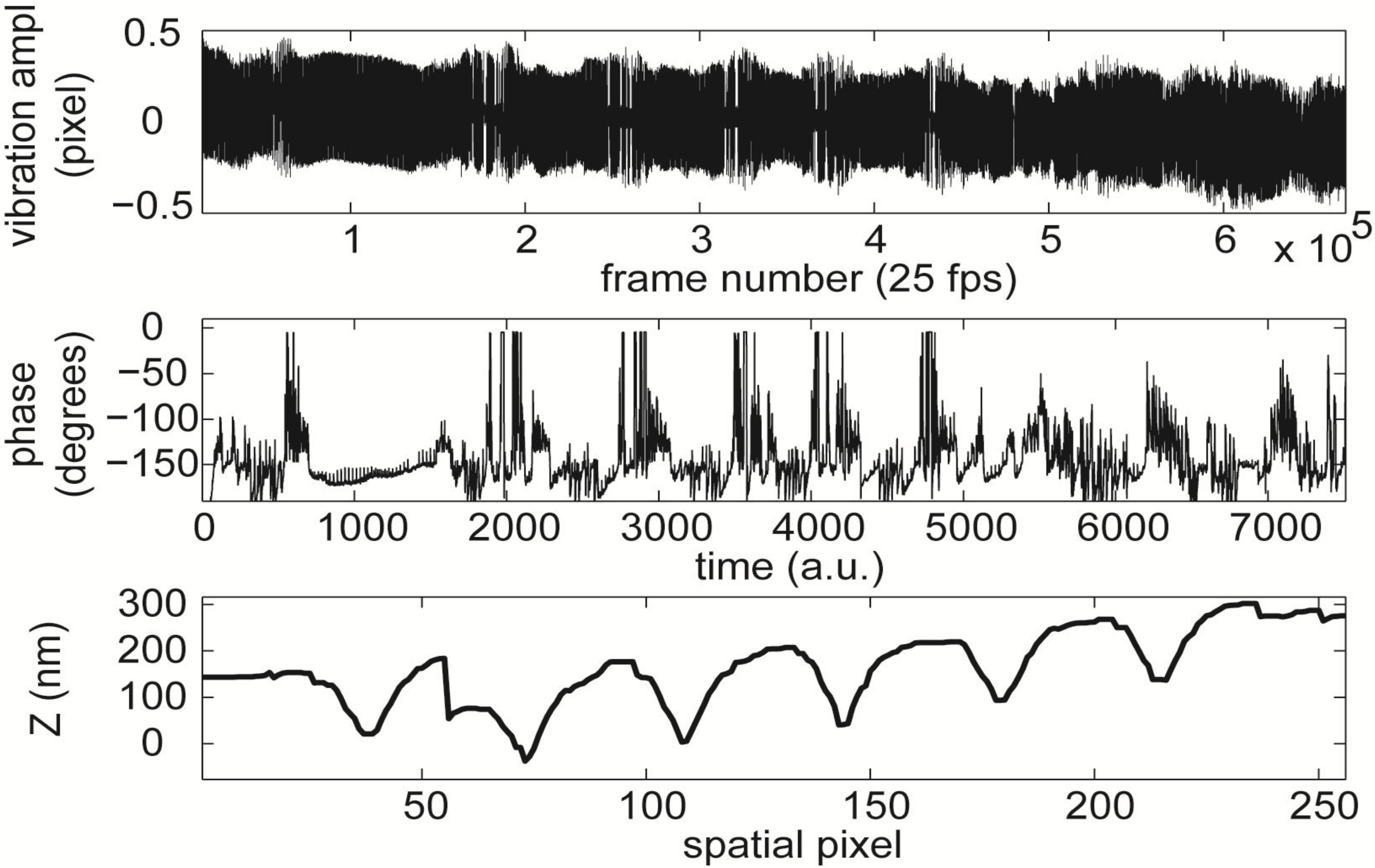

Position-Referenced-Microscopy for live-cell-culture monitoring

Patrick Sandoz, Rabah Zeggari, Luc Froehly, Jean-Luc Prétet, Christiane Mougin,
Position referencing in optical microscopy thanks to sample holders with out-of-focus encoded patterns,
Journal of Microscopy, 225, 293-303, 2007

July A. Galeano Zea, Patrick Sandoz, Émilie Gaiffe, Jean-Luc Prétet, Christiane Mougin,
Pseudo-periodic encryption of extended 2D surfaces for high accurate recovery of any random zone by vision,
International Journal of OptoMechatronics 4, 1, 65-82, 2010

July A. Galeano Z, Patrick Sandoz, Emilie Gaiffe, Sophie Launay, L. Robert, Maxime Jacquot, Fabienne Hirchaud, J.L. Prétet, Christiane Mougin,
Position-referenced microscopy for live cell culture monitoring,
Biomedical Optics Express 2, 5, 1307-1318, 2011
http://www.opticsinfobase.org/abstract.cfm?URI=boe-2-5-1307

Position-Referenced-Microscopy for live-cell-culture monitoring

Problematic

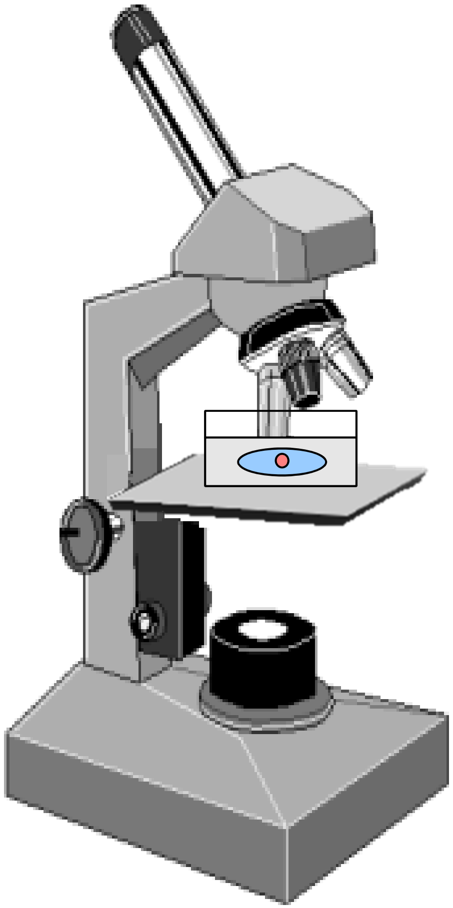

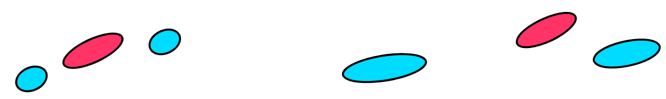

Image 1 **Image 2**

Biological Process ?

Fast → **Short period of Time**

Slow → **long period of Time**

Tools for long term cell-culture microscopy observation

Today: video microscopy

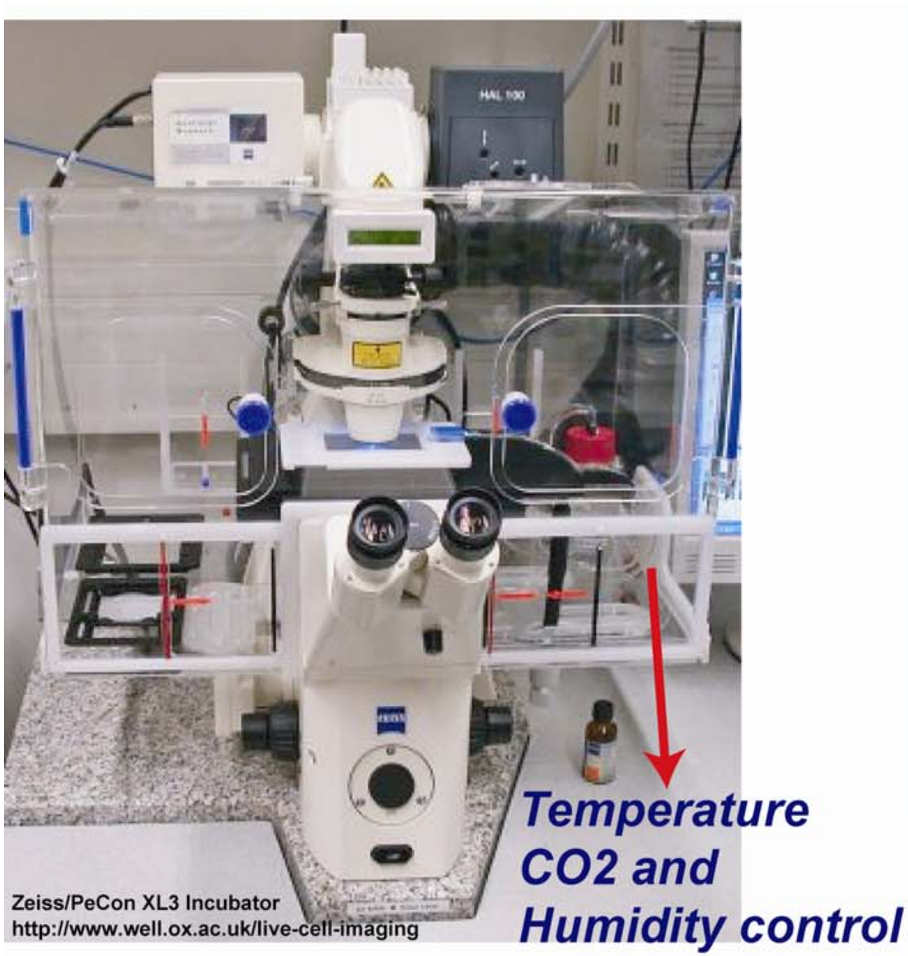

Proposal: culture dish transfers

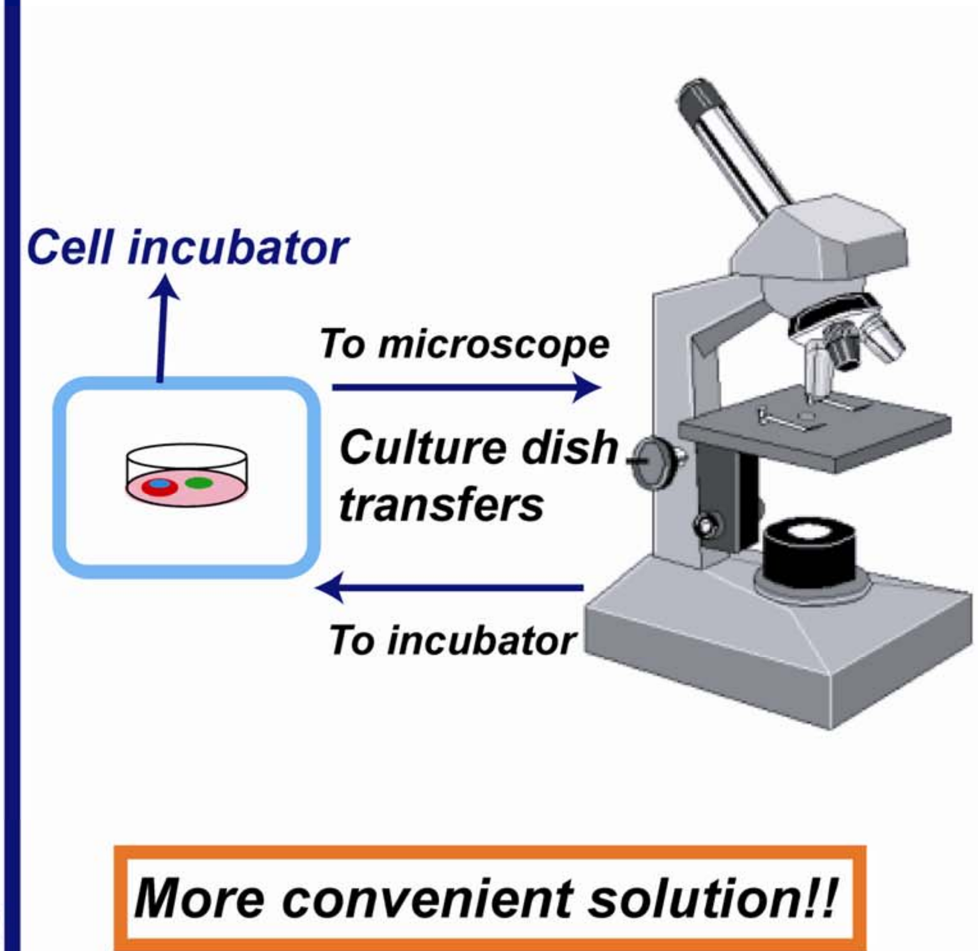

Monopolization of the equipment

Stage position limitations

Position Referenced Microscopy

(Subpixel accuracy in position recovery)

Principle of observation

Recording of two complementary images at different focus depths

The pattern image is representative of the cell culture location

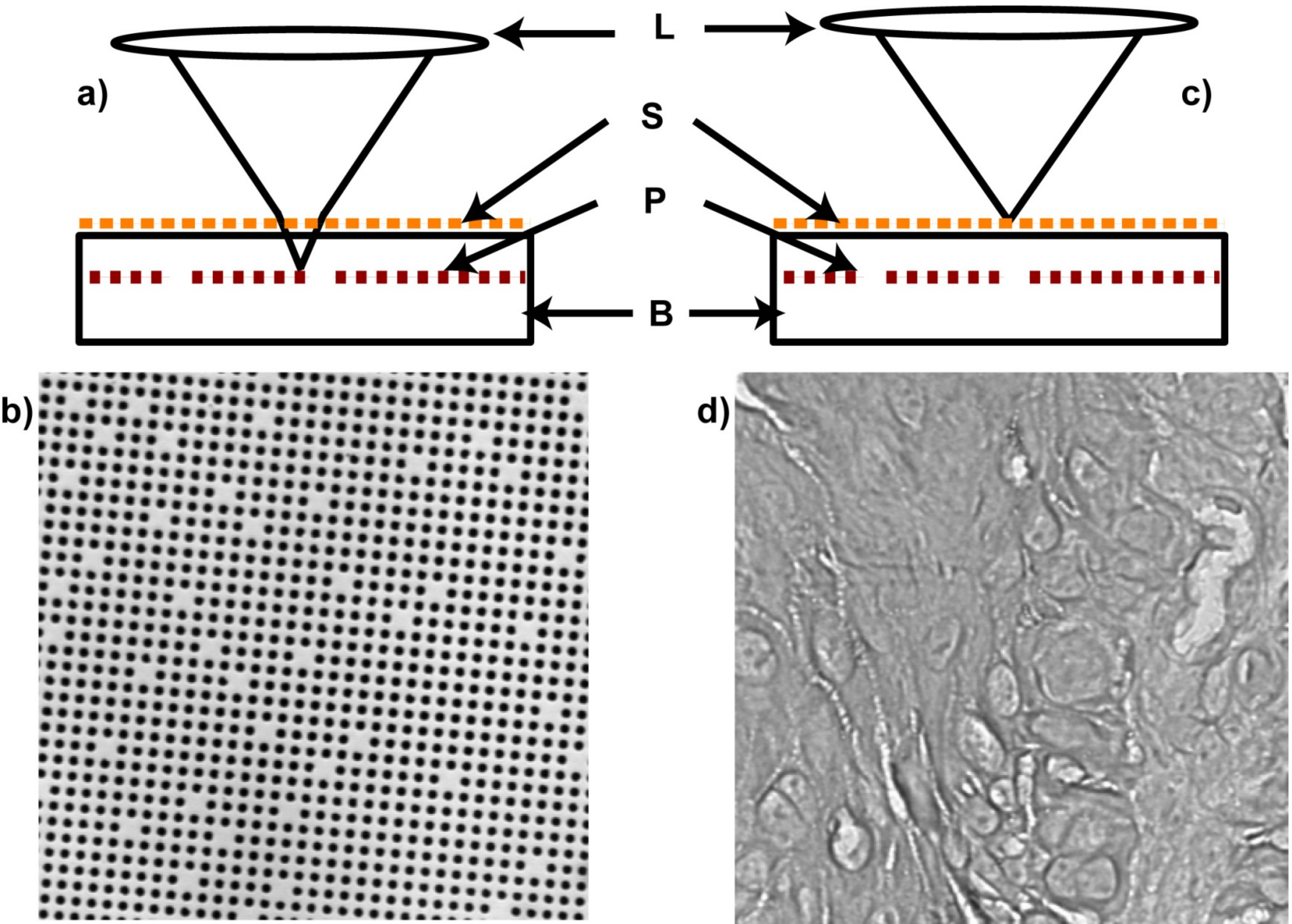

Technological realization of smart culture boxes

Photolithographic process

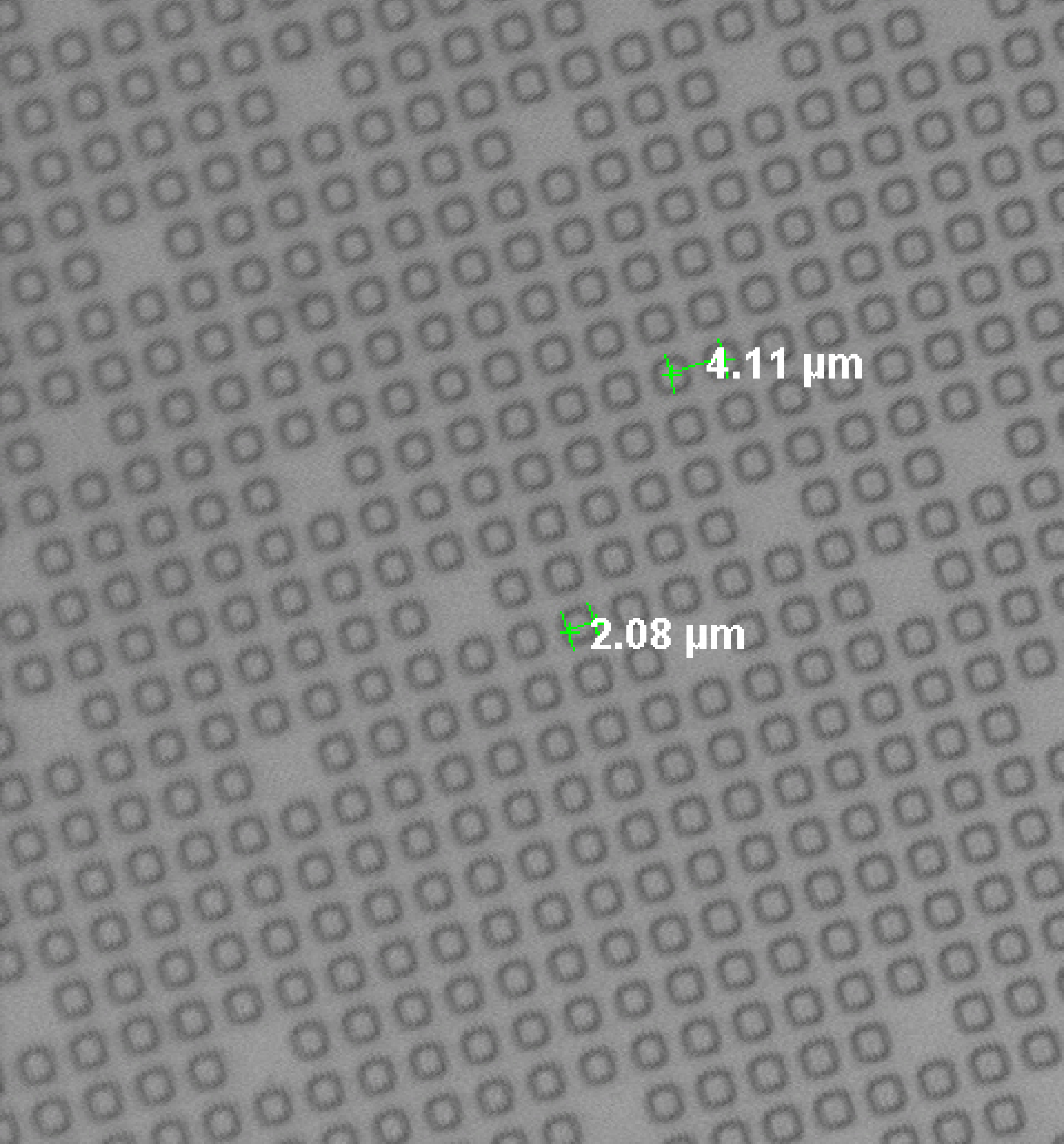

Instrumented culture dish

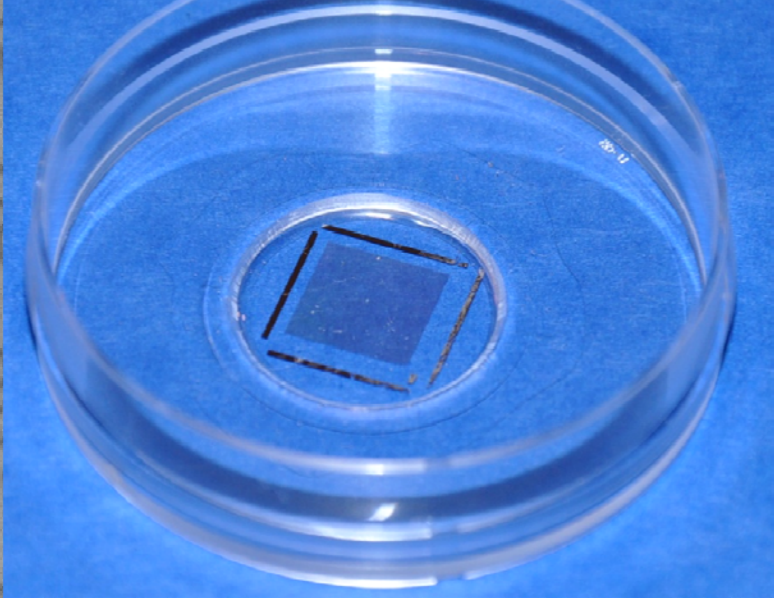

Software interface

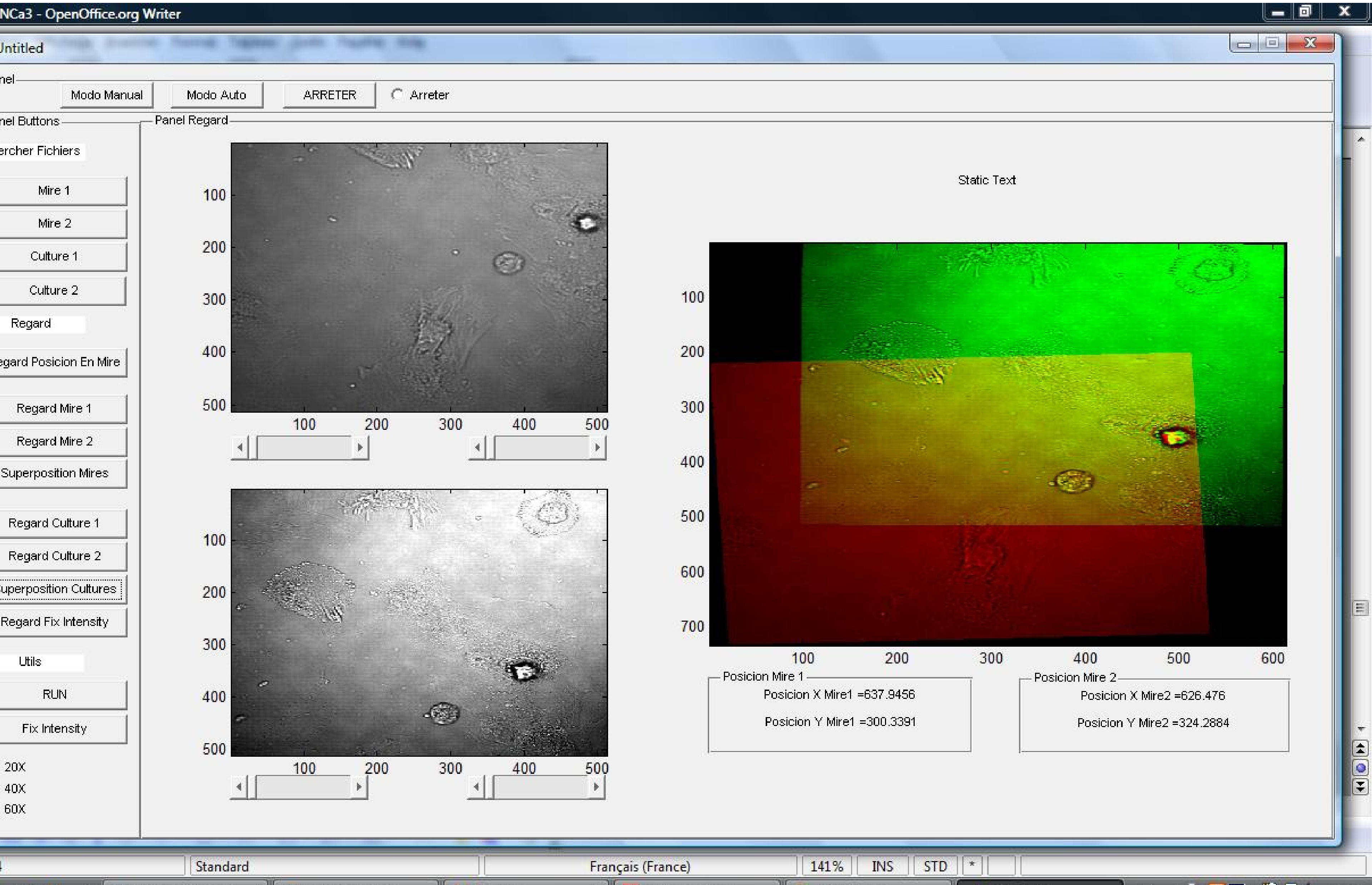

Iterative localization of the zones of interest

Registration of reference and current images in a common coordinate system

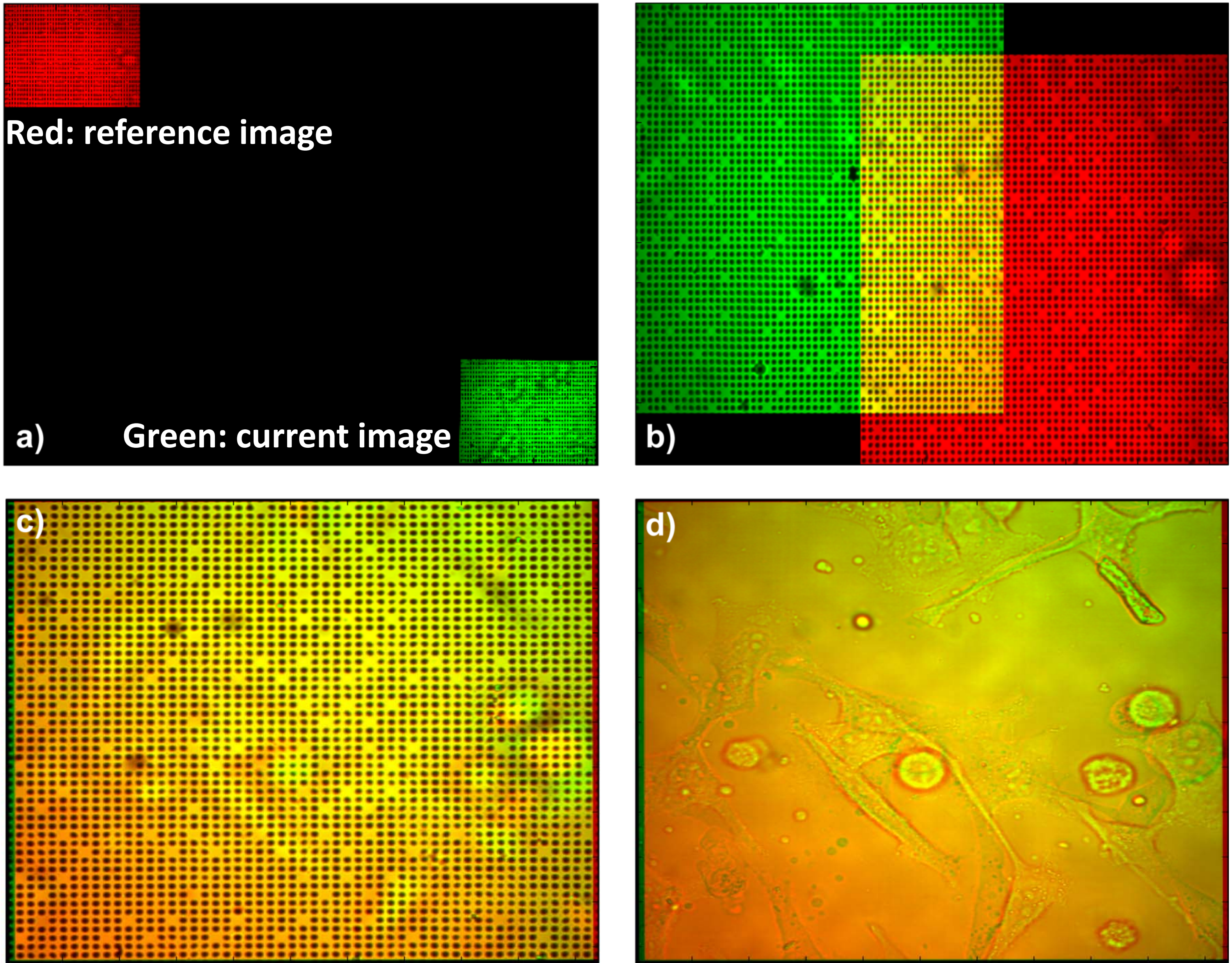

Video reconstruction of cell culture transformations

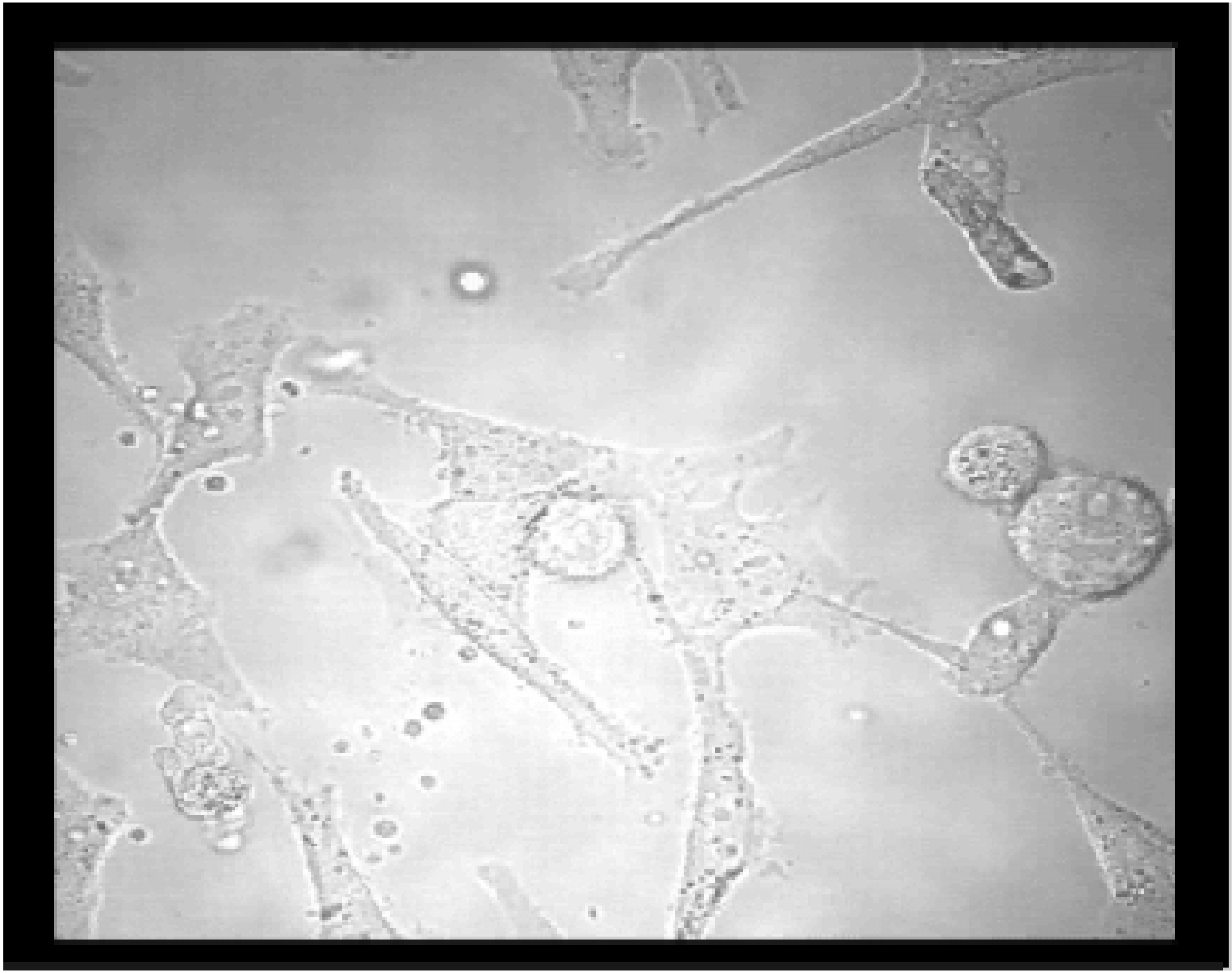

Human fibroblast cells observed in phase contrast mode (12h00)

Observation of the internalization of apoptotic bodies of cervical cancer cells by human fibroblast cells

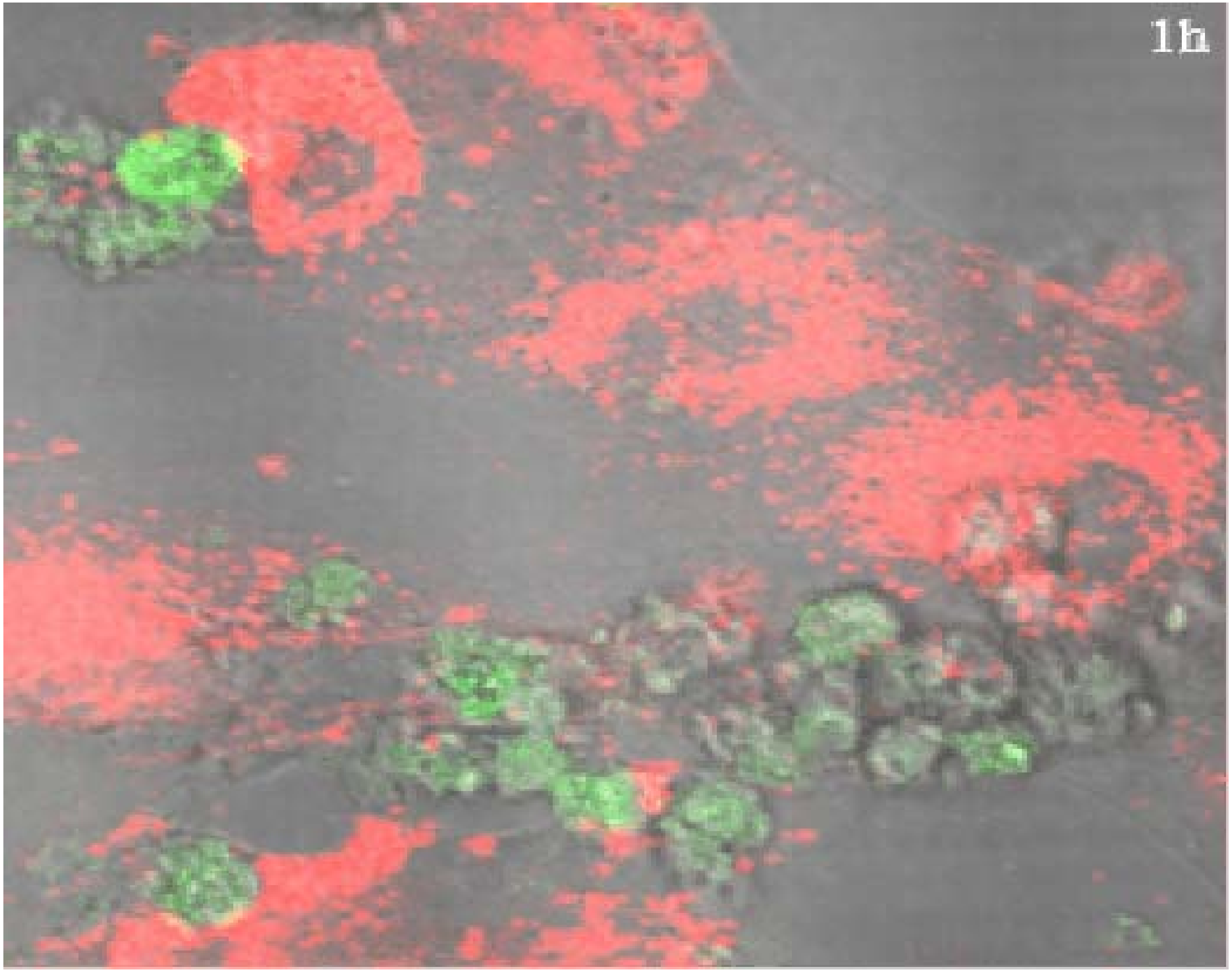

(confocal fluorescence mode)

Didactic experiment: characterization of a 440Hz tuning-fork

Patrick Sandoz, Jean-Michel Friedt, Émile Carry, Bertrand Trolard, Johnson Garzon Reyes,
Frequency domain characterization of the vibrations of a tuning fork by vision and digital image processing,
American Journal of Physics, 71, 1, p.20-26, 2009

Labtop controlled excitation and detection devices

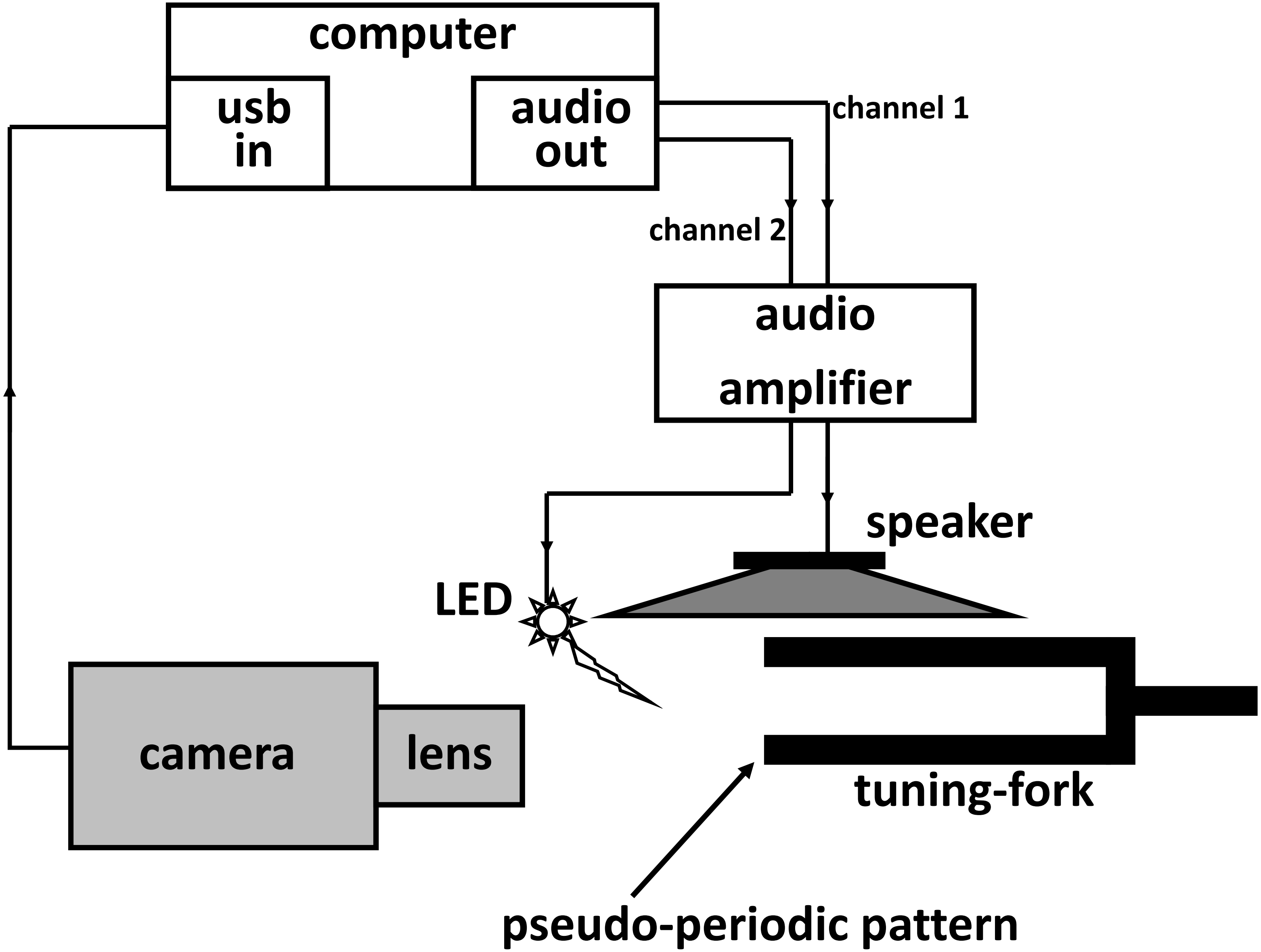

Low-cost experimental setup

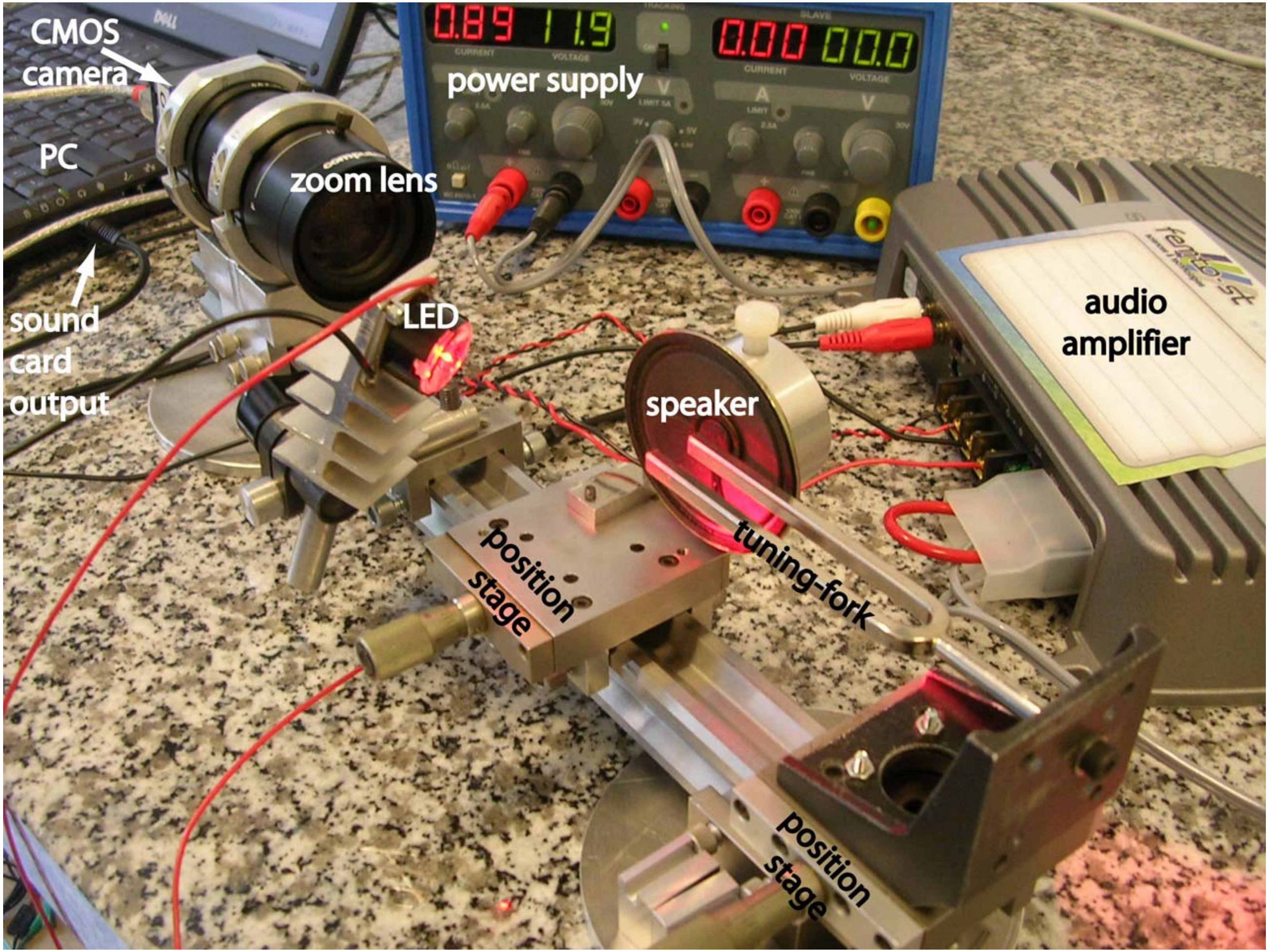

Pseudo-periodic pattern on one prong end face

Lines result from printing of a form with half-tone gray level (300dpi)

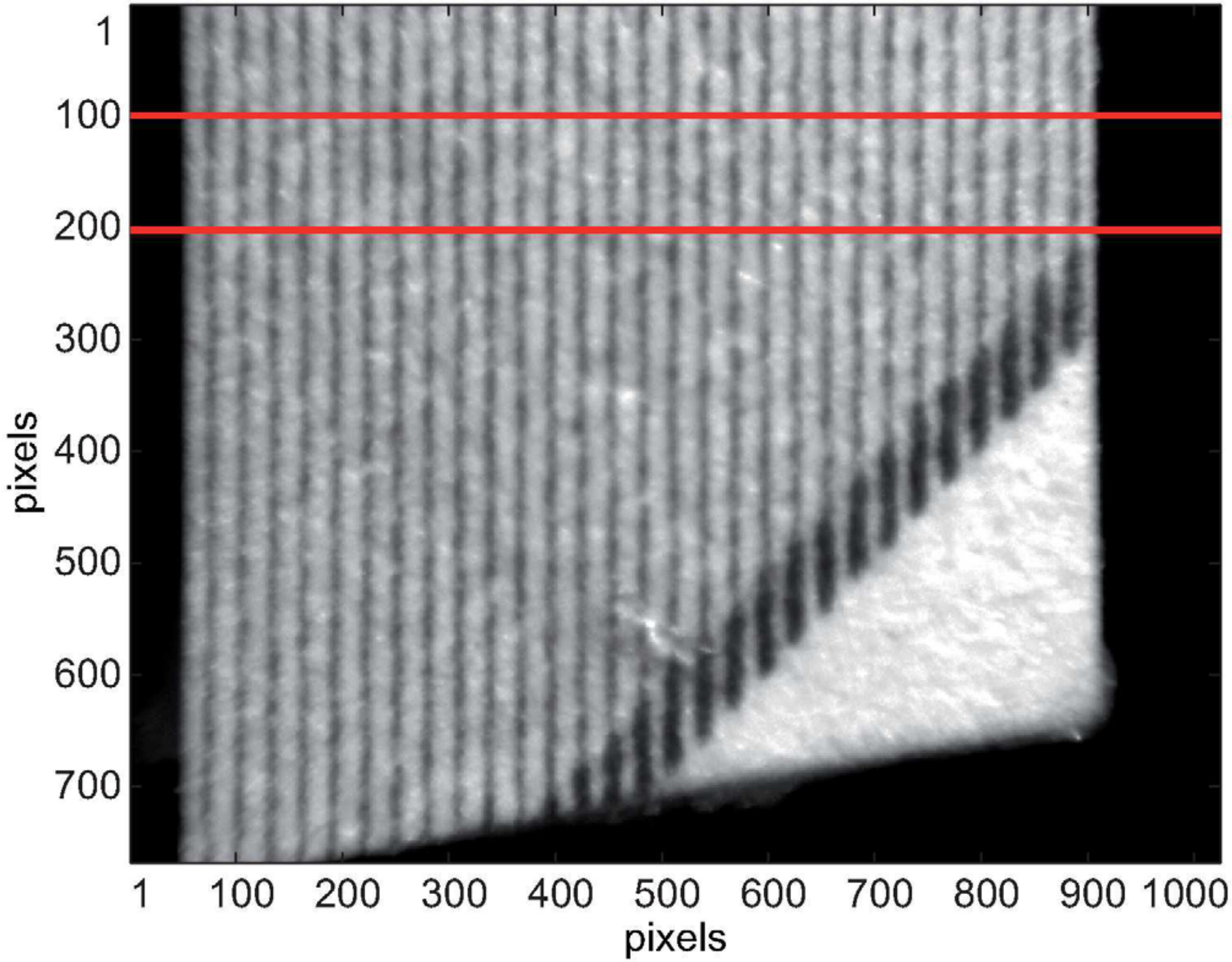

Lines form a reference pattern direclty stuck on the prong end face

Pseudo-periodic signal displacing along the pixel indexes

Signal to noise ratio enhancement by summing over lines 100 to 200

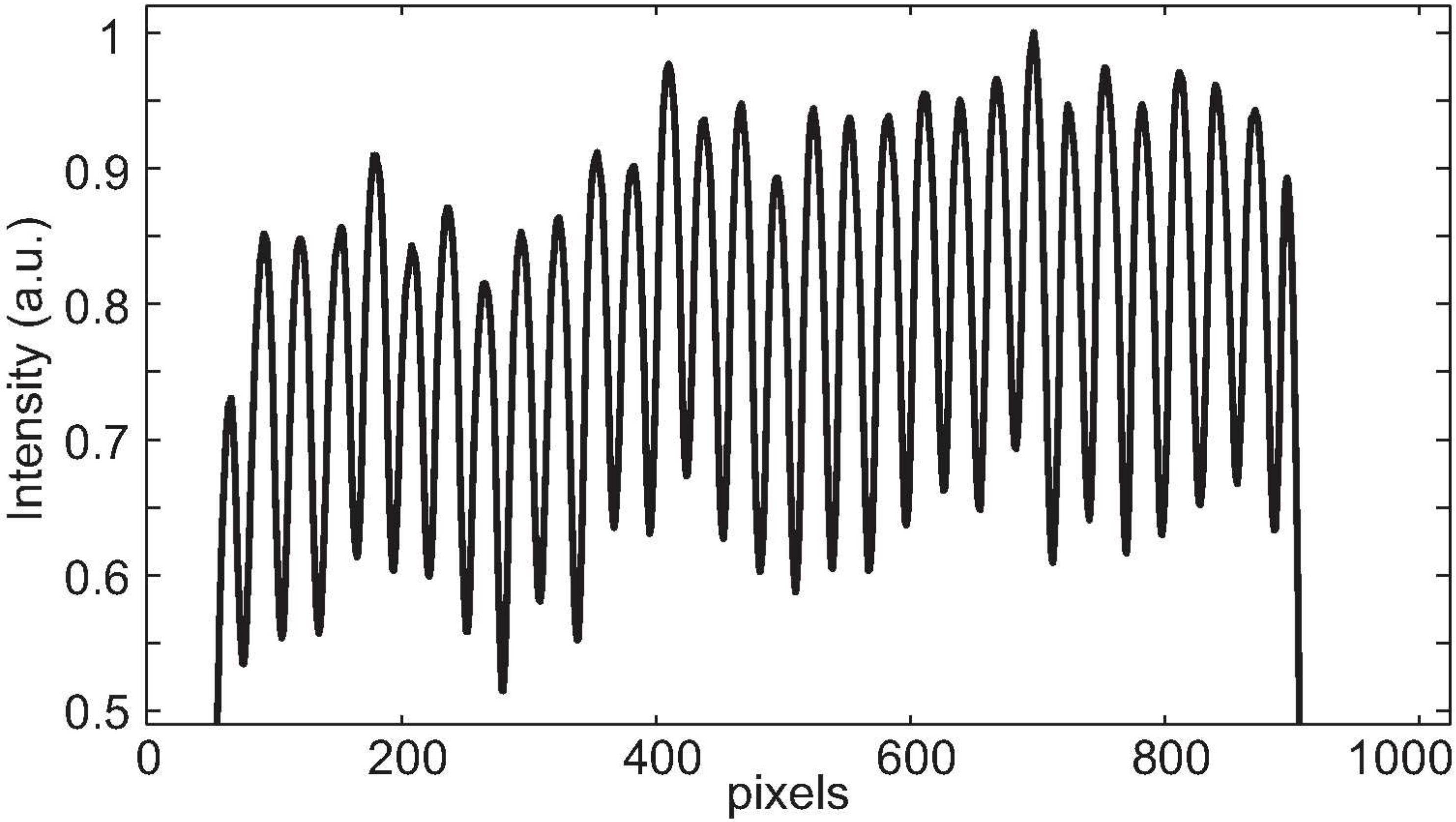

Signal processing has to extract the signal phase with respect to the image pixel frame

Gaussian-shaped analysis function in the complex plane

Function designed at the signal frequency

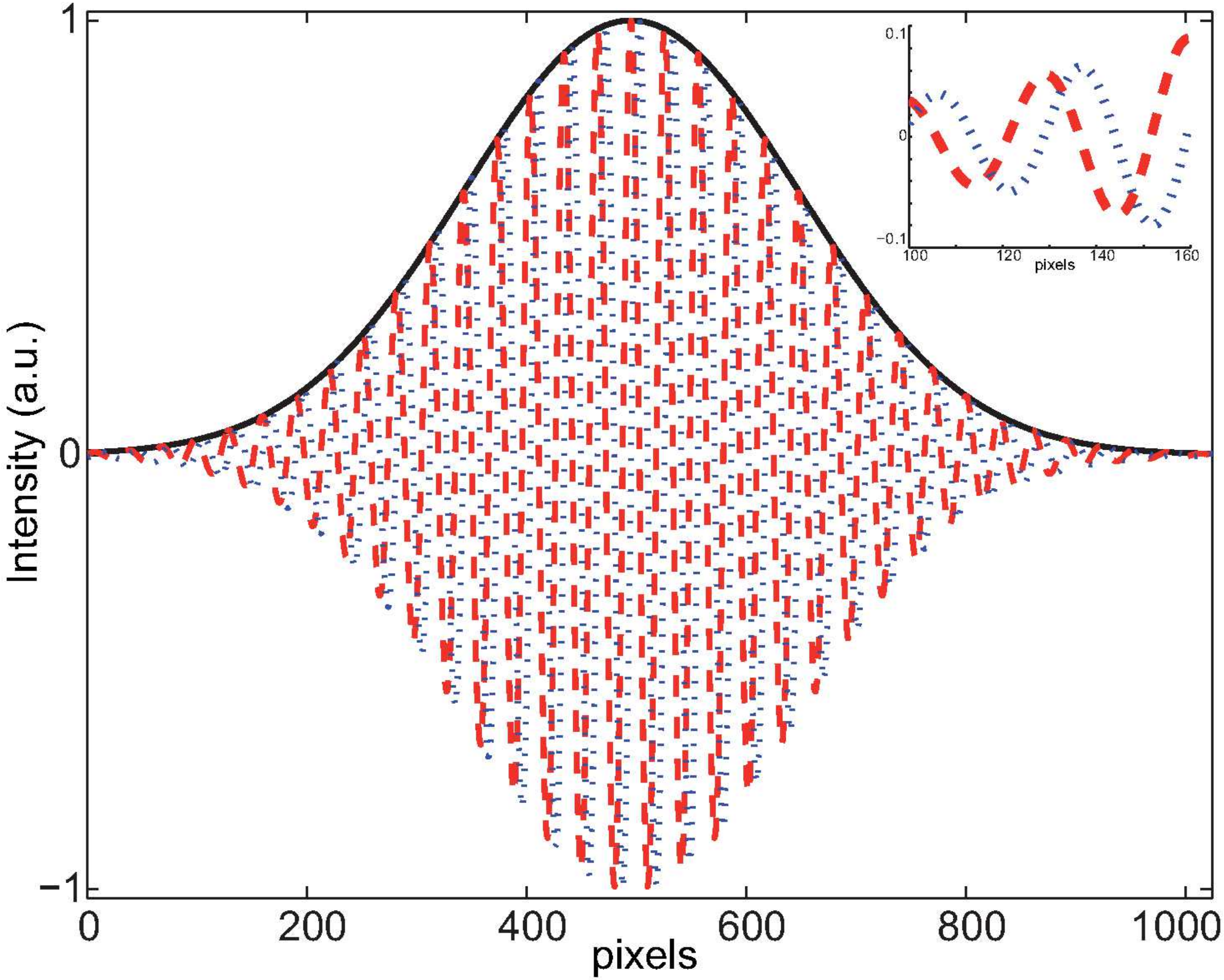

Red: real part

Blue: imaginary part

Observation of the tuning-fork vibration amplitude

The phase excursion describes the prong displacement (2π <=> 1 period)

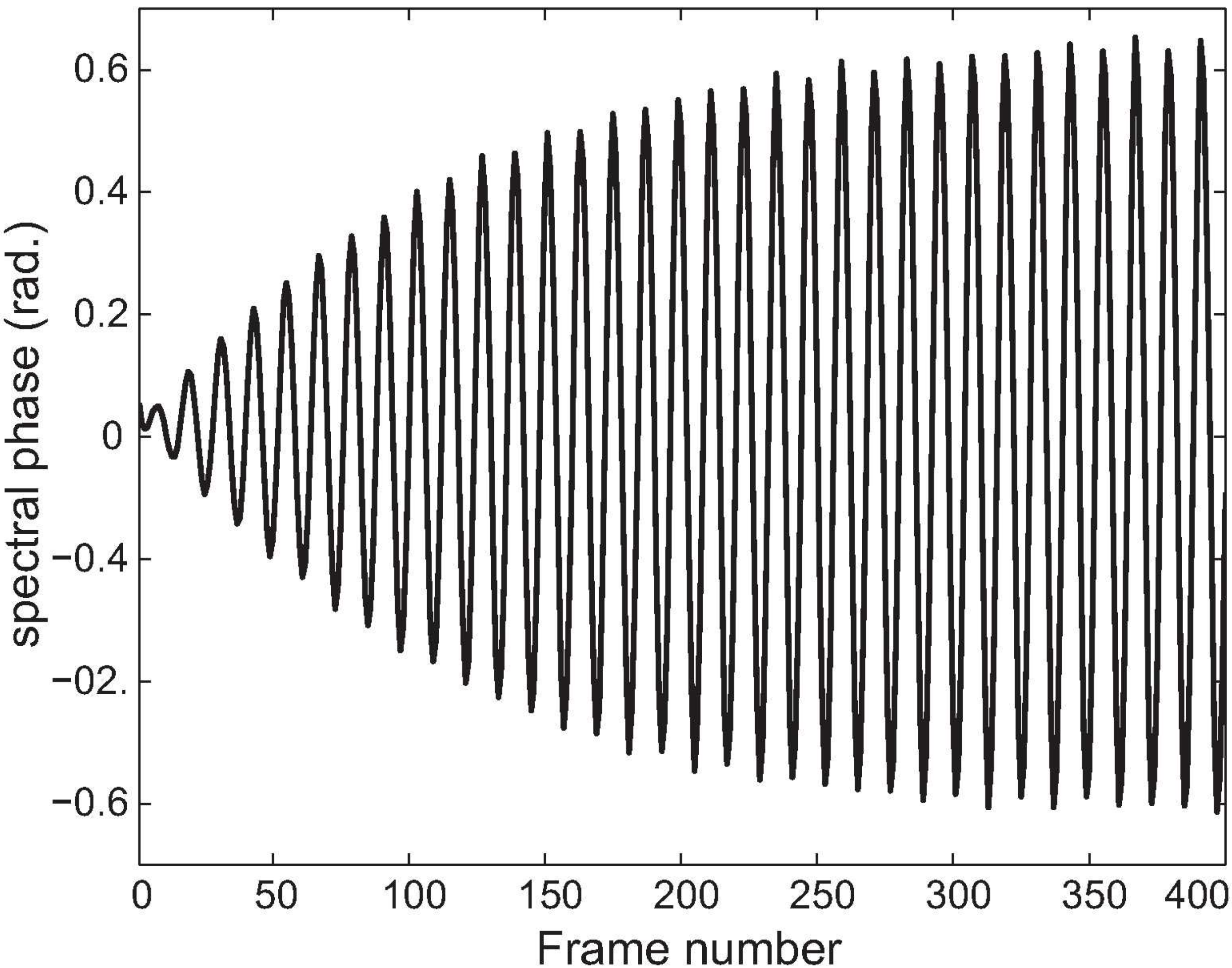

Excitation at resonance frequency.

1.25 Hz frequency shift between excitation and strobe illumination.

Observation of the tuning-fork vibration amplitude

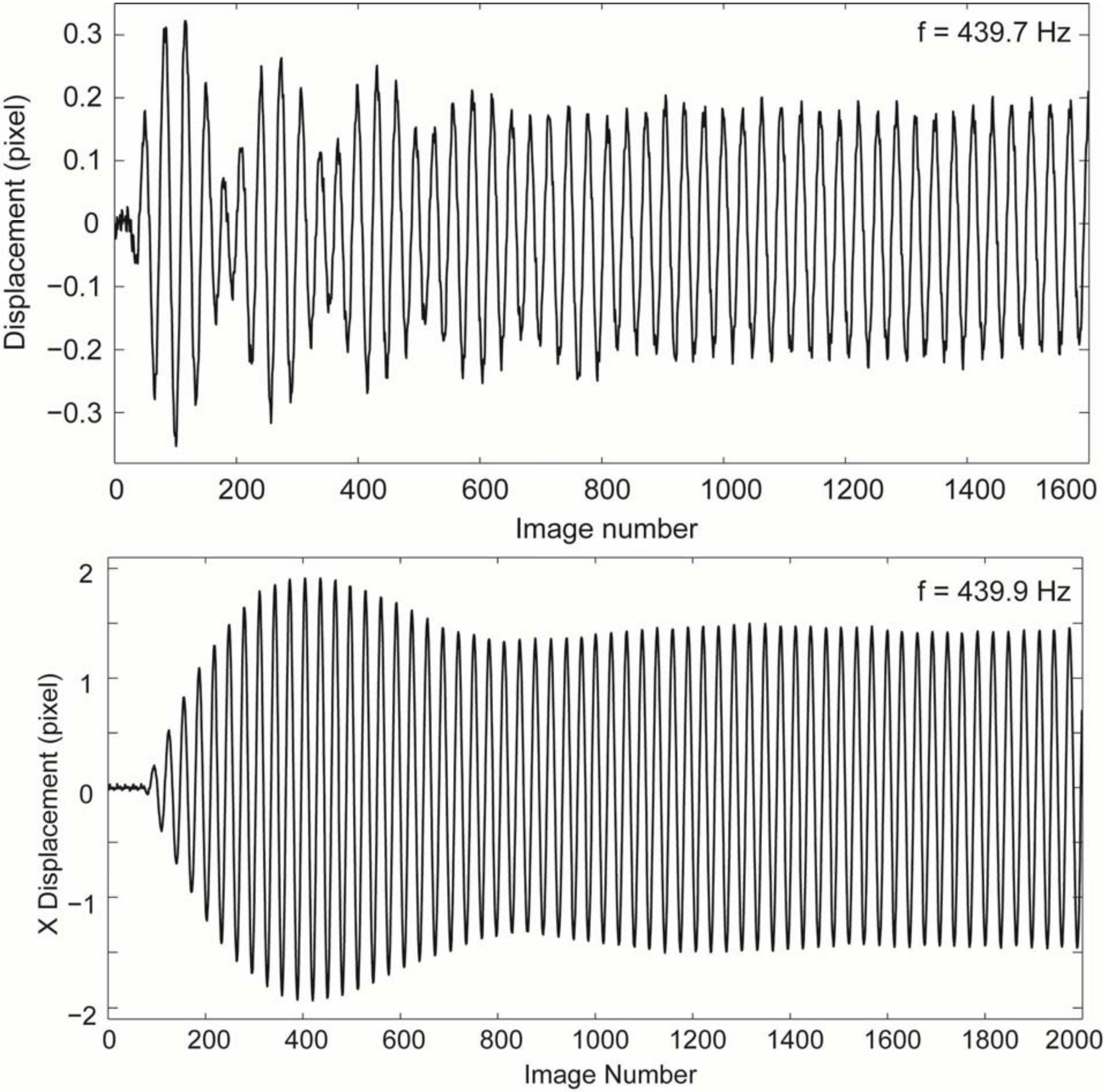

Excitation at different frequencies.

2 Hz frequency shift between excitation and strobe illumination.

The beat frequency corresponds to the frequency mismatch

Characterization of the tuning-fork resonance curve

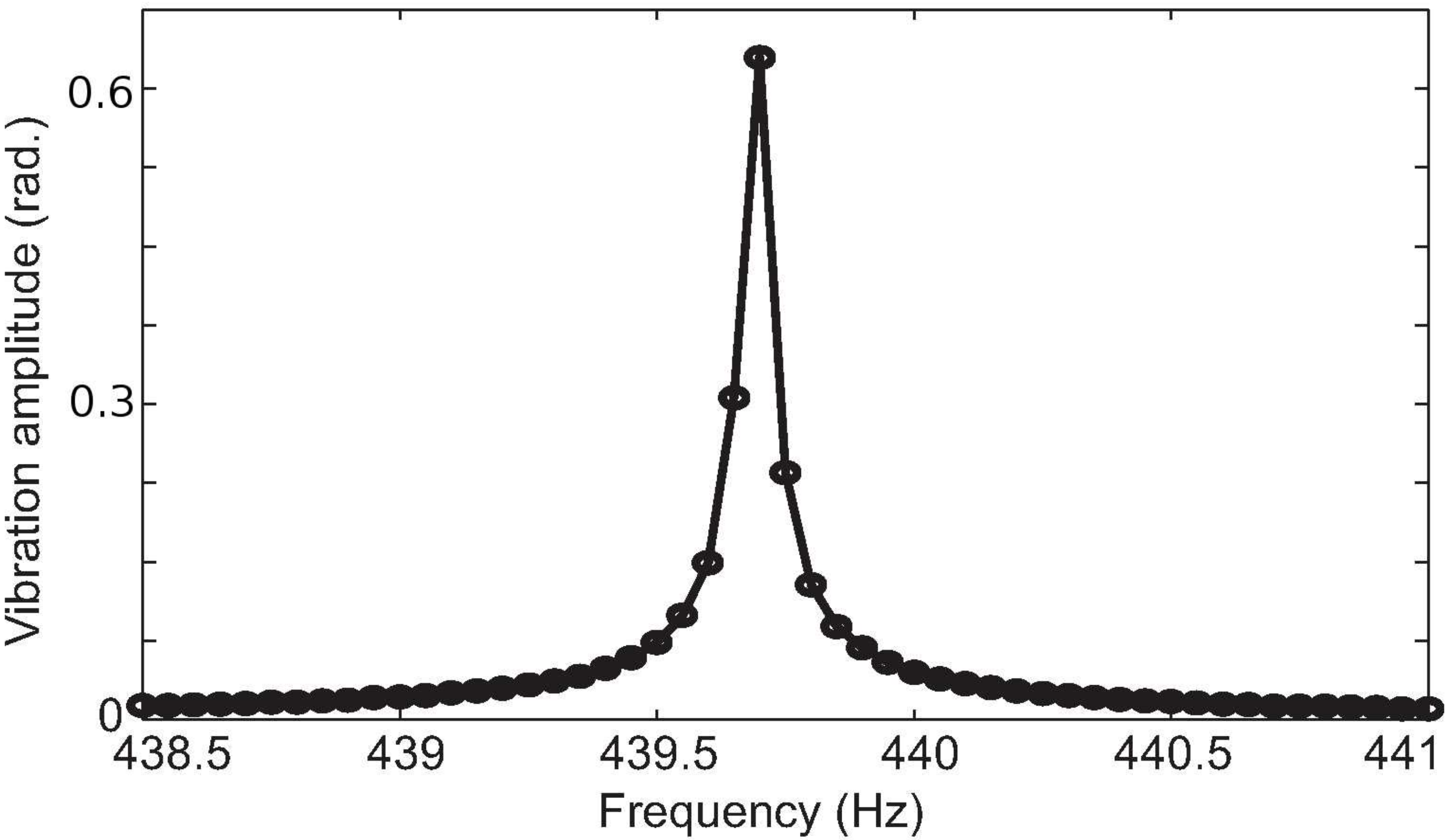

Resonance at 439.9 Hz

Recording time of only a few minutes with an automatic procedure

Thermal drift of the resonance frequency

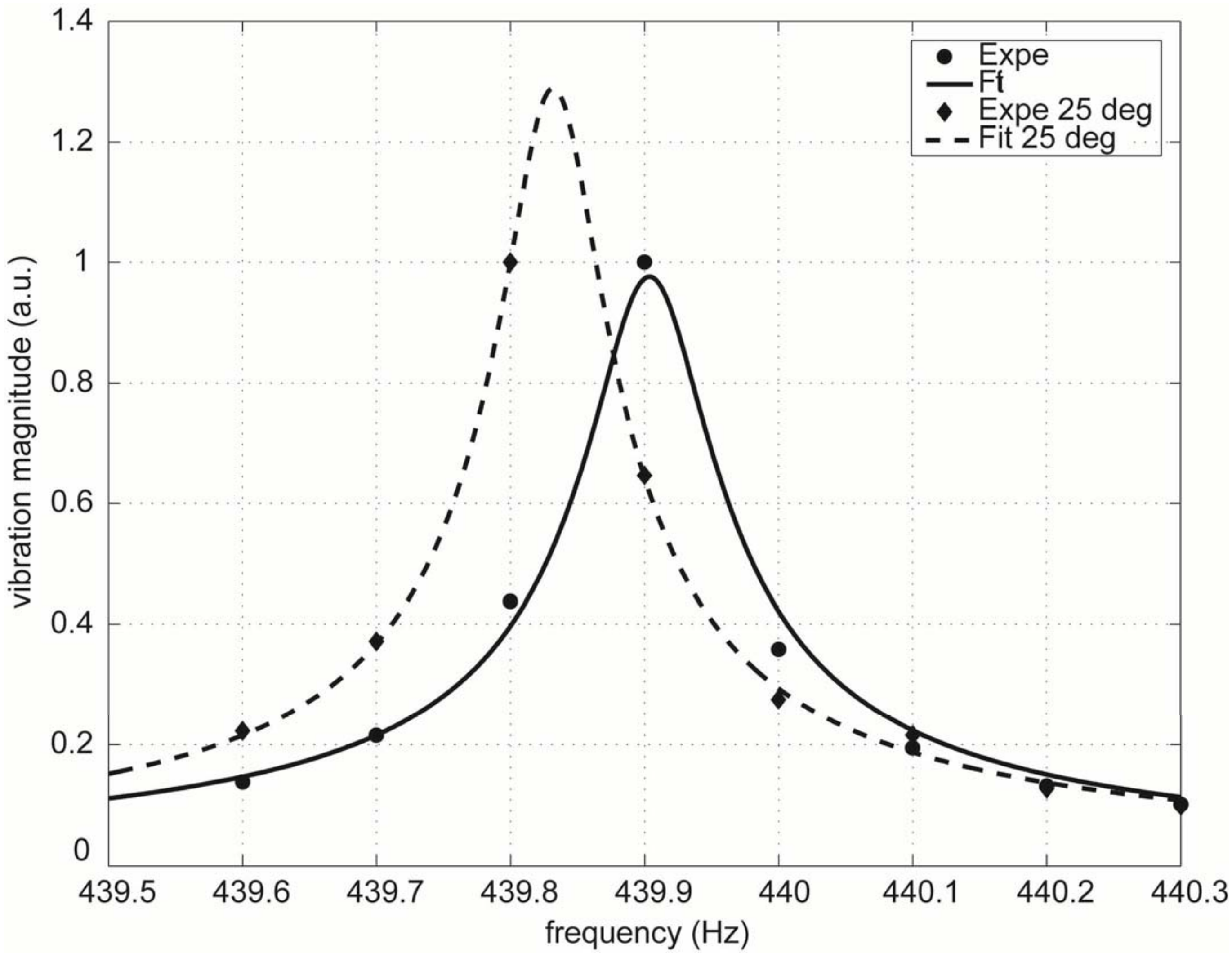

Resonance curves at different room temperatures (21° - 25°)

Frequency resonance shift of about 0.02 Hz per degree

5 Three dimensional measurement capabilities

Two approaches : - Interferometry

- Stereovision

Patrick Sandoz,
Nanometric Position and Displacement Measurement versus the Six Degrees of Freedom by Means of a patterned Surface Element,
Applied Optics, 44, (2005), no. 1, 1449–1453

Néstor A. Arias H., Patrick Sandoz, Jaime E. Meneses, Miguel A. Suarez, Tijani Gharbi,
3D Localization of a Labeled Target by means of a Stereo Vision Configuration with Subvoxel Resolution,
Optics Express 18, 23, 24152-24162 (2010).

Six degrees of freedom measurement with interferometry

Phase-shifting Interferometry (PSI)

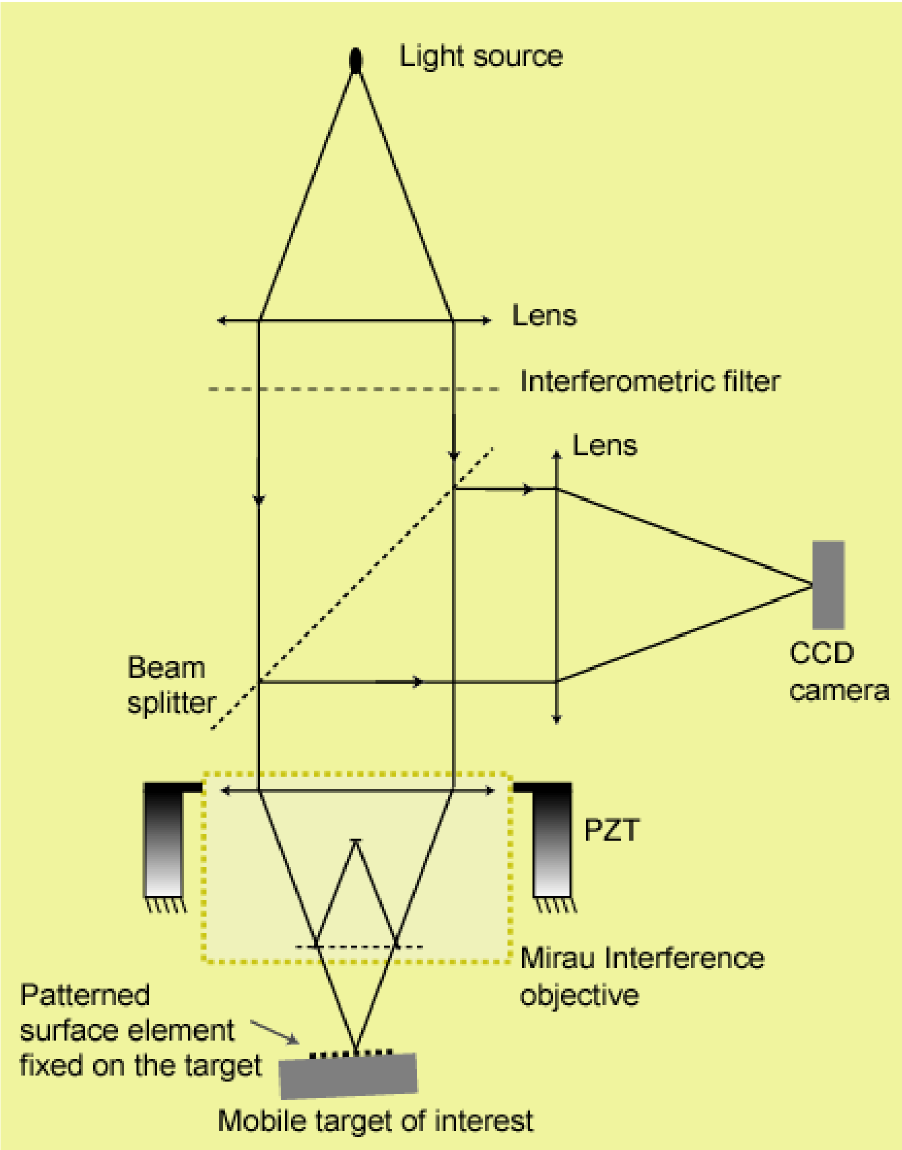

Micro-patterned surface sample

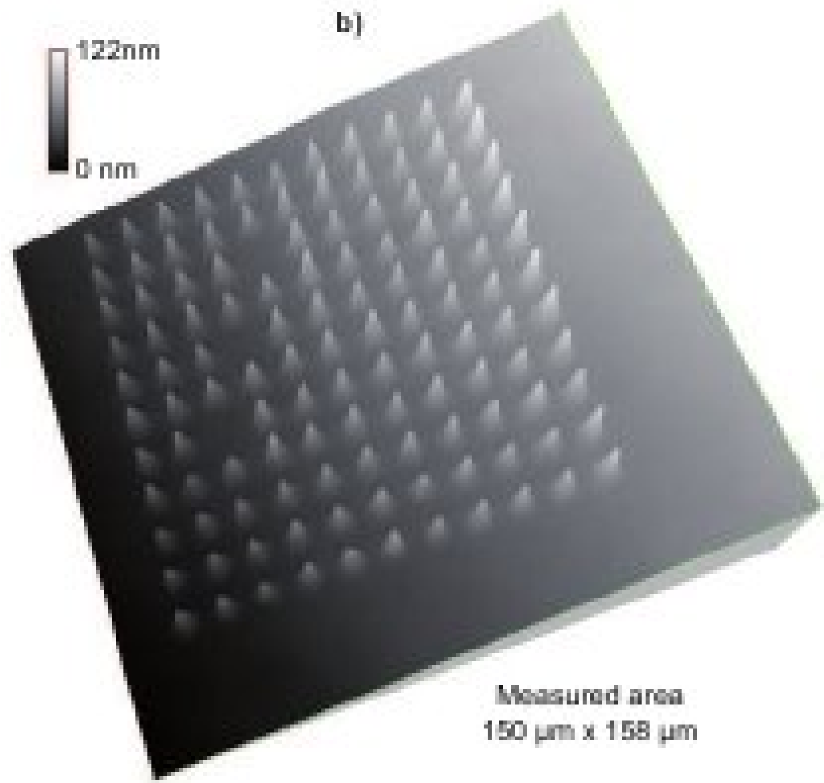

3D profile (PSI)

out-of-plane plane data from PSI

In-plane data from pattern

Six degrees of freedom measurement with interferometry

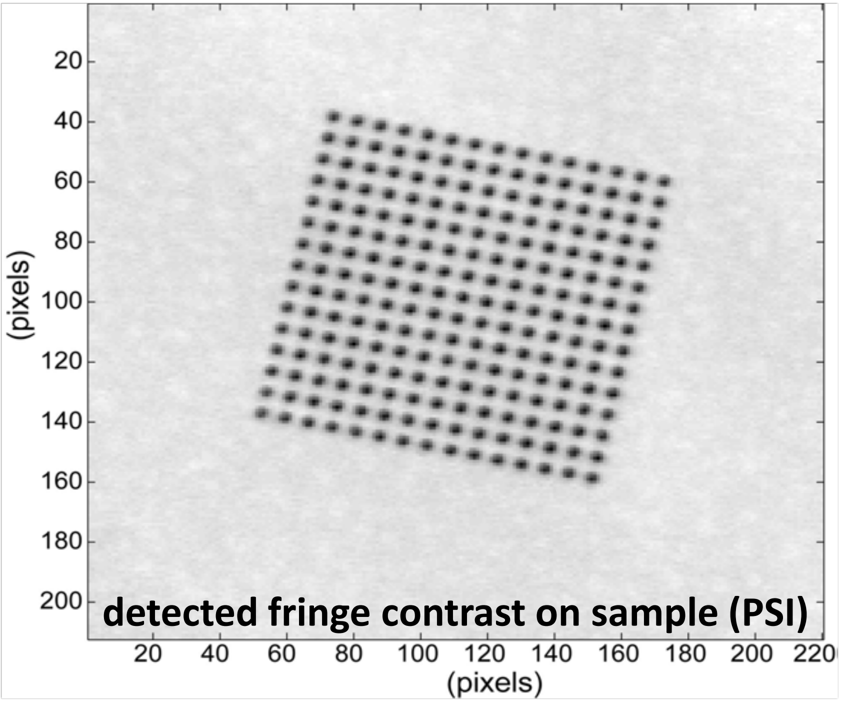

detected fringe contrast on sample (PSI)

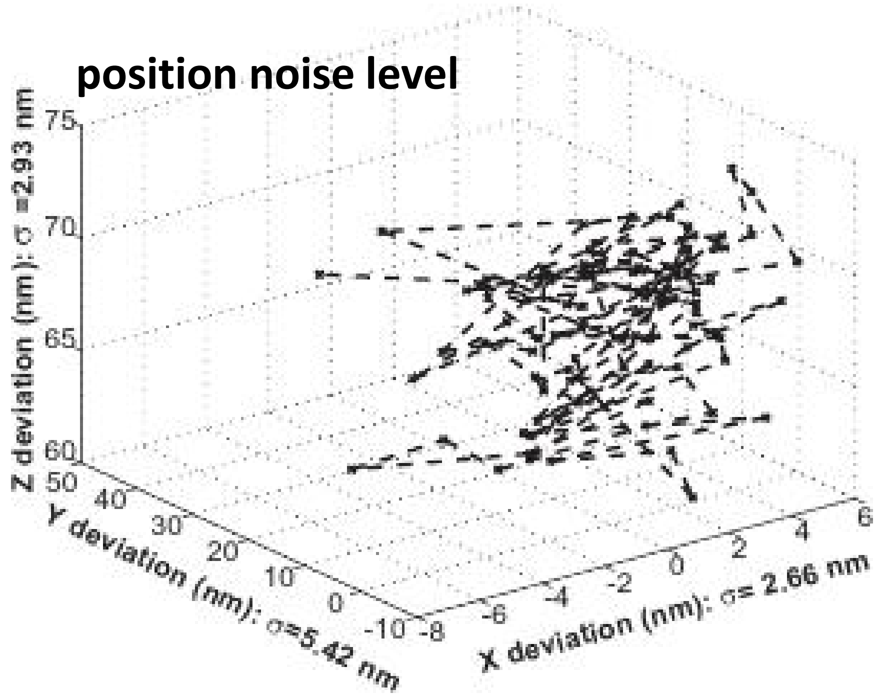

position noise level

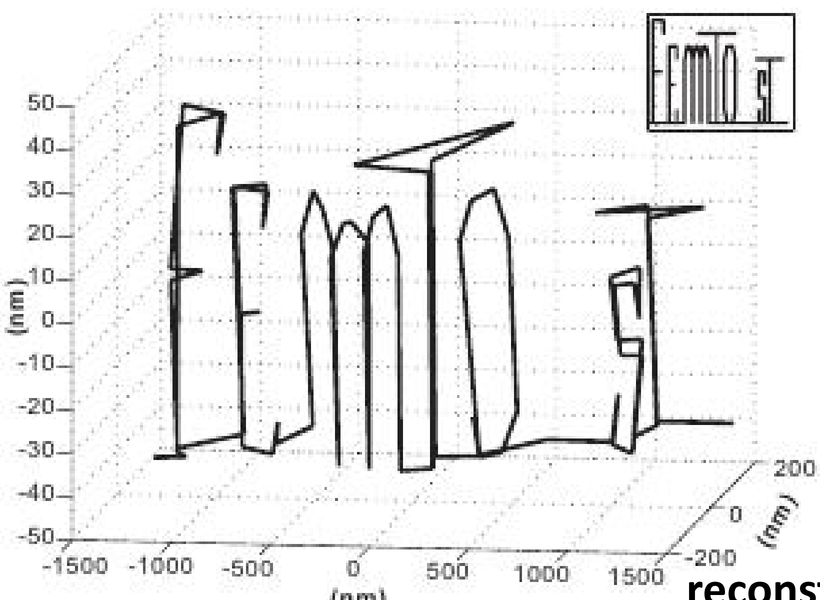

reconstructed 3D displacement

method specifications:

- 6 DOF sensing
- nanometre sensitivity in 3D
- slow rate
- 2π ambiguity along Z

Stereovision of a pseudo-periodic pattern (90° configuration)

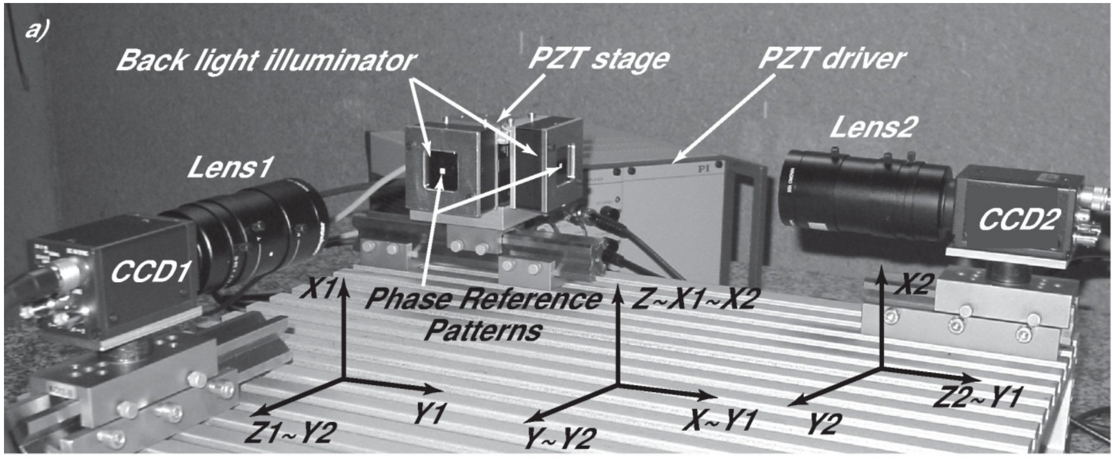

setup

specifications:

- working distance: 20cm
- magnification: 32.55 µm/pix
- estimated resolution: 29nm
- measurement range: 3cm

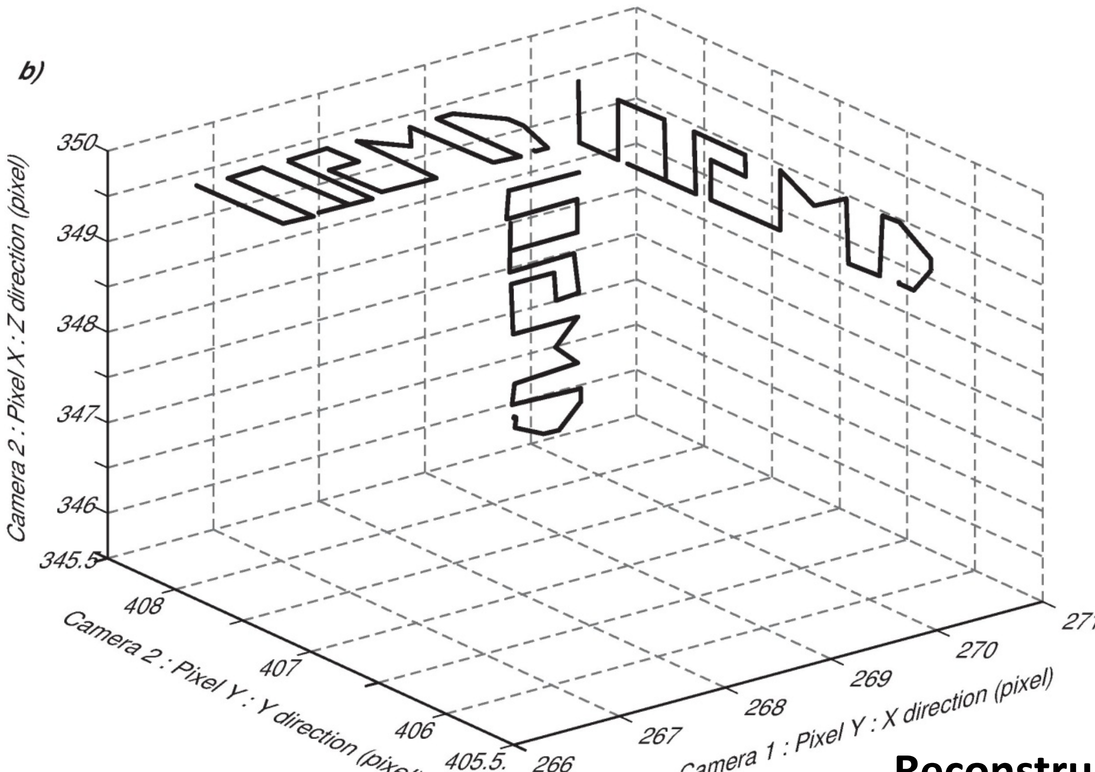

noise level

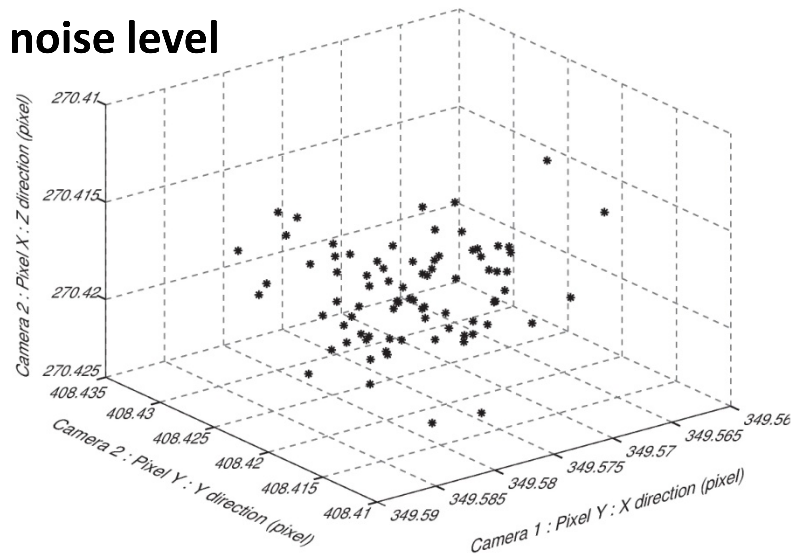

Reconstructed displacement

Stereovision of a pseudo-periodic pattern (±20° configuration)

unambiguous pattern with reference points

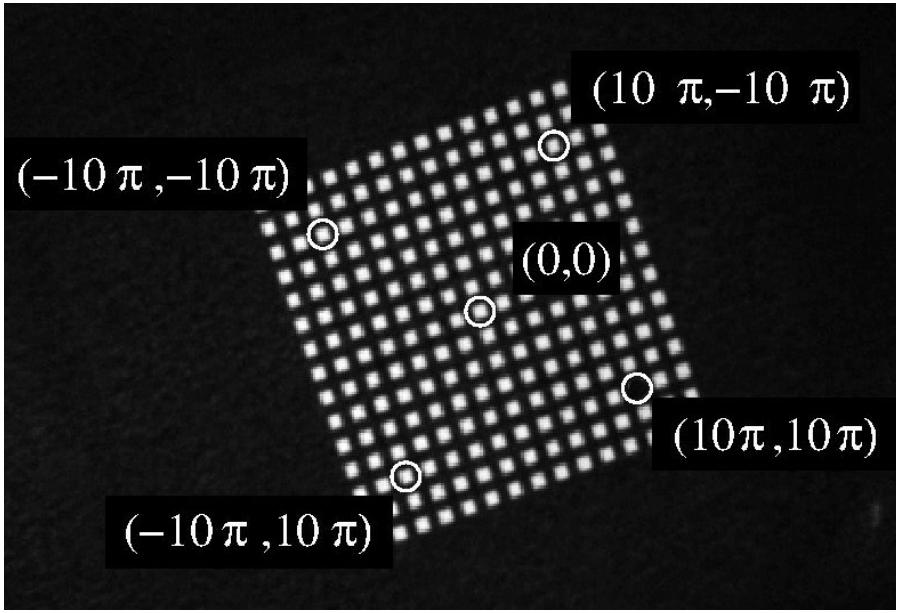

stereo setup

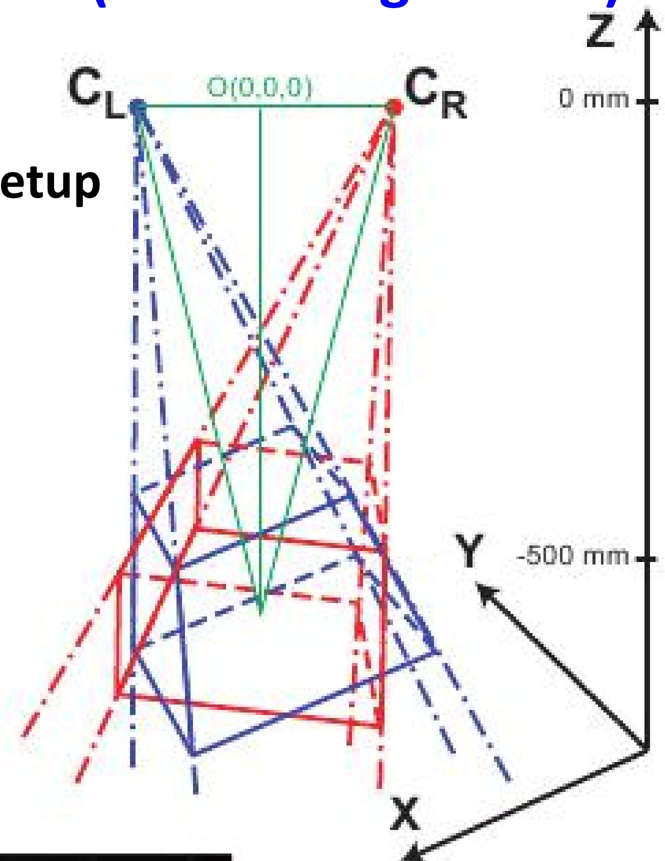

left and right recorded images

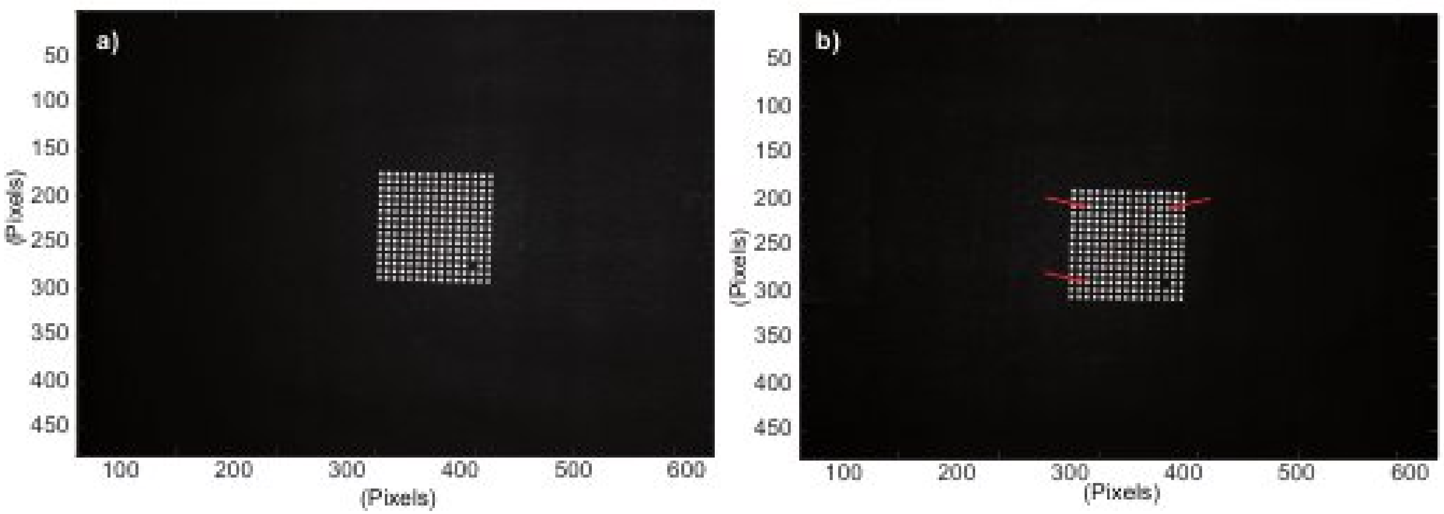

Stereovision of a pseudo-periodic pattern

worst

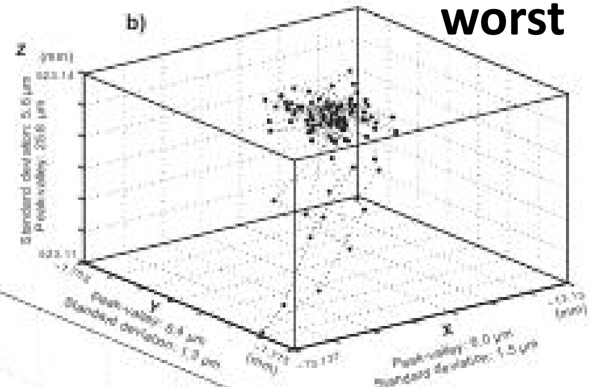

3D noise level

mean

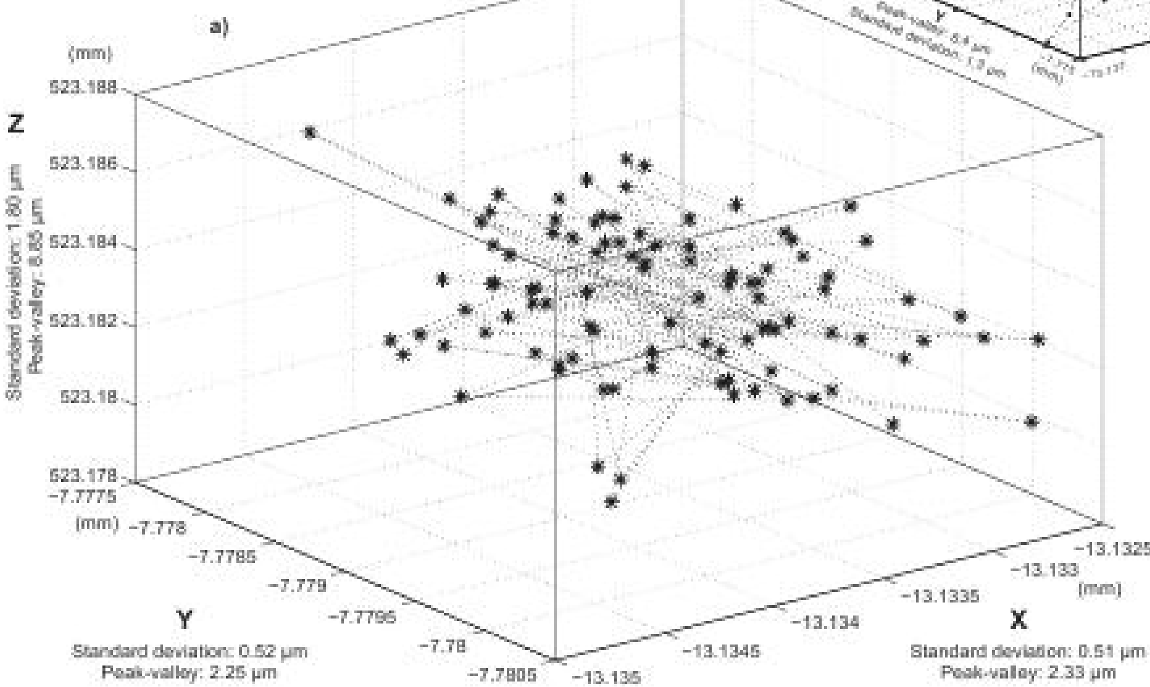

Position	Stand. Dev. (μm)		
	σ_X	σ_Y	σ_Z
Worst	1.50	1.26	5.64
Mean	0.53	0.52	2.06
Best	0.33	0.35	1.31

Angle	Stand. Dev. ($10^{-3} \cdot rad.$)		
	σ_{Θ_x}	σ_{Θ_y}	σ_{Θ_z}
Worst	0.193	0.177	0.176
Mean	0.174	0.170	0.169
Best	0.169	0.164	0.163

mean and worst position deviations observed (100 pts)

measurement distance of 50 cm

Stereovision of a pseudo-periodic pattern: 6 DoF sensing

Rotation ranges

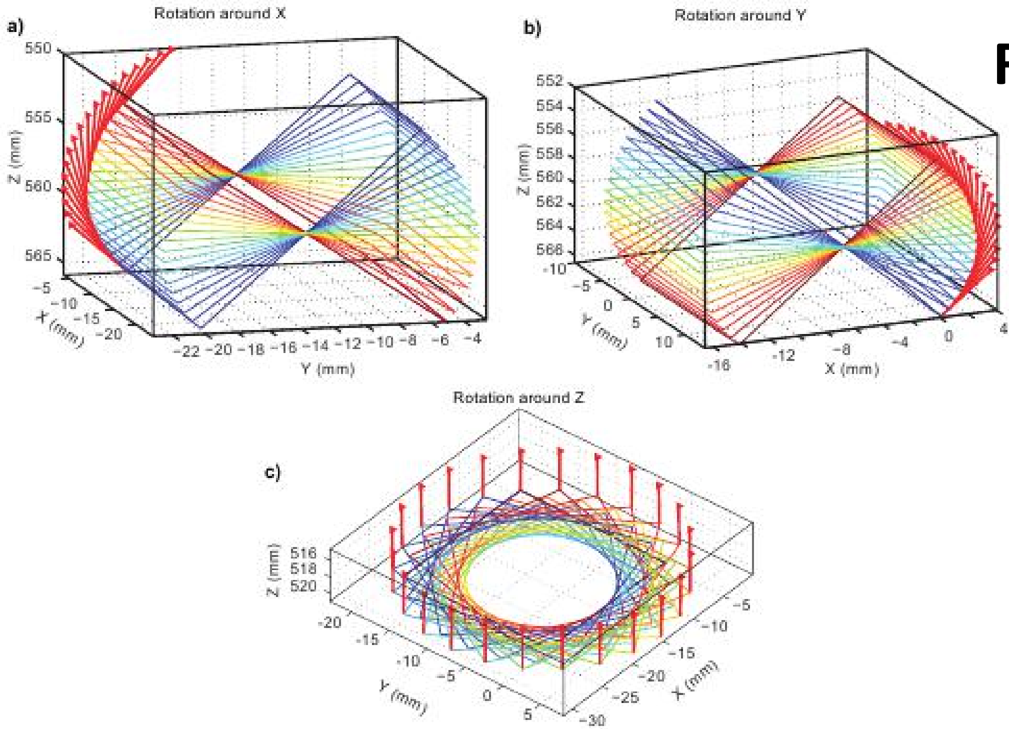

full scale: 2/3 of a single pixel

Reconstructed displacements

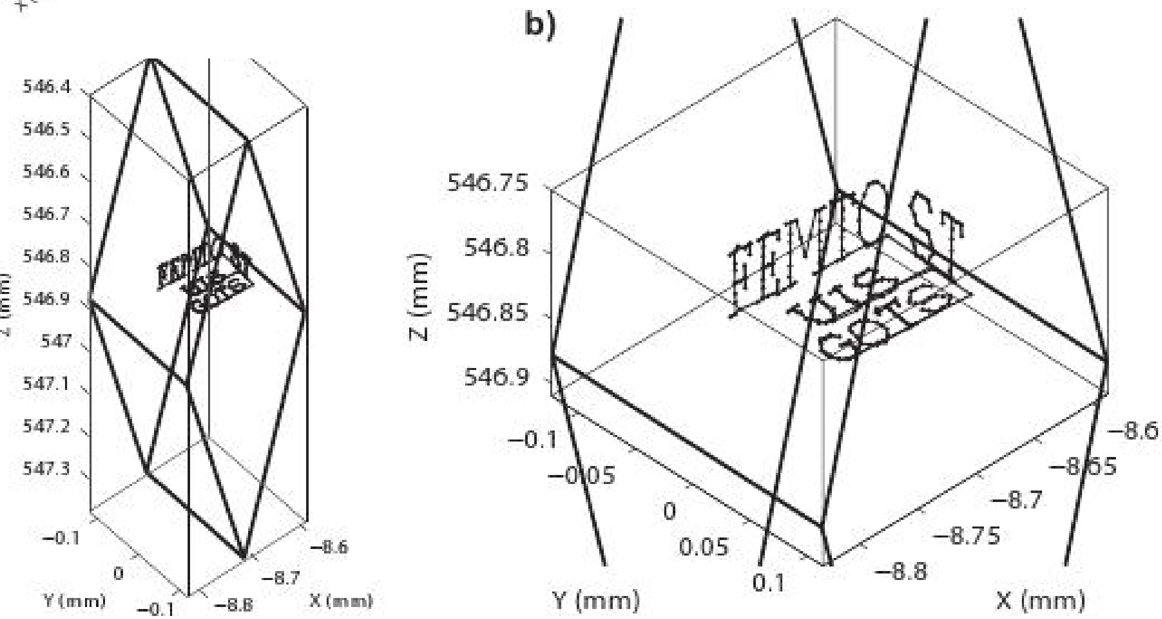

Summary and prospects

The Vernier principle can be transposed to digital image processing

Subpixel resolution can be obtained

typically better than 10^{-2} pixel with a standard camera

typically better than 10^{-3} pattern period in size

typically better than 10^{-3} degree in in-plane orientation

Multiscale method **(the imaging lens magnification acts as a scale adaptator)**

Self-calibrating method **(the pattern period forms a size reference)**

Various fields of applications : **(instrumentation, micro- & nano-technologies, biomedical, teaching, …)**